1-1-2012

Collagen Fiber Re-Alignment and Uncrimping in Response to Loading: Determining Structure-Function Relationships Using a Developmental Tendon Mouse Model

Kristin Suzanne Miller
University of Pennsylvania, krismiller17@gmail.com

Collagen Fiber Re-Alignment and Uncrimping in Response to Loading: Determining Structure-Function Relationships Using a Developmental Tendon Mouse Model

Abstract
Collagen fiber re-alignment and uncrimping are postulated mechanisms of structural response to load. It has been suggested that fibers re-orient in the direction of load and then "uncrimp" before collagen is tensioned and that in general, the structure is a result of the function tendons perform. However, little is known about how fiber re-alignment and uncrimping change in response to load, how this change relates to tendon mechanical properties, and if these changes are dependent on the underlying structure. Throughout postnatal development, dramatic structural and compositional changes occur in tendon. Postnatal tendons, with immature collagen networks, may respond to load in a different manner and timescale than mature collagen networks. Therefore, the overall objective of this study was to quantify the mechanical properties and structural response to load in a developmental mouse tendon model at 4, 10, 28 and 90 days old. Local collagen fiber re-alignment and crimp frequency were quantified throughout mechanical testing and local mechanical properties were measured. Throughout development, fiber re-alignment occurred at different points in the mechanical testing protocol. At early development, re-alignment was not identified until the linear (4 days) or toe-regions (10 days) of the mechanical test suggesting that fibers required a prolonged exposure to mechanical load before responding and that the immature collagen network present may delay re-alignment. The uncrimping of collagen fibers was identified during the toe-region of the mechanical test at all ages suggesting that crimp contributes to tendon nonlinear behavior. Additionally, results at 28 and 90 days suggested that collagen fiber crimp frequency decreased with increasing number of preconditioning cycles, which may affect toe-region properties. Mechanical properties and cross-sectional area increased throughout development. The insertion site demonstrated lower moduli values and a more disorganized fiber distribution compared to the midsubstance at all ages suggesting it experiences multi-axial loads. Further, the tendon locations demonstrated different re-alignment and crimp behaviors suggesting that locations may respond to load differently and develop at different rates. Results from this study suggest that structure affects the tendon's ability to respond to load and that the loading protocol applied may affect the measurement of mechanical properties.

Degree Type
Dissertation

Degree Name
Doctor of Philosophy (PhD)

Graduate Group
Bioengineering

First Advisor
Louis J. Soslowsky

Keywords
Collagen, Crimp, Nonlinear, Preconditioning, Re-Alignment, Supraspinatus Tendon

Subject Categories
Biomedical

COLLAGEN FIBER RE-ALIGNMENT AND UNCRIMPING IN RESPONSE TO LOADING: DETERMINING STRUCTURE-FUNCTION RELATIONSHIPS USING A DEVELOPMENTAL TENDON MOUSE MODEL

Kristin S. Miller

A DISSERTATION

In

Bioengineering

Presented to the Faculties of the University of Pennsylvania

in Partial Fulfillment of the Requirements for the Degree of Doctor of Philosophy

2012

Supervisor of Dissertation

_____

Louis J. Soslowsky, PhD, Fairhill Professor, Orthopaedic Surgery

Graduate Group Chairperson

_____

Beth A. Winkelstein, PhD, Professor, Bioengineering

Dissertation Committee
Dawn M. Elliott, PhD, (Committee Chair)
Professor, Biomedical Engineering, University of Delaware
David E. Birk, PhD
Professor, Pathology & Cell Biology, University of South Florida
Beth A. Winkelstein, PhD
Professor, Bioengineering, University of Pennsylvania

Acknowledgements

I would first like to thank the members of my committee for guiding me through the graduate experience. I would especially like to thank Dr. Louis Soslowsky, my advisor, for his mentorship and support throughout my time here. I am very grateful for his insight and dedication to training his students. I also thank Dr. Dawn Elliott, Dr. Beth Winklestein and Dr. David Birk for their time, valuable comments and suggestions throughout my studies.

I would also like to thank the entire McKay Laboratory, past and present, for the support and wonderful friendship over the past 5 years. In particular, I thank Spencer Lake, Nelly Andarawis-Puri and Joseph Sarver for their guidance, mentorship, patience and friendship. I thank Dr. Andrew Kuntz for his patience and time to introduce me to shoulder anatomy. I thank David Beason for countless hours of machining and design help. I am grateful for Cathy Peltz for her friendship and continued willingness to teach and mentor me. I thank Megan Farrell for her friendship and guidance. I'd like to thank Katie Reuther for her friendship and admirable work ethic. Thank you to Jennica Tucker for her help with histology and Nicholas Trasolini for your help with pilot studies and the in situ work.

I am also very grateful for Brianne Connizzo and Elizabeth Feeney. Thank you both for your hard work, dedication, persistence and contribution to this work, which would not have been possible without your efforts. Additionally, thank you Brianne for your hard work on the figures for this dissertation and the corresponding papers.

Additionally, none of this would have been possible without a strong support

system. I am extremely grateful and blessed to have family and friends who have been a constant encouragement throughout this process. Thank you to Deidre Sandrock and my teammates, past and present, on the Penn Women's Water Polo Team. To Alexis Crawley, thank you for your friendship and valuable insight. To David, Hilary and Harper Beason, thank you for letting me be a part of your family. I am extremely grateful for your friendship and encouragement. To the women of Joy in the Evening and Kelley Bergsma, thank you so much for your continued prayers and support, it has been an honor to serve beside and pray for such godly women and wonderful role models.

Further, none of this would have been possible without the love, support, and prayers of my family. I thank my parents, Greg and Cheryl, for always encouraging, supporting and believing in me. I am very grateful and blessed to be your daughter. I thank my brother, Brandon, for being an amazing example of honesty and purity of heart. I would also like to thank my grandparents, Wink, Cedar and Dorothy, for their constant prayers and support throughout my life. Lastly and most importantly, I would like to thank my Lord and Savior Jesus Christ, for blessing me with this opportunity and platform to serve, for giving me the grace and endurance to preserve, and for teaching me everyday how to sacrifice, work hard and love others above myself. You are my motivation and my efforts are for your glory.

ABSTRACT

COLLAGEN FIBER RE-ALIGNMENT AND UNCRIMPING IN RESPONSE TO LOADING: DETERMINING STRUCTURE-FUNCTION RELATIONSHIPS USING A DEVELOPMENTAL TENDON MOUSE MODEL

Kristin S. Miller

Louis J. Soslowsky

Collagen fiber re-alignment and uncrimping are postulated mechanisms of structural response to load. It has been suggested that fibers re-orient in the direction of load and then "uncrimp" before collagen is tensioned and that in general, the structure is a result of the function tendons perform. However, little is known about how fiber re-alignment and uncrimping change in response to load, how this change relates to tendon mechanical properties, and if these changes are dependent on the underlying structure. Throughout postnatal development, dramatic structural and compositional changes occur in tendon. Postnatal tendons, with immature collagen networks, may respond to load in a different manner and timescale than mature collagen networks. Therefore, the overall objective of this study was to quantify the mechanical properties and structural response to load in a developmental mouse tendon model at 4, 10, 28 and 90 days old. Local collagen fiber re-alignment and crimp frequency were quantified throughout mechanical testing and local mechanical properties were measured. Throughout development, fiber re-alignment occurred at different points in the mechanical testing protocol. At early development, re-alignment was not identified until the linear (4 days) or toe-regions (10 days) of the

mechanical test suggesting that fibers required a prolonged exposure to mechanical load before responding and that the immature collagen network present may delay re-alignment. The uncrimping of collagen fibers was identified during the toe-region of the mechanical test at all ages suggesting that crimp contributes to tendon nonlinear behavior. Additionally, results at 28 and 90 days suggested that collagen fiber crimp frequency decreased with increasing number of preconditioning cycles, which may affect toe-region properties. Mechanical properties and cross-sectional area increased throughout development. The insertion site demonstrated lower moduli values and a more disorganized fiber distribution compared to the midsubstance at all ages suggesting it experiences multi-axial loads. Further, the tendon locations demonstrated different re-alignment and crimp behaviors suggesting that locations may respond to load differently and develop at different rates. Results from this study suggest that structure affects the tendon's ability to respond to load and that the loading protocol applied may affect the measurement of mechanical properties.

Table of Contents

List of Tables

List of Figures

Chapter 1. Introduction

A. Introduction

Two postulated mechanisms of tendon structural response to load are collagen fiber re-alignment and fiber uncrimping. It has been suggested that collagen fibers re-orient in the direction of loading and then "uncrimp" before collagen is tensioned and that in general, the structure of tendon is a result of the function that tendon performs. However, little is known about how collagen fiber re-alignment and fiber uncrimping change in response to mechanical load and how a change in collagen structure relates to tendon mechanical properties. In particular, little is known about structural changes that occur during tendon preconditioning and if these changes are dependent on the number of preconditioning cycles. Additionally, it is not known if the uncrimping of collagen fiber occurs outside of the toe-region of the mechanical test. Identifying where these structural changes occur throughout the mechanical testing process is important in order to identify how tendons respond to mechanical load.

Further, it is important to determine if changes in the underlying structure of the tendon affect its ability to respond to mechanical load. Throughout postnatal development, dramatic structural and compositional changes occur in tendon.[4,6,63] Further, throughout postnatal development, supraspinatus tendons (SST) are expected to have different biomechanical properties and may not respond to load in the same manner as mature tendon.[1] The re-alignment or uncrimping of collagen fibers may be dependent on the inherent structure and composition of the tendon itself, in addition to the load it

experiences or the specific loading conditions applied (e.g., preconditioning). Postnatal tendons, with immature collagen fibrils, may respond to load in a much different manner and time scale than mature collagen fibers with mature fiber-fiber and fiber-matrix connections. While recent studies have begun to determine correlations between structure, composition and mechanics of developing tendons, the effect of developing tendon structure on collagen fiber re-alignment and fiber uncrimping is unknown.[1,9,40] A better understanding of tendon structure-function relationships will provide design parameters for therapeutic treatment of tendon injuries, tissue engineered constructs, and protocols for injury prevention.

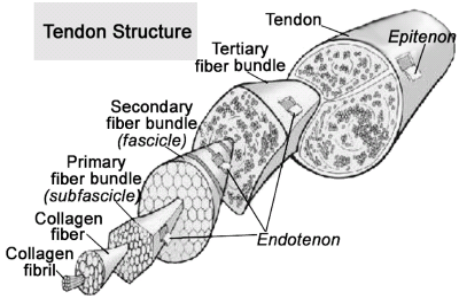

Figure 1.1 Tendon hierarchical structure.[46]

Tendon injuries are a common problem and resulted in over two million doctors office visits in the United States alone in 2001.[24] Tendons are subjected to repetitive motions and degeneration over time and are prone to both acute and chronic injuries. Tendon injuries heal slowly and rarely regain normal function.[28] This dissertation will provide a better understanding of how tendon responds to mechanical load and will identify potential correlations to tendon structure. This information is necessary to determine tendon structure-function relationships and subsequently the etiology of tendon injuries.

Therefore, the overall aim of this dissertation was to evaluate the structural response of tendon to mechanical load in a developmental mouse SST model. This dissertation will utilize an innovative quantitative method of crimp analysis and a

previously established crossed polarizer system to examine collagen fiber re-alignment under load. The quantitative crimp analysis was developed by adapting an established semi-quantitative flash-freezing method.[55] The crimp analysis will provide a "snap-shot" of crimp at specific quantifiable loads throughout a tensile mechanical testing protocol. Additionally, the quantitative crimp analysis method will be the first to quantitatively analyze fiber crimp during preconditioning. In addition, mouse supraspinatus tendon mechanical properties and collagen fiber re-alignment behavior have not been characterized throughout postnatal development due to their fragile nature and size. Further, this study is innovative in that it seeks to identify mechanisms of preconditioning and the toe-region by specifically quantifying collagen fiber re-alignment and uncrimping during loading throughout specific points in the mechanical test. The goal of this dissertation is to provide a better understanding of tendon structure-function relationships, in particular to understand the relationship between developing tendon structure and the ability of the tendon to respond to mechanical load, to improve our understanding of the process of tendon development, as well as to provide insights into tendon injuries with mechanical etiology.

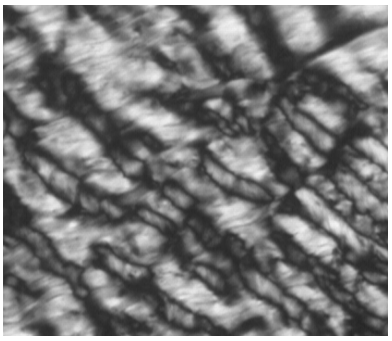

Figure 1.2 Collagen fiber crimp in tendon appears as alternating dark and light bands on polarized light. microscopy. Image size 100x100μm.

B. Background

B1. Tendon Structure and Composition

Tendon is a soft connective tissue that joins muscle to bone. It is a composite material with mainly parallel collagen fiber bundles surrounded by a gel-like extracellular matrix. The main constituent of fiber bundles is Type I collagen. Tendon extracellular matrix is composed primarily of water, minor collagens, proteoglycans and glycosaminoglycans (GAGs). Water represents 65-80% of wet weight, while type I collagen represents 65-80% of dry weight. Proteoglycans, such as decorin or biglycan, represent 1-5% of the dry weight of tendon.

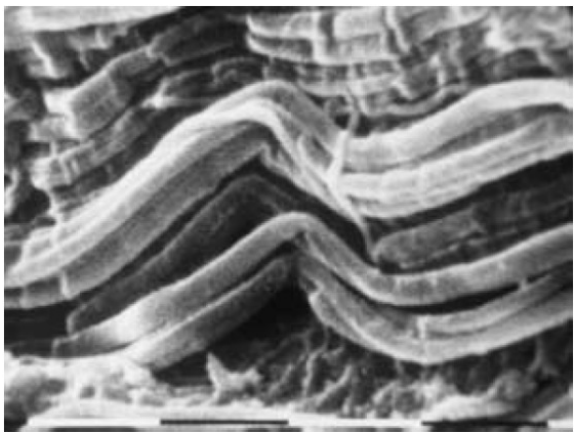

Figure 1.3 SEM image of relaxed Achilles tendon. Collagen fibril bundles arranged in a crimp pattern with a sharp top angle are evident. In the same crimp, single collagen fibrils drastically change direction form individual 'knots' termed 'fibrillar crimps'. As in each collagen fibril many 'knots' are often visible in the same tendon crimp.[14] Scale bar =1μm.

Tendon is hierarchical and highly organized. Initially, immature type I collagen fibril intermediates coalesce to form fibrils. As tendons mature, fibrils associate laterally to create a wide range of fibril diameter sizes.[11,32,63] These fibril segments are then assimilated into bundles which are incorporated into the developing matrix.[5] These bundles of fibrils are termed 'fibers' and considered the main functioning unit of collagen-based structures. Bundles of collagen fibrils have been found to be discontinuous in number from one serial section to another and the bundles rotated along the length serving to twine the composite fibrils in bundles.[5] Groups of collagen fibers then form fascicles, which in turn coalesce to form tendon (Fig 1.1). However, it is

currently not known how each hierarchical scale contributes to tendon mechanical properties and structural response to load. Further, it is not known how the rotation and twining of collagen fibril bundles affects tendon mechanical properties as it is commonly assumed that tendon fibers are packaged longitudinally as opposed to being physically intertwined. Collagen fibers are also highly viscoelastic and therefore their loading history is critical.[47]

Collagen exhibits a wavy or 'crimped' pattern that has been reported at multiple hierarchical scales.[14-17,19,44] It is thought that the crimp pattern influences tendon nonlinear mechanical behavior.[59,62] In histology, regions of the tendon appear as alternating dark and light bands under polarized light microscopy and are commonly identified as collagen fiber crimp (Fig 1.2). While these alterations of light and dark bands have been reported at the fiber, fascicle and tissue level scales,[14-17,19,44] discussions of collagen crimp in literature is primarily focused on the fascicle-level. Further, collagen fibrils in mature tendon have been examined under scanning electron microscopy (SEM) and appear to be composed of many "knots" of each single fibril termed 'fibrillar crimps' (Fig 1.3).[15] Fibrillar crimps are thought to follow a planar zig-zag with bending regions that

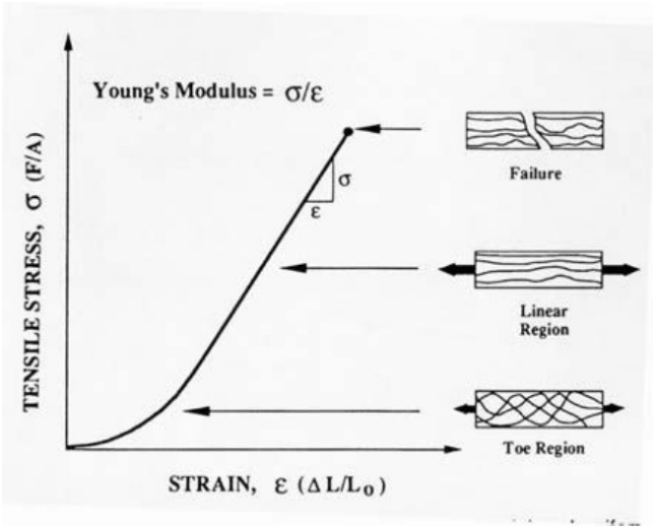

Figure 1.4 Sample nonlinear tendon stress-strain curve.[13]

act as flexible hinges.[14]

Crimp is thought to play a mechanical role in absorbing the initial load during elongation and then to recoil fibrils and fibers when tissues have to return to their initial length.[15] While the origin of collagen fiber crimp is unknown, it has been speculated to be dependent upon one or more of the following factors: mechanical impulses from the contraction of fibroblasts,[19,21] mechanical properties of collagen fibril and interfibrillar matrix,[21] the formation of elastin fibers,[33] blood circulation,[33] or fetal limb movements.[33] Additionally, a passive mechanical mechanism of fiber buckling caused by shrinkage of the matrix has been proposed as a possible mechanism for crimp initiation and development.

Cross-linking of collagen molecules provides structural integrity to collagen fibrils. Trivalent intermolecular pyridnoline crosslinks stabilize the fibrillar structure of collagen and are thought to contribute to tendon mechanical properties.[8] These cross-links are formed after spontaneous conversion of the immature, covalent crosslinks into more mature trivalent crosslinks with maturation.[8] Additionally, it is thought that proteoglycans and minor collagens may form non-covalent fibril-fibril interactions, which are necessary for mechanical integrity.[5]

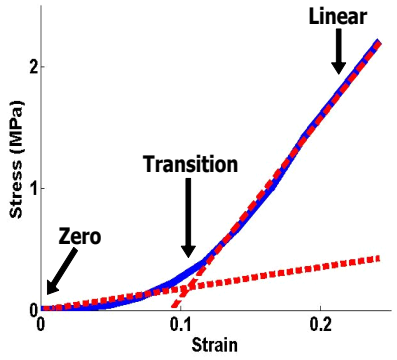

Figure 1.5 Example of a stress-strain curve with the bilinear curve fit with the transition and linear-strains denoted.

B2. Tendon Mechanics

Tendon is primarily a uniaxial tissue that transfers forces from muscle to bone. It is inhomogeneous, anisotropic, nonlinear and viscoelastic.[61] Tendon mechanical properties

vary with location, which is likely due to compositional variation and fiber organization of different regions.[25,26] Tendon mechanical properties are characterized by an initial low stiffness toe-region, followed by a high stiffness linear-region (Fig 1.4). The toe-region is thought to be caused by gradual recruitment of crimped collagen fibers.[20,61] After the toe-region, all collagen fibers are believed to be taut, supporting loading and the stress-strain curve becomes linear. While this understanding of fiber behavior has been speculated, it has not been rigorously studied nor quantified during loading. Additionally, the specific mechanisms of preconditioning and the toe-region are not yet fully understood.

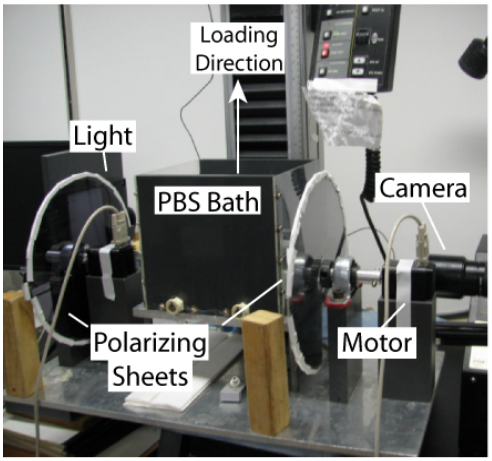

Figure 1.6 Angled side-view of the tendon tensile testing setup showing polarized light and imaging system: light source, rotating cross-polarized sheets, stepper motors, and camera.

The material properties of tendon, modulus and maximum stress, can be calculated from the stress-strain curve. Material properties are intrinsic measures of the quality of the tissue substance. Maximum stress is the highest stress obtained during a mechanical test. A bilinear curve fit can be applied to stress-strain data to calculate the transition strain (strain at which modulus transitions from the toe- and linear-region) and to quantify the moduli in the toe- and linear-regions (Fig 1.5). Linear modulus is calculated from the slope of the linear-region of the stress-strain curve while the toe-region modulus is calculated from the slope of the toe-region of the stress-strain curve. Time and history-

dependent viscoelastic properties can also be obtained. A stress-relaxation test requires stretching the tendon to a constant length and allowing the stress to vary over time. Percent relaxation is calculated from peak stress (highest stress after initial strain) and equilibrium stress (stress reached after relaxation has occurred). Material and viscoelastic parameters characterize the functional behavior of tendons.

Further, many studies have been conducted to evaluate tendon structure-function relationships. Tendon composition and structure has been shown to vary with the loading conditions seen by the tissue.[3] Additionally, correlations have been identified in the supraspinatus tendon between collagen fiber alignment and mechanical properties.[25] It has been postulated that the more disorganized collagen fiber alignment and lower moduli values demonstrated at the SST insertion site may be explained by a complex multi-axial loading environment experienced in vivo.[25] However, it is currently not known if the more disorganized collagen fiber distribution drives the decreased tensile mechanical properties or if the decreased tensile mechanical properties form in response to the multi-axial loads which then remodels the collagen network resulting in a more disorganized collagen fiber distribution. Structure-function relationships and the etiology of tendon structure and mechanical properties merits further examination.

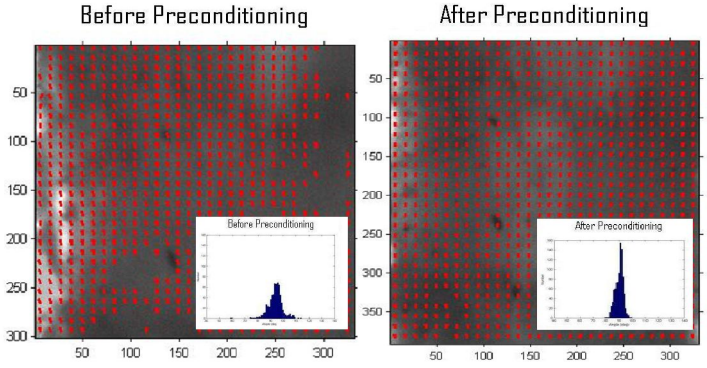

Figure 1.7 Sample alignment maps and histograms before and after preconditioning showing an increase in alignment (Decrease in VAR).

B3. Collagen Fiber Re-alignment

To better understand how structure correlates to mechanical function, it is necessary to determine how the structure of tendon responds to mechanical load. Determining where collagen fibers re-align in the direction of loading during mechanical testing is an important step towards understanding tendon structural response to the presence of mechanical load. Additionally, measuring collagen fiber distributions throughout the mechanical test provides structural information, which may correlate with local tendon mechanical properties, improving our understanding of tendon structure-function relationships. Several techniques have been used recently for the analysis of fiber architecture of tendon and other fiber-reinforced soft tissues.[35,36,41,56,57] Our laboratory has recently developed a cross-polarizer technique for mechanically testing while simultaneously taking a series of images to measure fiber architecture in small sections of human SST.[25,26] This device consists of a tensile testing system (Instron, Norwood, MA) integrated with a polarized light setup, consisting of a linear backlight (Dolan-Jenner, Boxborough, MA), 90°-offset rotating polarizer sheets (Edmund Optics, Barrington, NJ)

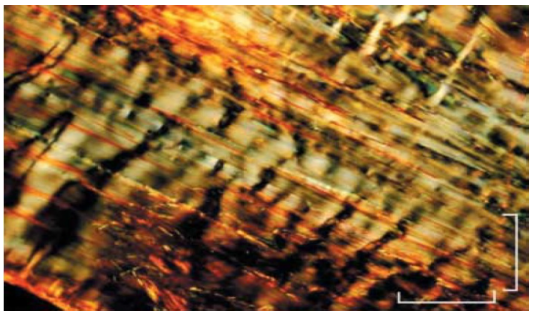

Figure 1.8 Polarized light micrograph of relaxed Achilles tendon. The alternating light and dark transverse bands indicate collagen fiber crimp.[13] Scale bar =100μm.

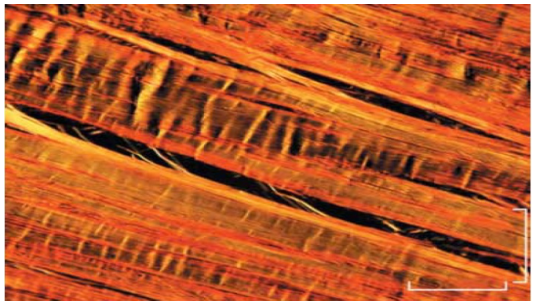

Figure 1.9 Polarized light micrograph of stretched Achilles tendon. Note some areas with collagen fiber bundles running straight and parallel to the long axis of the tendon with no birefringence, and other areas where birefringence is observed and reveals flattened crimps.[13] Scale bar =100μm.

on either side of the test sample, and a digital camera (Basler, Exton, PA) (Fig 1.6). Additionally, this device has been used in studies examining the rat SST and the rat subscapularis tendon.[30,51] A large shift in collagen fiber re-alignment was identified during preconditioning in the rat SST model (Fig 1.7).[30] Preconditioning is thought to provide tendons with a consistent "history," allowing stress-strain results to become repeatable for rigorous evaluation and comparison across experiments. While it is widely accepted that preconditioning is important, structural changes that occur during preconditioning are not well understood. Previous studies have suggested re-alignment of collagen fibers as one proposed mechanism of preconditioning.[30,37,48,49] However additional studies are necessary to further understand the role of collagen fiber re-alignment during preconditioning, as well as throughout the entire mechanical test to improve knowledge of how tendon responds to mechanical load.

Figure 1.10 Grading scale for semi-quantitatively analyzing number of crimped fibers in ligament following stress relaxation and creep tests.[55] Image sizes 140μm x140μm.

B4. Collagen Fiber Crimp

The uncrimping of collagen fibers, in addition to fiber re-alignment, is a suggested mechanism of tendon response to mechanical load. Collagen crimp has been suggested to explain the toe-region of the stress-strain curve.[20,61] While crimp has been extensively studied at slack or unknown load conditions,[14-17,22] few studies have examined crimp at specific, quantifiable loading conditions. Further, the effect of preconditioning on fiber

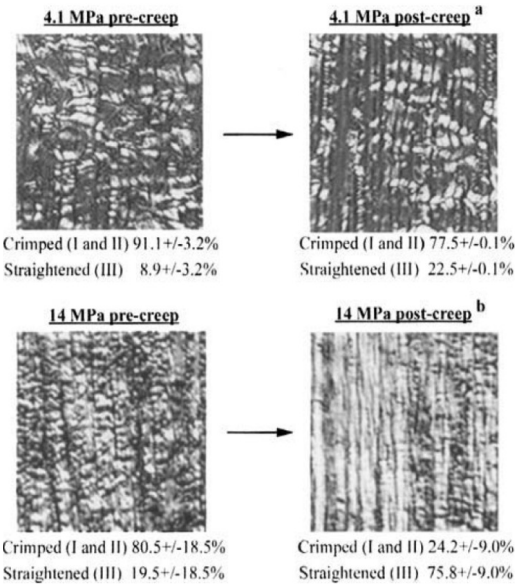

Figure 1.11 Significant decreases in crimped fibers and increases in straight fibers were evident after creep tests in ligament tested at both loading levels.[55] Image sizes 280μm x280μm.

crimp has not been examined and fiber uncrimping may occur during preconditioning.

Studies estimate that the uncrimping of collagen fibers occurs when the tendon has reached 1-5% strain (Fig 1.8, crimped; Fig 1.9, uncrimped fibers).[20,38,39,59] Further, in a study examining the rat tail tendon fascicle, straightening of collagen fibers has been reported at 1 and 2% strain and by the end of the toe-region, all fascicles were uncrimped and realigned in the direction of load.[44] It is possible that the level of strain necessary to transition to the linear-region is dependent on the tendon location in the body as well as structure and required function. While results from the rat tail tendon fascicle studied found no evidence of fiber re-alignment or uncrimping following the toe-region, tendon level studies in the rotator cuff tendons have demonstrated that fiber re-alignment continues until tendon failure.[25,30,51] In addition, tendon fascicles demonstrated a nonuniform uncrimping of collagen fibers along the length of the tendon,[20] which suggests that tendon crimp may vary locally at a larger hierarchical scale. Examining the role of collagen fiber crimp during preconditioning and the toe-region of the stress-strain curve will advance the field's understanding of how tendon responds to mechanical load.

Additionally, the relationship between collagen fiber crimp and re-alignment throughout mechanical testing has not been extensively studied. Fiber crimp has been noted to appear deeper after repeated cycles of loading in the toe-region, while fibers appeared more highly aligned than initial testing values, suggesting that fiber crimp may be an entirely different mechanism that collagen fiber re-alignment.[58]

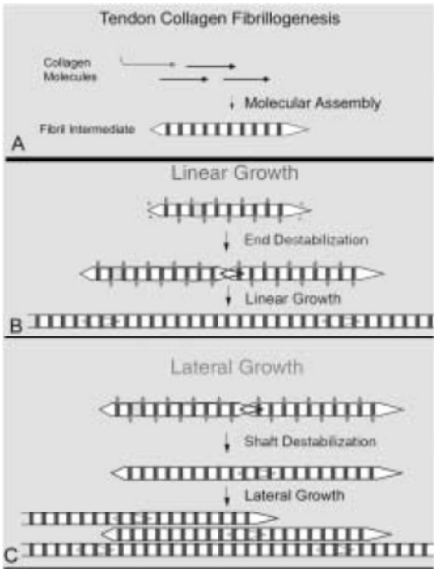

Figure 1.12 Tendon fibrillogenesis. (A) Molecular assembly of type I collagen generates the fibril intermediate. (B) In the linear growth step, the intermediates in (A) grow by end-to-end growth to generate longer fibrils. (C) In the lateral growth step, there is a lateral association and growth of the developing fibrils.[63]

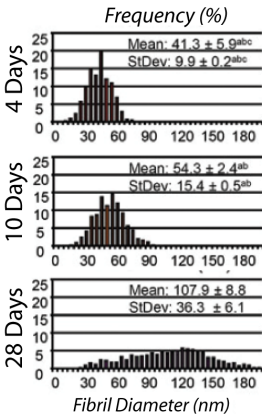

Figure 1.13 Frequency distribution of fibril diameters demonstrated an increased fibril diameter and fibril diameter distribution throughout postnatal development.[1]

To examine collagen fiber crimp during loading, a semi-quantitative measurement of crimp analysis has been used to capture crimp at specific points during creep and stress relaxation tests in ligament.[7,55] In these studies, the samples were flash frozen while still loaded in the mechanical testing system immediately following the prescribed loading regimen. Flash freezing the samples while they are still attached to the mechanical test grips allows crimp to be characterized at specific loads and test points.[55] In ligament, creep has been assessed before and after creep and stress relaxation tests to two load levels. Ligaments were flash frozen at each test point, immediately embedded in OCT, frozen and then sectioned on

a cryotome. Sections were stained with hematoxylin and Sirius red and examined using polarized light microscopy and image software. The percent crimped area was qualitatively graded into three categories (substantial crimp, intermediate, minimal) (Fig 1.10).[55] No significant differences were found in the crimp patterns measured before and after stress-relaxation at either loading condition.

However, significant decreases in crimped fibers and increases in straight fibers were evident after creep for ligaments tested at both loading levels (Fig 1.11). In tensile loading of tendons, it has been noted that when tendons are stretched the crimps decrease in number and appear to flattened with an increase in crimp top angle.[14] However, under scanning electron microscopy (SEM) and transmission electron microscopy (TEM), it was noted that fibrillar crimps were still present even though tendon level crimps had disappeared.[14] Overall these studies have begun to characterize collagen fiber crimp in the presence of load but have yet to specifically quantify crimp behavior throughout an entire mechanical testing protocol or in the presence of

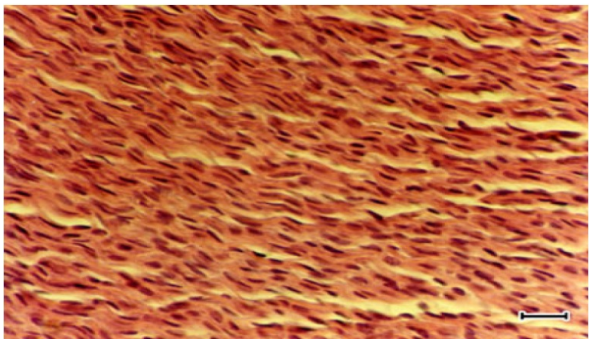

Figure 1.14 Longitudinal section of superficial digital flexor tendon of newborn rabbit demonstrates immature tenocytes partially aligned along the long axis of the tendon. Tissue shows primitive crimping and high cellularity.[33] Scale bar =20μm.

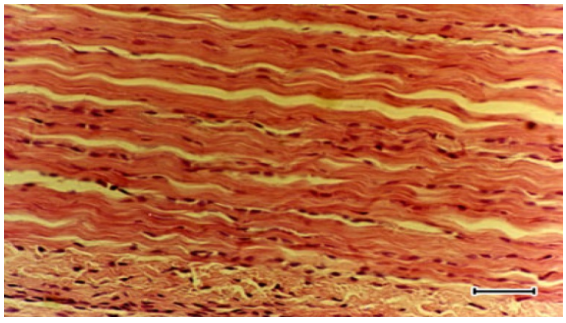

Figure 1.15 Longitudinal section of 28 day old rabbit tendon showing fewer cells per unit area and improved alignment of fibers from early development.[33] Scale bar =40μm.

preconditioning. These studies suggest that crimp may influence mechanical properties and merits more extensive examination.

B5. Tendon Development

Throughout postnatal development, dramatic structural and compositional changes occur in tendon. The development of tendon hierarchical structure during collagen fibrillogenesis can be marked by at least three stages.[4,6,63] Initially, collagen molecules

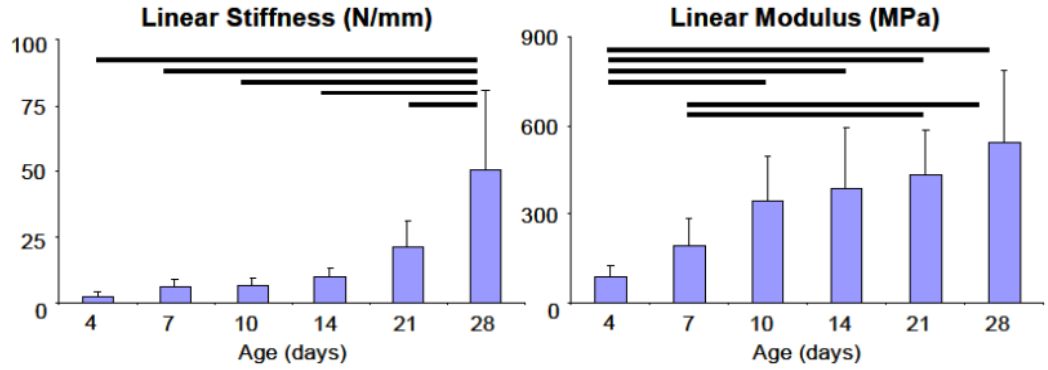

Figure 1.16 Linear stiffness and modulus significantly increased with age in a postnatal Achilles tendon $p<0.05$.[1]

assemble extracellularly to form fibril intermediates. These fibril intermediates assemble end-to-end during linear fibril growth (Fig 1.12). Fibrils then associate laterally to generate larger diameter fibrils during lateral fibril growth. The distribution of collagen fibril diameter size changes throughout development.[31-34] During early development, the distribution is small consisting of mainly small diameter fibrils (Fig 1.13). However, throughout development, the distribution increases as fibrils coalesce to form

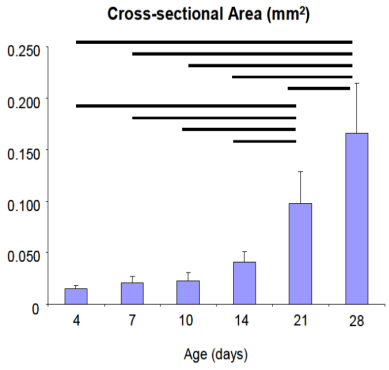

Figure 1.17 Achilles tendon cross-sectional area increases throughout postnatal development. $p<0.05$. [1]

larger diameter fibrils, while some remain unaltered (Fig 1.13). Changes in collagen fibril diameter begin during the onset of locomotion .[11] It is thought that the larger diameter fibrils withstand higher tensile stress than small diameter fibrils.[9,34] Previous studies have identified moderate correlations between mean fibril diameter with fascicle stiffness and maximum load.[9] Additionally, there is a weak correlation between fascicle modulus and maximum stress.[9] Fibrillogenesis is thought to be regulated by fibril-associated macromolecules, such as decorin and biglycan[23,27,40,43,60,63] and fibril-associated collagens with interrupted triple helices (FACITS) such as collagen XII and XIV.[2,50]

Collagen fiber crimp is established in tendon during embryonic development when the tissue is rapidly increasing in length and collagen content (Fig 1.14).[21,45] Additionally, age related changes in collagen fiber crimp behavior have been reported throughout development (Fig 1.14 and 1.15).[10,19,33,45] Two week old rat tail tendon required a smaller percent strain to eliminate the extinction bands (signifying collagen crimp) than older tendons (29 months).[10] Crimp length was found to be proportional to tail length and has been shown to increase with age until

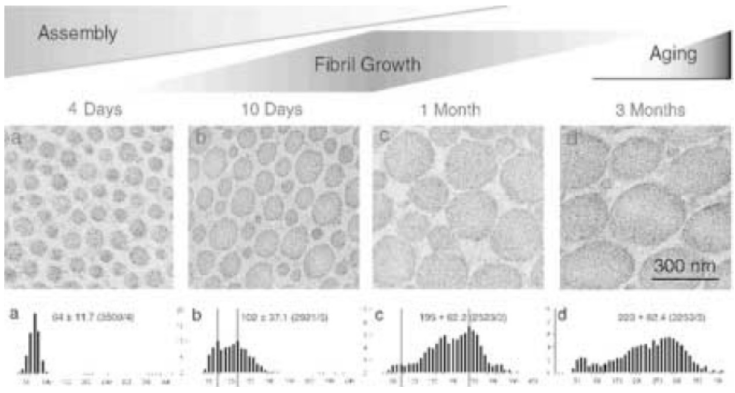

Figure 1.18 Collagen fibril structure during development in mouse tendons. Transmission electron micrographs of transverse sections from mouse flexor tendons and the diameter distributions at each stage of development (a-d). Bar 300 nm. [12]

maturity.[10] In regards to mechanical properties, the toe-region of the stress-strain curve shortens with age while the linear modulus increases (Fig 1.16).[1,10] Cross-sectional area of the tendon also increases with age (Fig 1.17).[1]

Several in vivo animal models of development are available including previous work performed in the chicken,[4,6,42,45] rat,[31,43] mouse[1,63] and rabbit.[33] The mouse model is attractive for developmental studies based on availability of previous knowledge of the stages of fibrillogenesis.[1,63] At 4 days old, a normal distribution of small diameter fibrils is present and fibril intermediates begin their initial assembly (Fig 1.18). At ten days, the transition from fibril assembly to growth begins. By thirty days old, fibril growth continues until maturation. A broad distribution of fibril diameters is present and larger diameter fibrils are characteristic. By three months of age, the tendon is mature and has completed growth. Fibril diameters only change modestly with large diameter fibrils begin more prominent in the oldest tendons. Documented stages of fibrillogenesis in the mouse provide confidence that tendon structure is changing throughout development and provides an acceptable model system for studying how changing structure affects tendon's ability to respond to mechanical load. In addition to this, the mouse model is attractive as it provides pote ntial for future knockout studies and offers the ability to quantify GAG or crosslink contribution. Further, the SST has been shown to be an effective model to study re-alignment of collagen fibers due to the tendon's more disorganized collagen fiber distribution.[25,26] In particular, the SST is an effective model to study structure-function relationships as its insertion site has been shown to demonstrate a complex gradation of structural, mechanical and compositional properties

(Fig 1.19).[54] In particular, the SST's insertion site has been noted to have a more disorganized collagen fiber distribution and lower moduli values compared to the midsubstance location.[25] However, it is not known if the insertion site demonstrates a disorganized uniaxial population of fibers or if it is organized as an anastomosing network[5] with highly regulated intermodal distances and periodic branching. Previous work in the mouse SST model has investigated the formation of the tendon-to-bone insertion site throughout development.[18,53] Local expression of extracellular matrix and growth factor genes changed throughout mouse SST development.[18] A robust insertion site formation as previously described in was not seen until 21 days after birth (Fig 1.20).[54] The results from these studies indicate that the ability of tendon to structurally respond to load may vary by location throughout development. Additionally, further research is necessary to better understand how the insertion site and tendon midsubstance communicate and transmit load to each other as the insertion site develops.

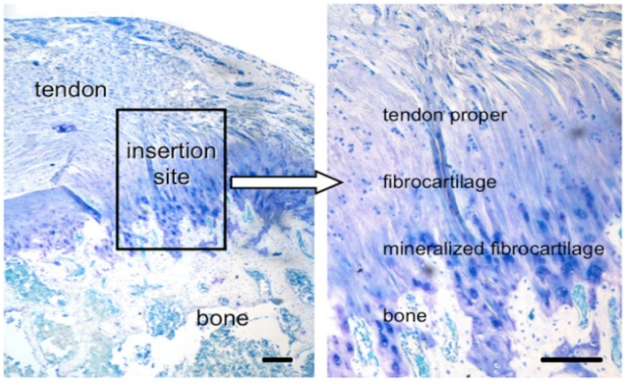

Figure 1.19 Tendon attaches to bone across a functionally graded fibrocartilaginous transition site.[52] Scale bar = 200mm.

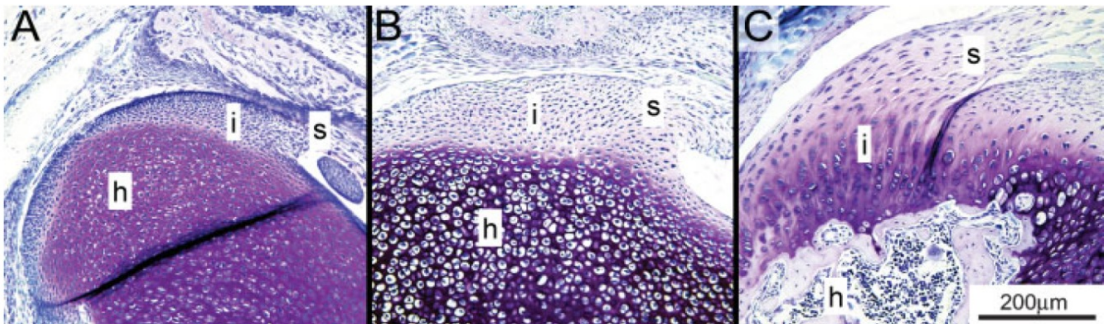

Figure 1.20 A fibrocartilaginous transition zone did not develop between the supraspinatus and the humeral head until postnatal timepoints. (A) 15.5 days post conception; (B) neonatal; (C) 21 days postnatal. s, supraspinatus tendon; h, humeral head; i, interface.[18]

C. Specific Aims and Hypotheses

The overall aim of this bioengineering study is to investigate tendon structural response to load throughout postnatal development. The overall objective is to use postnatal development to identify if underlying changes in tendon structure affect the tendons ability to structurally respond to load, specifically by quantifying collagen fiber re-alignment and crimp behavior throughout the mechanical testing process. The specific aims and hypotheses are as follows:

Specific Aim 1: To determine developmental changes in local mechanical properties.

Hypothesis 1: Local differences between midsubstance and insertion site modulus will be detectable at late postnatal development and at maturity.

This hypothesis is based on previous studies that showed that the mouse tendon-to-bone insertion site is not fully formed until 21 days postnatal development.[18] Therefore, we anticipate that the insertion site location will demonstrate a lower linear modulus compared to the midsubstance location after 21 days postnatal.

Specific Aim 2: To quantify local collagen fiber re-alignment and uncrimping of developing tendon in response to mechanical loading.

Hypothesis 2a: The largest amount of collagen fiber uncrimping will occur in the toe-region of the mechanical test regardless of age.

This hypothesis is based on previous work indicating that the toe-region of the mechanical test is explained primarily by the uncrimping of collagen fibers.[20,29,62] We postulate that initial fiber re-alignment in the direction of loading will occur before fiber uncrimping[30,37] and that the uncrimping of collagen fibers will be confined to the toe-region regardless of developmental age.

Hypothesis 2b: In mature tendon, the largest amount of collagen fiber re-alignment will occur during preconditioning regardless of number of cycles. In postnatal tendons, the largest amount of collagen fiber re-alignment will occur during the toe-region but re-alignment will also occur during 20 cycles of preconditioning.

This hypothesis was based on previous work that demonstrated a large shift in collagen fiber re-alignment towards the direction of load during preconditioning in a mature rat SST tendon.[30,37] We hypothesize that mature mouse tendon will behave similarly and demonstrate the largest shift during preconditioning regardless of the number of preconditioning cycles as mature fibers will quickly respond and re-align toward the direction of loading, even in response to very small loads. Additionally previous work has demonstrated throughout early postnatal development, tendons have an immature collagen fibril architecture and network,[4,6,63] therefore we hypothesize that in early development, postnatal tendons will not respond to mechanical load as quickly as mature

tendons, therefore the largest shift in re-alignment will occur at the beginning of the toe-region. Re-alignment may also be present at the end of the extended 20 cycle preconditioning protocol as fibers are given longer to respond and re-orient in the direction of loading.

Hypothesis 2c: Alignment differences between the midsubstance and insertion site will be detectable at late postnatal development and at maturity.

This hypothesis is based on previous histological and biochemical data, which demonstrated that the mouse supraspinatus insertion site was not fully formed until 21 days postnatal,[18] suggesting that it has begun to experience and respond to complex loads. It is expected that alignment differences between the midsubstance and insertion sites will be detectable at 28 days and 90 days postnatal.

Specific Aim 3: To determine relationships between mechanical response and structure through a linear correlation.

Hypothesis 3a: Locally, a more organized collagen distribution will significantly predict stronger linear modulus.

This hypothesis is based on previous work which identified a negative correlation between collagen fiber alignment and linear modulus in a human SST tendon.[25]

In summary, examining collagen fiber re-alignment and fiber uncrimping during loading throughout development provides an exciting opportunity to determine if tendon response to preconditioning is dependent on underlying structure and number of cycles. Additionally, this dissertation will determine if fiber uncrimping is limited to the toe-region regardless of tendon age. A better understating of how tendons respond to

mechanical load will aid the interpretation and understanding of mechanical properties obtained from mechanical tests and how they relate to physiologic conditions. Additionally, this work will further elucidate tendon structure-function relationship throughout postnatal development.

D. Chapter Overviews

This thesis consists of 7 chapters. Chapter 1 is an introduction and provides the necessary background information for the studies described in the subsequent chapters. Chapter 1 also includes a summary of tendon composition, structure and mechanics. Additionally, it provides background information on the significance and measurement techniques to investigate collagen fiber re-alignment and fiber uncrimping. It also provides background on the model system chosen to investigate collagen fiber re-alignment and uncrimping in tendon, the developmental mouse supraspinatus tendon. A background in collagen fibrillogenesis throughout postnatal development is described. In addition, background on the development of the mouse supraspinatus tendon-to-bone insertion site is given. All of this information serves as a foundational framework for the chapters that follow.

Chapter 2 presents work that provides the foundation for the development of the Aims and Hypotheses of this thesis. Chapter 2 utilized a mature rat SST model to examine collagen fiber re-alignment throughout a mechanical testing protocol. Collagen fiber re-alignment was found to occur primarily during preconditioning and the ramp-to-failure in a mature rat model. The inhomogeneity of the SST was also examined by comparing local collagen fiber distributions, cross-sectional area and mechanical

properties of the midsubstance location of the SST to the tendon-to-bone insertion site location.

Chapter 3 addresses Aims 1, 2 and 3 by evaluating collagen fiber re-alignment, mechanics, and subsequent correlations between alignment and mechanics in a mature mouse SST model. This Chapter utilizes a typical uniaxial mechanical testing device that has been integrated with a polarized light set-up to simultaneously take images for collagen fiber alignment analysis while mechanically testing. Collagen fiber distributions will be evaluated throughout the mechanical test and mechanical properties and cross-sectional area will be measured at the insertion site and midsubstance locations. The information presented in this chapter will serve as a baseline for comparisons with the postnatal development time points examined in Chapter 5.

Chapter 4 addresses Aim 2 by presenting an established semi-quantitative method and new quantitative method for evaluating collagen fiber crimp frequency throughout mechanical testing in a mature mouse SST model. This was accomplished by flash freezing tendon samples immediately following the prescribed mechanical loading protocol while the tendons were still loaded in the mechanical testing device to prevent tendon relaxation or recovery of crimp behavior during histology preparation. Details on the development of the new software to quantify collagen fiber crimp will be provided in this chapter. Chapter 4 presents baseline data on changes in collagen fiber crimp frequency throughout the mechanical test, in the presence of 3 different preconditioning protocols as well as local comparisons between the insertion site and midsubstance locations in a mature mouse SST model. In addition to introducing the quantitative

software, the information presented in this chapter will serve as a baseline for the comparisons of crimp frequency and crimp behavior throughout postnatal development, which will examined in Chapter 6.

Chapter 5 addresses Aims 1, 2 and 3 by evaluating collagen fiber re-alignment behavior throughout the mechanical test as well as mechanical properties and correlations between alignment and mechanics throughout postnatal development. This was accomplished using similar methods as described in Chapter 3. Resolution of the collagen fiber alignment analysis was modified for time points during early development to ensure a consistent resolution across all time points for comparisons between developmental ages. Data from Chapter 3 is used to draw comparisons across developmental ages and to identify correlations between structure and function throughout postnatal development.

Chapter 6 addresses Aim 2 and utilizes the techniques described in Chapter 4 to examine local collagen fiber crimp frequency in a developmental mouse SST tendon throughout the mechanical testing protocol and in response to 3 preconditioning regimes. Data from Chapter 4 is used to draw comparisons between crimp frequency with increasing developmental age and crimp behavior throughout the mechanical test. Finally, in Chapter 7 overall conclusions will be drawn from the studies described in Chapters 2-6. Potential future directions of this research will also be discussed.

E. References

1. Ansorge HL, Adams S, Birk DE, Soslowsky LJ: Mechanical, compositional, and structural properties of the post-natal mouse Achilles tendon. **Ann Biomed Eng 39:**1904-1913
2. Ansorge HL, Meng X, Zhang G, Veit G, Sun M, Klement JF, et al: Type XIV Collagen Regulates Fibrillogenesis: PREMATURE COLLAGEN FIBRIL GROWTH AND TISSUE DYSFUNCTION IN NULL MICE. **J Biol Chem 284:**8427-8438, 2009
3. Benjamin M, Ralphs JR: Fibrocartilage in tendons and ligaments--an adaptation to compressive load. **J Anat 193 (Pt 4):**481-494, 1998
4. Birk DE, Nurminskaya MV, Zycband EI: Collagen fibrillogenesis in situ: fibril segments undergo post-depositional modifications resulting in linear and lateral growth during matrix development. **Dev Dyn 202:**229-243, 1995
5. Birk DE, Southern JF, Zycband EI, Fallon JT, Trelstad RL: Collagen fibril bundles: a branching assembly unit in tendon morphogenesis. **Development 107:**437-443, 1989
6. Birk DE, Zycband EI, Woodruff S, Winkelmann DA, Trelstad RL: Collagen fibrillogenesis in situ: fibril segments become long fibrils as the developing tendon matures. **Dev Dyn 208:**291-298, 1997
7. Boorman RS, Norman T, Matsen FA, 3rd, Clark JM: Using a freeze substitution fixation technique and histological crimp analysis for characterizing regions of

strain in ligaments loaded in situ. **J Orthop Res 24:**793-799, 2006

8. Couppe C, Hansen P, Kongsgaard M, Kovanen V, Suetta C, Aagaard P, et al: Mechanical properties and collagen cross-linking of the patellar tendon in old and young men. **J Appl Physiol 107:**880-886, 2009

9. Derwin KA, Soslowsky LJ: A quantitative investigation of structure-function relationships in a tendon fascicle model. **J Biomech Eng 121:**598-604, 1999

10. Diamant J, Keller A, Baer E, Litt M, Arridge RG: Collagen; ultrastructure and its relation to mechanical properties as a function of ageing. **Proc R Soc Lond B Biol Sci 180:**293-315, 1972

11. Dressler MR, Butler DL, Wenstrup R, Awad HA, Smith F, Boivin GP: A potential mechanism for age-related declines in patellar tendon biomechanics. **J Orthop Res 20:**1315-1322, 2002

12. Ezura Y, Chakravarti S, Oldberg A, Chervoneva I, Birk DE: Differential expression of lumican and fibromodulin regulate collagen fibrillogenesis in developing mouse tendons. **J Cell Biol 151:**779-788, 2000

13. Fox AJS, Bedi A, Rodeo SA: The Basic Science of Articular Cartilage: Structure, Composition and Function. **Sports Health: A Multidisciplinary Approach. 1:**461-468, 2009

14. Franchi M, Fini M, Quaranta M, De Pasquale V, Raspanti M, Giavaresi G, et al: Crimp morphology in relaxed and stretched rat Achilles tendon. **J Anat 210:**1-7, 2007

15. Franchi M, Ottani V, Stagni R, Ruggeri A: Tendon and ligament fibrillar crimps

give rise to left-handed helices of collagen fibrils in both planar and helical crimps. **J Anat 216:**301-309

16. Franchi M, Quaranta M, Macciocca M, Leonardi L, Ottani V, Bianchini P, et al: Collagen fibre arrangement and functional crimping pattern of the medial collateral ligament in the rat knee. **Knee Surg Sports Traumatol Arthrosc 18:**1671-1678

17. Franchi M, Raspanti M, Dell'Orbo C, Quaranta M, De Pasquale V, Ottani V, et al: Different crimp patterns in collagen fibrils relate to the subfibrillar arrangement. **Connect Tissue Res 49:**85-91, 2008

18. Galatz L, Rothermich S, VanderPloeg K, Petersen B, Sandell L, Thomopoulos S: Development of the supraspinatus tendon-to-bone insertion: localized expression of extracellular matrix and growth factor genes. **J Orthop Res 25:**1621-1628, 2007

19. Gathercole LJ, Keller A: Crimp morphology in the fibre-forming collagens. **Matrix 11:**214-234, 1991

20. Hansen KA, Weiss JA, Barton JK: Recruitment of tendon crimp with applied tensile strain. **J Biomech Eng 124:**72-77, 2002

21. Herchenhan A, Kalson NS, Holmes DF, Hill P, Kadler KE, Margetts L: Tenocyte contraction induces crimp formation in tendon-like tissue. **Biomech Model Mechanobiol**

22. Hurschler C, Provenzano PP, Vanderby R, Jr.: Scanning electron microscopic characterization of healing and normal rat ligament microstructure under slack

and loaded conditions. **Connect Tissue Res 44:**59-68, 2003

23. Kalamajski S, Oldberg A: The role of small leucine-rich proteoglycans in collagen fibrillogenesis. **Matrix Biol 29:**248-253

24. Lake SP, Ansorge HL, Soslowsky LJ: Animal models of tendinopathy. **Disabil Rehabil 30:**1530-1541, 2008

25. Lake SP, Miller KS, Elliott DM, Soslowsky LJ: Effect of fiber distribution and realignment on the nonlinear and inhomogeneous mechanical properties of human supraspinatus tendon under longitudinal tensile loading. **J Orthop Res 27:**1596-1602, 2009

26. Lake SP, Miller KS, Elliott DM, Soslowsky LJ: Tensile properties and fiber alignment of human supraspinatus tendon in the transverse direction demonstrate inhomogeneity, nonlinearity, and regional isotropy. **J Biomech 43:**727-732

27. Lechner BE, Lim JH, Mercado ML, Fallon JR: Developmental regulation of biglycan expression in muscle and tendon. **Muscle Nerve 34:**347-355, 2006

28. Lin TW, Cardenas L, Soslowsky LJ: Biomechanics of tendon injury and repair. **J Biomech 37:**865-877, 2004

29. Masic A, Bertinetti L, Schuetz R, Galvis L, Timofeeva N, Dunlop JW, et al: Observations of multiscale, stress-induced changes of collagen orientation in tendon by polarized Raman spectroscopy. **Biomacromolecules 12:**3989-3996

30. Miller KS, Edelstein, L., Connizzo, B. K., and Soslowsky, L. J... Effect of Preconditioning and Stress Relaxation on Local Collagen Fiber Re-Alignment: Inhomogeneous Properties of Rat Supraspinatus Tendon. **Journal of**

Biomechanical Engineering In press, 2012

31. Moore MJ, De Beaux A: A quantitative ultrastructural study of rat tendon from birth to maturity. **J Anat 153:**163-169, 1987

32. Nakagawa Y, Majima T, Nagashima K: Effect of ageing on ultrastructure of slow and fast skeletal muscle tendon in rabbit Achilles tendons. **Acta Physiol Scand 152:**307-313, 1994

33. Oryan A, Shoushtari AH: Histology and ultrastructure of the developing superficial digital flexor tendon in rabbits. **Anat Histol Embryol 37:**134-140, 2008

34. Parry DA, Craig AS, Barnes GR: Tendon and ligament from the horse: an ultrastructural study of collagen fibrils and elastic fibres as a function of age. **Proc R Soc Lond B Biol Sci 203:**293-303, 1978

35. Quinn KP, Bauman JA, Crosby ND, Winkelstein BA: Anomalous fiber realignment during tensile loading of the rat facet capsular ligament identifies mechanically induced damage and physiological dysfunction. **J Biomech 43:**1870-1875

36. Quinn KP, Winkelstein BA: Altered collagen fiber kinematics define the onset of localized ligament damage during loading. **J Appl Physiol 105:**1881-1888, 2008

37. Quinn KP, Winkelstein BA: Preconditioning is correlated with altered collagen fiber alignment in ligament. **J Biomech Eng 133:**064506

38. Rigby BJ: Effect of Cyclic Extension on the Physical Properties of Tendon Collagen and Its Possible Relation to Biological Ageing of Collagen. **Nature**

202:1072-1074, 1964

39. Rigby BJ, Hirai N, Spikes JD, Eyring H: The Mechanical Properties of Rat Tail Tendon. **J Gen Physiol 43:**265-283, 1959

40. Robinson PS, Huang TF, Kazam E, Iozzo RV, Birk DE, Soslowsky LJ: Influence of decorin and biglycan on mechanical properties of multiple tendons in knockout mice. **J Biomech Eng 127:**181-185, 2005

41. Sacks MS, Chuong CJ: Characterization of collagen fiber architecture in the canine diaphragmatic central tendon. **J Biomech Eng 114:**183-190, 1992

42. Scott JE, Hughes EW: Proteoglycan-collagen relationships in developing chick and bovine tendons. Influence of the physiological environment. **Connect Tissue Res 14:**267-278, 1986

43. Scott JE, Orford CR, Hughes EW: Proteoglycan-collagen arrangements in developing rat tail tendon. An electron microscopical and biochemical investigation. **Biochem J 195:**573-581, 1981

44. Screen HR, Lee DA, Bader DL, Shelton JC: An investigation into the effects of the hierarchical structure of tendon fascicles on micromechanical properties. **Proc Inst Mech Eng H 218:**109-119, 2004

45. Shah JS, Palacios E, Palacios L: Development of crimp morphology and cellular changes in chick tendons. **Dev Biol 94:**499-504, 1982

46. Sharma P, Maffulli N: Tendon injury and tendinopathy: healing and repair. **J Bone Joint Surg Am 87:**187-202, 2005

47. Silver FH, Kato YP, Ohno M, Wasserman AJ: Analysis of mammalian connective

tissue: relationship between hierarchical structures and mechanical properties. **J Long Term Eff Med Implants 2:**165-198, 1992

48. Sverdlik A, Lanir Y: Time-dependent mechanical behavior of sheep digital tendons, including the effects of preconditioning. **J Biomech Eng 124:**78-84, 2002

49. Teramoto A, Luo ZP: Temporary tendon strengthening by preconditioning. **Clin Biomech (Bristol, Avon) 23:**619-622, 2008

50. Thierry L, Geiser AS, Hansen A, Tesche F, Herken R, Miosge N: Collagen types XII and XIV are present in basement membrane zones during human embryonic development. **J Mol Histol 35:**803-810, 2004

51. Thomas S, Miller, KS., Soslowsky, LJ.: The Upper Band of the Subscapularis Tendon in the Rat has Altered Mechanical and Histologic Properties. **Journal of Shoulder and Elbow Surgery**, 2012

52. Thomopoulos S, Hattersley G, Rosen V, Mertens M, Galatz L, Williams GR, et al: The localized expression of extracellular matrix components in healing tendon insertion sites: an in situ hybridization study. **J Orthop Res 20:**454-463, 2002

53. Thomopoulos S, Kim HM, Rothermich SY, Biederstadt C, Das R, Galatz LM: Decreased muscle loading delays maturation of the tendon enthesis during postnatal development. **J Orthop Res 25:**1154-1163, 2007

54. Thomopoulos S, Williams GR, Gimbel JA, Favata M, Soslowsky LJ: Variation of biomechanical, structural, and compositional properties along the tendon to bone insertion site. **J Orthop Res 21:**413-419, 2003

55. Thornton GM, Boorman RS, Shrive NG, Frank CB: Medial collateral ligament autografts have increased creep response for at least two years and early immobilization makes this worse. **J Orthop Res 20:**346-352, 2002

56. Tower TT, Neidert MR, Tranquillo RT: Fiber alignment imaging during mechanical testing of soft tissues. **Ann Biomed Eng 30:**1221-1233, 2002

57. Tower TT, Tranquillo RT: Alignment maps of tissues: I. Microscopic elliptical polarimetry. **Biophys J 81:**2954-2963, 2001

58. Viidik A: Simultaneous mechanical and light microscopic studies of collagen fibers. **Z Anat Entwicklungsgesch 136:**204-212, 1972

59. Viidik A: Tensile strength properties of Achilles tendon systems in trained and untrained rabbits. **Acta Orthop Scand 40:**261-272, 1969

60. Watanabe M, Nojima M, Shibata T, Hamada M: Maturation-related biochemical changes in swine anterior cruciate ligament and tibialis posterior tendon. **J Orthop Res 12:**672-682, 1994

61. Woo SL, Debski RE, Zeminski J, Abramowitch SD, Saw SS, Fenwick JA: Injury and repair of ligaments and tendons. **Annu Rev Biomed Eng 2:**83-118, 2000

62. Woo SL, Johnson GA, Smith BA: Mathematical modeling of ligaments and tendons. **J Biomech Eng 115:**468-473, 1993

63. Zhang G, Young BB, Ezura Y, Favata M, Soslowsky LJ, Chakravarti S, et al: Development of tendon structure and function: regulation of collagen fibrillogenesis. **J Musculoskelet Neuronal Interact 5:**5-21, 2005

Chapter 2. The Effect of Preconditioning and Stress Relaxation on Local Collagen Fiber Re-Alignment: Inhomogeneous Properties of the Rat Supraspinatus Tendon

A. Introduction

This chapter will investigate the effects of preconditioning and stress relaxation on local collagen fiber re-alignment in addition to local mechanical properties in a rat supraspinatus tendon model.

Cyclic preconditioning is a commonly accepted initial component of most tendon mechanical testing protocols. Preconditioning provides tendons with a consistent "history" and stress-strain results become repeatable, allowing for rigorous evaluation and comparison. Protocols frequently involve the repeated stretching of a sample to a sub-failure load in order to produce a repeatable mechanical response.[5,10,15,27] The internal structure of tendon changes in response to each loading cycle. After applying repeated cycles, a steady-state is reached at which no further changes will occur unless the cycling routine is changed.[10]

While it is widely accepted that preconditioning is important, changes that occur during preconditioning are not well understood. Micro-structural alterations, such as re-arrangement of collagen fibers, is one proposed mechanism of preconditioning.[18,23,24] Recently, a strong correlation between changes in collagen fiber alignment and changes in the mechanical response of ligament during cyclic tensile preconditioning has been

reported.[18] The correlation found between reduced force response during preconditioning and change in fiber alignment after preconditioning suggests that viscoelastic effects and microstructural reorganization both contribute to the time-and-history dependence of mechanical properties.[18] However, the dependence of collagen fiber re-alignment during preconditioning on tendon location has not yet been examined. Additionally, collagen fiber re-alignment during stress relaxation or a tensile ramp-to-failure following preconditioning has not been examined in tendon.

Additionally, recent studies have shown that collagen fiber re-alignment varies by tendon location.[13,14] The tendon-to-bone insertion site of the supraspinatus tendon experiences higher strains and has been shown to have a more disorganized fiber distribution compared to the tendon midsubstance.[13,21,25,32] Therefore, the objective of this study was to locally measure collagen fiber re-alignment and corresponding mechanical properties throughout tensile mechanical testing, in order to address mechanisms of preconditioning and stress relaxation, as well as tissue nonlinearity and inhomogeneity in the rat supraspinatus tendon model. We hypothesized that fiber re-alignment will be greatest in the toe-region of the ramp-to-failure test, but that a change in circular variance will also occur during preconditioning, despite the small loads used in the mechanical testing protocol. Additionally, we hypothesize that the collagen fiber distribution will become more disorganized throughout the stress relaxation test and that the mechanical properties and initial collagen fiber alignment will be greater in the midsubstance location of the tendon compared to the tendon-to-bone insertion site.

B. Methods

B1. Sample Preparation

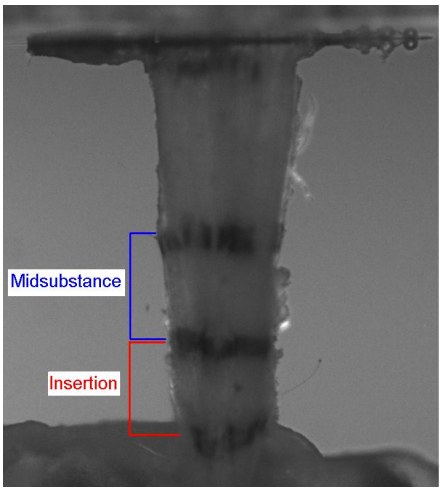

Figure 2.1 Stain lines denoted tendon insertion site and midsubstance locations for alignment and optical strain analysis.

This study was approved by the University of Pennsylvania IACUC. Twenty-two Sprague-Dawley rats (400-450g) were sacrificed and supraspinatus tendons (SST) were removed for mechanical testing. All soft tissue was removed from around the tendon, leaving the supraspinatus muscle-tendon unit attached to the humerus. The supraspinatus muscle was removed. Fine dissection of the tendon was performed under a dissection microscope to ensure that all remaining fascia was removed from the tendon. Verhoeff stain lines were placed on the tendons denoting the insertion site and tendon midsubstance for optical strain analysis, to denote regions for alignment analysis and to define the gauge section. The first stain line was placed at the tendon-to-bone insertion site on the humerus as described previously,[17] and the remaining stain lines were placed at 2, 4, 7 and 9 mm from the insertion site (Fig 2.1). Cross-sectional area at each location was measured using a noncontact laser device with a resolution of 2 μm.[9] The humerus was embedded in a holding fixture with the use of polymethylmethacrylate (PMMA). After the PMMA had set, the humeral head was sanded down to prevent the bone from impeding light from passing through the tendon insertion site for polarized light analysis. A small pilot study confirmed that failure properties were not altered after sanding down the humeral head. A second coating of PMMA was applied to prevent failure at the growth plate. The holding fixture was

inserted into a custom testing fixture. The proximal end of the tendon was glued between two pieces of sandpaper and placed in custom grips for tensile testing. All samples had an initial gauge length of 7 mm and had an average width and thickness of 3 mm x 0.4 mm respectively.

B2. Mechanical Testing and Data Analysis

Samples were placed in a 37º phosphate buffered saline (PBS) bath and loaded in a tensile testing system (Instron, Norwood, MA) integrated with a polarized light setup, consisting of a linear backlight (Dolan-Jenner, Boxborough, MA), 90°-offset rotating polarizer sheets (Edmund Optics, Barrington, NJ) on either side of the test sample, and a digital camera (Basler, Exton, PA) (Fig 2.2).[13] Prior to testing, the encoder embedded in the stepper motor (Fig 2.2) (Lin Engineering, Santa Clara, CA) that rotates the polarizer sheets was initialized by resetting the encoder value with the polarizer sheets set at a position corresponding to 0º of angular rotation. A small pilot study was performed to determine the position corresponding to 0º. This study evaluated several reference points by overlaying the quiver plot outputs from the alignment analysis onto the images of tendon obtained from the optical analysis. At the position corresponding to 0º of angular rotation, the quiver

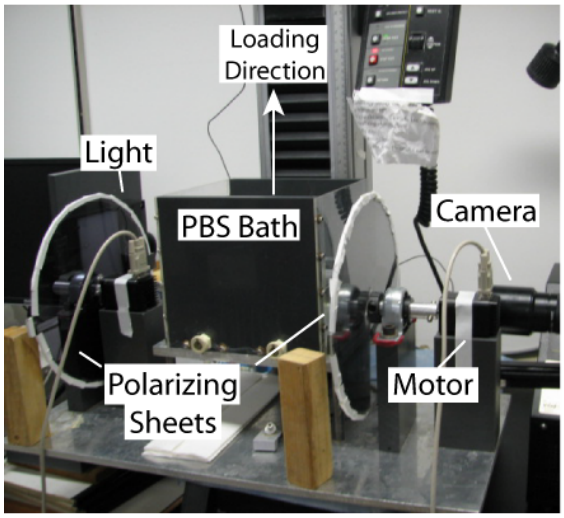

Figure 2.2 Angled side-view of the tendon tensile testing setup showing polarized light and imaging system: light source, rotating cross-polarized sheets, stepper motors, and camera.

plots were found to align with native tendon fiber direction. To determine biomechanical properties, tensile testing along the long axis of the tendon was performed using a 100 N load cell with a resolution of 0.001N for all tests.

This study utilizes an established uniaxial mechanical testing protocol for rat rotator cuff tendon mechanical testing to examine and compare tendon mechanical properties at specific locations and in response to different treatments.[16] At several points throughout the mechanical testing protocol, sets of 14 images were acquired as the polarizers rotated through a 125° range for measurement of fiber alignment during loading as previously described.[14] Initially, samples were preloaded to a nominal load (0.01 N) and then preconditioned under load control for 10 cycles between 0.1 N and 0.5 N. Preconditioning cycles were performed at an average frequency of 0.22 ± 0.03 Hertz and cycled between 0.98 ± 0.06 percent and 1.13 ± 0.03 percent grip-to-grip strain. Preconditioning is performed before the stress relaxation and ramp-to-failure tests to provide all samples with a consistent loading history to allow for more consistent and simplified mathematical interpretation of mechanical properties. The preconditioning loads used in this study were selected to ensure that the tendons

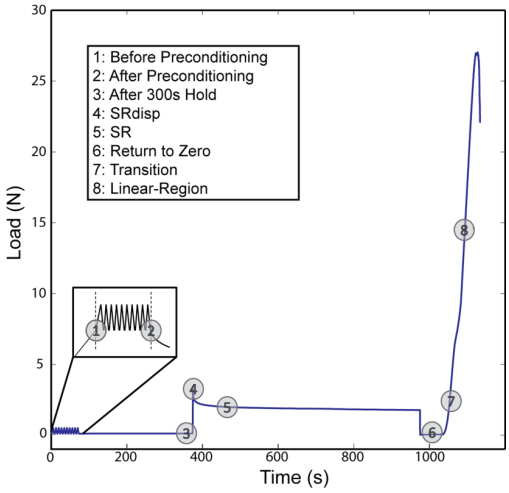

Figure 2.3 Load-time graph of a representative sample undergoing the mechanical testing protocol. 14-image alignment maps were taken for alignment analysis at 1) before preconditioning, 2) after preconditioning, 3) after preconditioning following a 300 second hold, 4) after the SR displacement, 5) during SR, 6) after SR following a return to zero displacement, 7) at the transition strain, and 8) at a point in the linear-region.

would not be damaged during preconditioning and were selected based on pilot studies with intact and injured and repaired rat SSTs. The loads are low to enable the preconditioning protocol to be applied for both injured and intact tendon to compare their mechanical properties across studies. One 14 image alignment map was acquired both before preconditioning (but after the preload was administered) and immediately following the 10^{th} cycle of preconditioning to determine if the spread of the collagen fiber distribution changed during preconditioning (that collagen fiber re-alignment occurred) (Fig 2.3; Points 1 & 2 respectively).

After returning to the lower load limit of 0.1N following the 10^{th} cycle of preconditioning, a 300 second hold was applied to allow the tissue to equilibrate before the stress relaxation test. In addition to the alignment map taken immediately following the 10 preconditioning cycles, an additional alignment map was acquired at the end of the 300 second hold to determine if collagen fiber alignment changed over the 300 second time course (Fig 2.3; Point 3). Next, to measure viscoelastic properties, samples were then subjected to a relative ramp of a 0.42 mm grip-to-grip displacement at a rate of 0.35mm/second, followed by a 600 second hold to reach an equilibrium load. A series of alignment maps was taken every 5 seconds during the stress relaxation test to determine if the initial 0.42 mm grip-to-grip displacement as well as the subsequent 600 second hold affected the collagen fiber distribution.

Immediately following the 600 second hold, samples were returned to zero displacement by being displaced 0.42 mm at a rate of -0.35mm/second. In order to measure toe-region properties during the ramp-to-failure, samples were returned to zero-

displacement via displacement control, therefore some samples maintained a nominal load during the 60 second hold. Pilot studies demonstrated that a return to zero displacement was more consistent and repeatable than a return to zero load. An additional alignment map was taken following the return to zero displacement (Fig 2.3; Point 6). Following the 60 second hold, a ramp to failure was applied at a rate of 0.21mm/second. Alignment map images were taken every 5 seconds during the ramp-to-failure. Images were also obtained every 5 seconds for optical strain analysis during the ramp-to-failure.

A custom Matlab program (Matlab, Natick, MA) was used to optically track stain lines during the ramp-to-failure as previously described.[6] Strain at the insertion site was determined by optically tracking the displacements between stain line 1 and 2 (located 2 mm away from the tendon-to-bone insertion site) (Fig 2.1). Regions of PMMA directly adjacent to the tendon-to-bone insertion site were selected for stain line 1. Strain at the midsubstance location was determined by optically tracking the displacement between stain line 2 and 3 (2 and 4 mm away from the tendon-to-bone insertion site respectively) (Fig 2.1). A small pilot study was performed comparing manual tracking of the stain lines to computer automated tracking via texture correlation. The results from this study confirmed that the fluctuations in image intensity throughout the ramp-to-failure due to tendon collagen fiber re-alignment did not affect the automated displacement tracking.

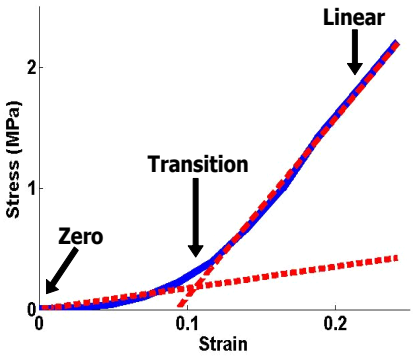

Figure 2.4 Example of a stress-strain curve with the bilinear curve fit and zero, transition and linear-strains.

Stress was calculated as force divided by initial area. A pilot study examined the best model to fit the load-to-failure data and determined the most accurate way to compare the optical strains measured to fiber re-alignment. A structural fiber recruitment model,[16] an exponential model, and a bilinear fit model were all used on a subset of data. The pilot study determined that the bilinear fit model provided the most consistent and accurate representation of the data and therefore was implemented for this study (Fig 2.4). A bilinear curve fit was applied to the stress-strain data to quantify transition stress, transition strain and the moduli in the toe- and linear-regions from the stress-strain data. Following the bilinear fit analysis, points representing the toe- and linear-regions of the stress-strain curve were selected to examine how the collagen fiber distributions changed during the toe- and linear-regions of the stress-strain curve. Alignment maps from the transition strain (calculated from the bilinear fit) and a point in the linear-region were selected for fiber alignment analysis.

Fiber alignment was calculated from the image sets as described.[13] Briefly, images of the tendon surface were divided into rectangular areas (30-wide x 30-long = 900 areas). Pixel intensities were summed by area per image and plotted against angle of polarizer rotation. A sine wave was fitted to the intensity-angle data to determine the angle corresponding to minimum pixel intensity, which represents the average direction of the area's collagen fiber alignment. A limitation of the crossed polarizer method is that fiber angles can only be calculated within a 90º range (±45º to the predominant fiber direction) rather than the entire possible range of orientations. To overcome this limitation, fibers were assumed to re-align in the direction of loading as previously described.[13] Circular

variance (VAR), a measure of the distribution of collagen fiber alignment (from eqn. 26.17 Zar et. al.), was calculated at several points throughout the mechanical test.[2,33] VAR was calculated for fiber distributions before preconditioning (BP), immediately after preconditioning (AP), following a 300 second hold before stress relaxation (300h), immediately after the SR displacement (SRdisp), at the end of the SR test (SR), after the SR test following a return to zero displacement (zero), at a point representing the toe-

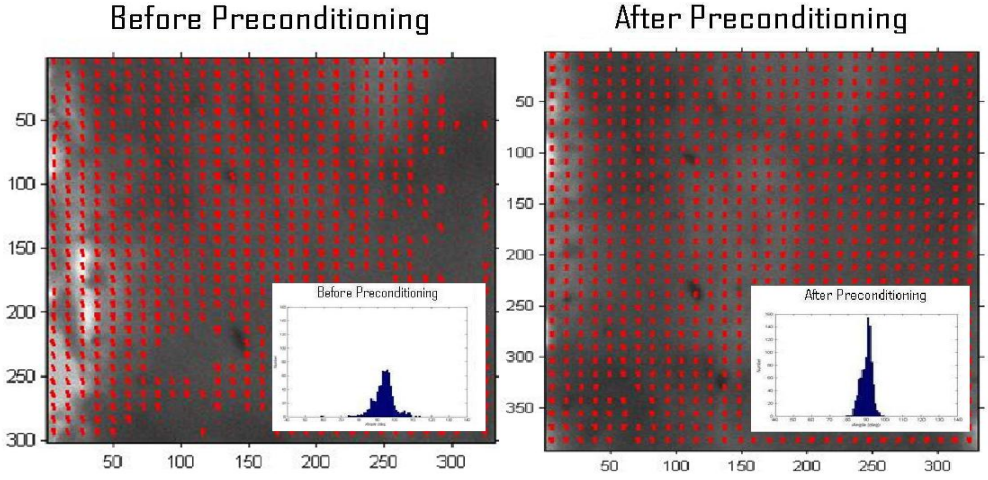

Figure 2.5 Sample alignment maps and histograms before and after preconditioning showing an increase in alignment (Decrease in VAR).

region of the stress-strain curve, and at a point representing the linear-region of the stress-strain curve (Fig 2.3). Fiber re-alignment throughout the mechanical test was evaluated by comparing VAR values at two mechanical testing points. Collagen fiber re-alignment was said to occur during that region of the mechanical test if the difference of fiber distributions was found to be statistically significant. Fiber re-alignment during preconditioning was evaluated by comparing VAR values before and after preconditioning. Similar methods were used to determine fiber re-alignment during the 300 second hold following preconditioning, during the SR, after a return to zero

displacement following SR, as well as in the toe- and linear-regions of the stress-strain curve. Mean angle values were calculated for collagen fiber distributions at each location for all mechanical test regions examined.

B3. Statistical Analysis

Shapiro-Wilk tests indicated non-normally distributed data for VAR values. As a result, non-parametric statistical tests were used for evaluating fiber re-alignment. Changes in fiber alignment (Friedman test) were compared for tendon location (midsubstance vs. insertion) and for the mechanical test region (preconditioning, stress-relaxation, toe- and linear-region). Bonferroni corrections were used for multiple comparisons to remain conservative in our data interpretation and significance ($p<0.0125 = 0.05/4$) was determined using Wilcoxon signed-rank post-hoc tests. VAR data is presented as median ± interquartile range and statistics are paired comparisons. Mechanical parameters were evaluated with parametric statistics. Changes in parameters were compared for tendon location (midsubstance vs. insertion). Data is presented as mean ± standard deviation.

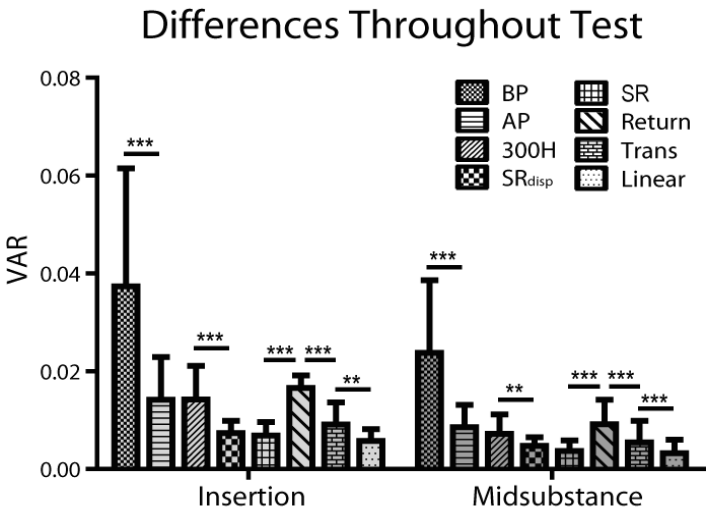

Figure 2.6 Circular variance (VAR) values demonstrate increasing alignment (Decreased VAR) during preconditioning, the displacement for SR and in the toe- and linear-regions for midsubstance and insertion site. A decrease in alignment (Increased VAR) was noted following the return to zero displacement for both locations. (sig=*$p<0.0125$, ** $p<0.0025$, ***$p<0.00025$).

C. Results

VAR values and mean angle were examined at several stages of the mechanical test. Similar results were found for re-alignment behavior and mean angle changes at each location. During preconditioning, VAR values demonstrate significant re-alignment under tension (decreasing VAR) (Figs 2.5 & 2.6). Additionally, the mean angle shifted an average of 4º in the midsubstance and 5.5º at the insertion site location during preconditioning. No significant changes in re-alignment were found during the 300 second hold at either location (Fig 2.6). After the initial displacement was performed for the SR test, a decrease in VAR (increase in organization) was found at both locations (Fig 2.6). However, no significant changes in re-alignment were found throughout the 600 second stress relaxation test for either location (Fig 2.6). Following the stress relaxation test, the sample was returned to zero displacement and a more disorganized collagen fiber distribution was found at both locations (Fig 2.6). Finally, the collagen fiber distribution became more organized (decrease in VAR) throughout the ramp to failure. Significant differences in collagen fiber distributions were found at both the toe- and linear-regions

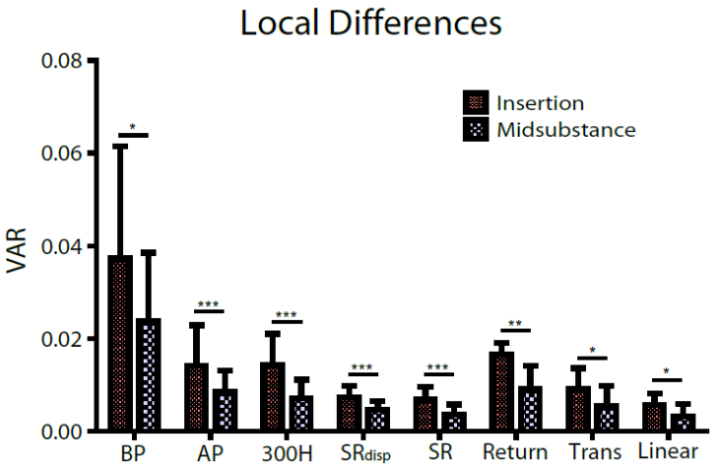

Figure 2.7 Circular variance (VAR) values demonstrate inhomogeneous fiber distributions throughout all regions of the mechanical testing protocol. (*p<0.0125, ** p<0.0025, ***p<0.00025=sig.)

at both locations (Fig 2.6).

Locally, VAR values were significantly different (less organized at the insertion site compared to the midsubstance) at all mechanical testing points (Fig 2.7). Linear-region moduli were significantly greater in the midsubstance than in the insertion site (1.6x greater, Fig 2.8) and a trend was present for the toe-region moduli (Fig 2.9). Additionally, moduli values demonstrated that both the insertion site and midsubstance locations were highly nonlinear (~10x linear/toe-region ratio). Transition strain (determined from the stress-strain data) was higher for the insertion site than for the midsubstance location (Fig 2.10). Cross-sectional area was greater at the insertion site compared to the midsubstance location (Fig 2.11).

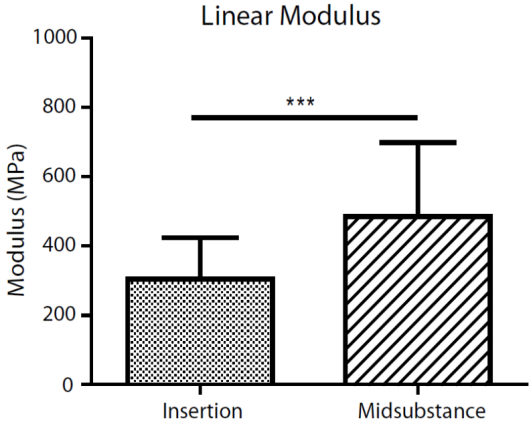

Figure 2.8 Linear modulus values obtained from the linear-region of the stress-strain curve. Insertion site linear modulus is lower than the midsubstance indicating inhomogeneous mechanical properties of the rat SST. (***p<0.00025=sig.)

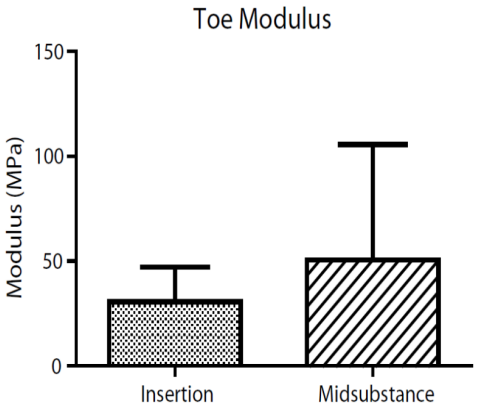

Figure 2.9 Toe modulus values obtained from the toe-region of the stress-strain curve. Insertion site linear modulus is lower than the midsubstance indicating inhomogeneous mechanical properties of the rat SST.

D. Discussion

This study found a correlation between cyclic preconditioning and early re-alignment of collagen fibers regardless of location. Contradictory to our hypothesis, the largest amount of collagen fiber re-alignment

occurred during preconditioning (Figs 2.5, 2.6, 2.12 and 2.13). Additionally, the largest shift in mean angle also occurred during preconditioning. While previous work has noted some collagen fiber re-alignment during preconditioning, the large shift in alignment seen at such small loads in the present study was surprising.[27,29] These findings suggest that the re-alignment of collagen fibers may be an underlying mechanism of preconditioning as well as a potential explanation for the increase in tendon strength seen after preconditioning in highly aligned tendons. This result supports previous studies examining the post-preconditioning mechanical response of patellar and Achilles tendons.[19,24] Preconditioning has been postulated to be associated with a change in the stress-free configuration, a shift of the toe-region of the stress-strain curve to higher strains and a decrease in crimp period in a recent study in rat tail tendon fascicles.[11] The midsubstance location of the rat SST consists mainly of parallel oriented fibers that can be gradually re-oriented toward the direction of loading during preconditioning cycles. Additionally, a vector correlation algorithm has recently been used in ligament to detect microstructural changes in collagen fiber alignment during preconditioning and found a strong correlation between collagen fiber rotation and changes in force.[18] The mean angle shift towards 90º found in the present study during preconditioning supports the concept that fibers re-align in the direction of loading and could account for the changes in mechanical response noted post-preconditioning.[3,20,22,27] Additionally, no changes in alignment were found following the 300 second hold applied post-preconditioning (Figs 2.6, 2.12, 2.13). These findings indicate that holding the tendon at a constant load for 300 or less seconds may not signal a decrease in collagen fiber alignment with short

recovery times. It is possible that the response of collagen fibers depends not only on the amount of relaxation time, but also the initial displacement and loading history. While it is known that the stiffness of the tissue is dependent on the tendon loading history,[29] the effect of loading history on collagen fiber re-alignment and how it may influence the ability of fibers to return to their initial alignment is currently unknown. After the 300 second hold was performed, a 0.42 mm grip-to-grip displacement was performed. Following the displacement, VAR values decreased, demonstrating an increase in collagen fiber organization at both locations.

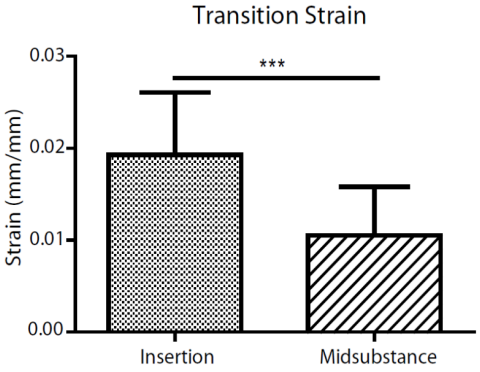

Figure 2.10 Local optical strain values required to reach the transition (intersection of the toe- and linear-regions of the stress-strain curve) is shown for both locations. A higher local, optical strain is necessary for the insertion site of the tendon to transition to the linear-region than for the tendon midsubstance. (***p<0.00025=sig.)

Next, a 600 second stress relaxation test was performed. Contrary to our hypothesis, no change in collagen fiber re-alignment was found during the stress relaxation test (Figs 2.6, 2.12, 2.13). Interestingly, crimp analysis in rabbit medial collateral ligament revealed no changes in collagen fiber crimp behavior before and after stress relaxation tests, while fibers were recruited during creep tests,[26] supporting the idea that the microstructural

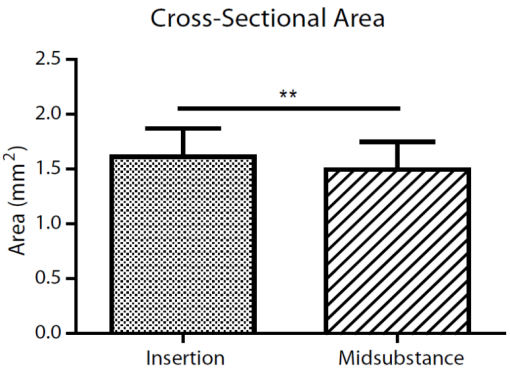

Figure 2.11 Local cross-sectional area is shown for both locations. A higher cross-sectional area was found at the insertion site compared to the midsubstance location. (**p<0.0025=sig.)

mechanisms of creep and stress relaxation are different.[10] This finding together with the lack of collagen fiber re-alignment during stress relaxation in the present study suggests that a shift in the structural organization of collagen fibers may not be responsible for stress relaxation.

Following the stress relaxation test, samples were returned to zero displacement and a decrease in collagen fiber organization (increased VAR) was found compared to the distribution imaged at the end of the stress relaxation test at both the midsubstance and insertion site locations. This finding suggests that returning to a reference point (marked by a decrease in both load and displacement) may cause a decrease in collagen fiber

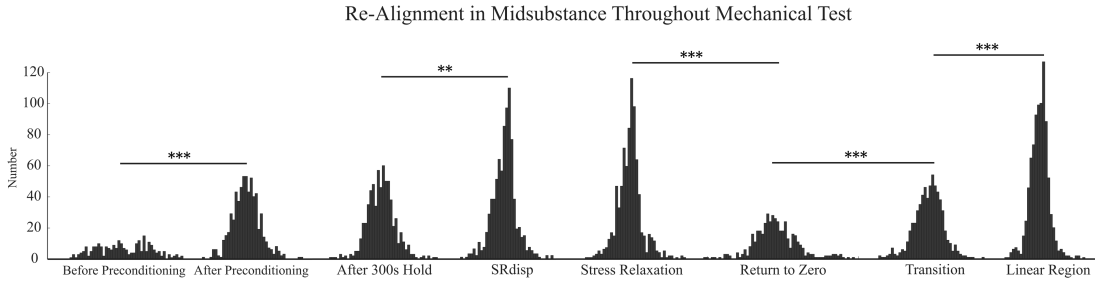

Figure 2.12 Midsubstance histograms for a representative sample show increasing alignment during preconditioning, during the displacement for the stress relaxation test, followed by a decrease in alignment after returning to zero-displacement and increases in toe-region (comparing return to zero and transition) and linear-region (comparing transition and linear-region). (*p<0.0125, ** p<0.0025, ***p<0.00025=sig.)

alignment at both locations allowing the tendon's collagen fibers to re-orient away from the direction of loading. This supports previous work in which a tissue-equivalent demonstrated a recovery of fiber alignment during a stress-free return to zero-displacement, but not during a return to zero-force suggesting that fiber re-alignment away from the direction of loading occurred only after a return to an un-stretched length during unloading.[27] While the majority of fiber re-alignment occurred during

preconditioning in our study, significant re-alignment was also found throughout the tensile ramp-to-failure test in both the toe- and linear-regions of the stress-strain curve for both the midsubstance and insertion site locations (Fig 2.6). Additionally, no significant differences in collagen fiber organization were found between the two "rest" points (after the 300 second hold and following the return to zero displacement) at either locations. It has been postulated that recovery and stress relaxation are two different processes, controlled by different mechanisms and occur at different rates.[7] While loading occurs via forced displacement, recovery loads result from internal processes in the unloaded state, this study indicates that collagen fiber re-alignment away from the direction of load following a return to zero-displacement may be a potential mechanism of tendon recovery and merits further study.[7]

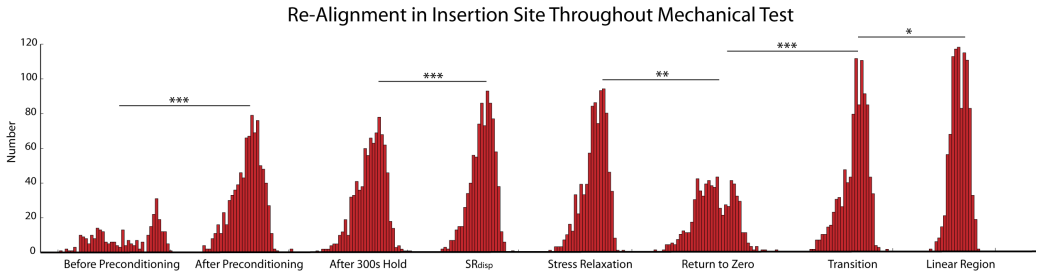

Figure 2.13 Insertion site histograms for a representative sample show increasing alignment during preconditioning, during the displacement for the stress relaxation test, followed by a decrease in alignment after returning to zero-displacement and increases in toe-region (comparing return to zero and transition) and linear-region (comparing transition and linear-region). (*p<0.0125, ** p<0.0025, ***p<0.00025)

Further, this study reports the inhomogeneous, nonlinear mechanical properties and fiber alignment of the rat SST. After examining collagen fiber re-alignment throughout the entire mechanical testing protocol, similar patterns in collagen fiber re-alignment were found for fiber distributions between the midsubstance and insertion site locations at

all mechanical testing points, indicating that the tendon functions as a continuous unit. Furthermore, local differences in cross-sectional area, linear modulus, transition strain and collagen fiber alignment, at all regions of the mechanical loading profile, demonstrate that the rat SST is inhomogeneous. The lower linear modulus (Fig 2.8) and higher VAR values (signifying increased disorganization) found at the insertion site compared to the midsubstance location demonstrate that the multi-axial loads experienced at the SST insertion may affect both the structure and mechanics of the tissue. Additionally, a higher strain was required for the insertion site to reach the linear region than the tendon midsubstance (Fig 2.10). This suggests that the more disorganized insertion site may require more microstructural changes before it is able to transition to the linear region of the stress-strain curve, such as collagen fiber crimp, which is believed to explain the toe-region of the stress-strain curve.[1,4,8,30,31]

This study is not without limitations. First, the crossed polarizer method used in this study can only measure fibers ±45º of the tendon long axis (90º total range), instead of the full 180º range that would contain all possible fiber orientations. While other methods are available to determine collagen fiber orientation, we selected the crossed polarizer method as it is the simplest method to provide the data necessary for analysis to test our study hypotheses. An angle value correction was applied based on the assumption that fibers must reorient toward the direction of loading. Secondly, the observations of collagen fiber re-alignment behavior made in this study were for one specific mechanical testing protocol. Despite this limitation, this study provides insight into the understanding of tendon fiber re-alignment throughout the mechanical testing

protocol in addition to examining potential mechanisms of preconditioning and stress relaxation. While collagen fiber re-alignment at the low loads seen during the applied preconditioning protocol may be a function of the mechanical testing protocol, imposed uniaxial boundary conditions, or removal of the native tension in the tendon, it is still important to understand what effects or influence the mechanical testing protocol and experimental design set up itself has on the measured mechanical properties since these are commonly used in the biomechanical testing literature and interpreting such data for clinical relevance. Preload and specific preconditioning protocols are not consistently reported in tendon literature. Further, there is a lack of consensus on the appropriate form of preconditioning as well as magnitudes of load to be used during preconditioning. This study identified a significant re-alignment of collagen fibers during preconditioning despite the small magnitude of the loads applied. The results from this study suggest that collagen fibers re-align in the presence of load, even if the magnitude of the load is very small. However, future studies are necessary to examine the effect of increasing the magnitude of the load reached during preconditioning on collagen fiber alignment and mechanical properties as it is possible that a higher magnitude may respond in a larger shift in collagen fibers towards the direction of loading and a further shift of the stress-strain curve while may have implications on mechanical properties, in particular during the toe-region. The results of this study suggest that the mechanical testing protocol itself may have implications on the consistency and repeatability of the mechanical properties measured; therefore, it is important to report the potential effects of preconditioning protocols, their implications on interpretations of mechanical properties and relating

future ex vivo work to the physiologic condition. Additionally, further studies are necessary to examine the effect of different types of preconditioning protocols on collagen fiber alignment and mechanical properties. As it is possible that applying small cycles of preconditioning before a ramp to failure may result in different collagen fiber re-alignment behavior than testing protocols which cycle samples repeatedly and then measure moduli values from the Nth cycle. It is possible that comparing mechanical properties from tests with differing preconditioning protocols may not allow for consistent and interpretable comparisons across studies. Further, this study provides valuable data regarding the specific mechanical and organizational properties of the rat SST. Additionally, the study reports information on how the collagen fiber distribution changes in response to various loading conditions. Collagen fiber distribution in relation to tendon macroscopic deformation is an important component of structurally based continuum models and it is important to be able to predict mechanical behavior during initial loading as well as during unloading and reloading as many physiologic loads are cyclic.[7,12] Finally, the samples used in this study were frozen, not fresh samples as is most commonly used in biomechanical testing of tendon tissue. It should be noted that cardiovascular studies have identified that freezing may result in changes in structure, such as fiber re-alignment or the breaking of crosslinks, which may be similar to the changes induced by preconditioning.[28] Fresh samples demonstrated greater hysteresis and required more cycles before stress-strain results became consistent and repeatable compared to frozen samples.[28] These results indicate that fresh samples may demonstrate larger shifts in collagen fiber re-alignment during preconditioning and merit further

study.

In Chapters 3 and 4, our laboratory will investigate if the amount of collagen fiber re-alignment is dependent on the preconditioning protocol and in Chapter 5 the potential effect of local changes in collagen fiber crimp on transition strain will be investigated. It is possible that the insertion site displays a higher frequency of collagen fiber crimp requiring an increased strain to reach the linear-region as noted in this study. Further studies are necessary to evaluate structural changes throughout a variety of mechanical testing protocols to determine if the changes observed are a result of the strain-rate, amount of load versus the type of loading (load control, displacement control). Finally, the amount of time and conditions necessary for collagen fiber orientation to return to its original orientation is currently unknown. Future studies incorporating longer rest intervals are necessary to determine what conditions are necessary for fibers to re-align away from the direction of loading and return to their initial configuration.

In summary, it was shown here that collagen fiber re-alignment towards the direction of load occurred during preconditioning, the 0.42mm displacement, and during the ramp-to-failure. Additionally, a decrease in collagen fiber alignment was noted during a return to zero displacement. Further, the insertion site of SST was found to have a larger CSA, lower linear modulus, higher transition strain and a more disorganized collagen fiber distribution than the tendon midsubstance. These results indentify a correlation between collagen fiber re-alignment and preconditioning and provide further insight into the structure-function relationships of tendon.

.

E. References

1. Abrahams M: Mechanical behaviour of tendon in vitro. A preliminary report. **Med Biol Eng 5:**433-443, 1967
2. Berens P: CircStat: A MATLAB Toolbox for Circular Statistics. **Journal of Statistical Software 31:**1-21, 2009
3. Billiar KL, Sacks MS: A method to quantify the fiber kinematics of planar tissues under biaxial stretch. **J Biomech 30:**753-756, 1997
4. Broom ND: The stress/strain and fatigue behaviour of glutaraldehyde preserved heart-valve tissue. **J Biomech 10:**707-724, 1977
5. Carew EO, Barber JE, Vesely I: Role of preconditioning and recovery time in repeated testing of aortic valve tissues: validation through quasilinear viscoelastic theory. **Ann Biomed Eng 28:**1093-1100, 2000
6. Derwin KA, Soslowsky LJ, Green WD, Elder SH: A new optical system for the determination of deformations and strains: calibration characteristics and experimental results. **J Biomech 27:**1277-1285, 1994
7. Duenwald SE, Vanderby R, Jr., Lakes RS: Stress relaxation and recovery in tendon and ligament: experiment and modeling. **Biorheology 47:**1-14
8. Evans JH, Barbenel JC: Structural and mechanical properties of tendon related to function. **Equine Vet J 7:**1-8, 1975
9. Favata M: Scarless Healing in the Fetus: Implications and Strategies for Postnatal Tendon Repair **Ph.D. thesis. University of Pennsylvania.**, 2006
10. Fung YC: **Biomechanics : mechanical properties of living tissues, ed 2nd.** New

York: Springer-Verlag, 1993

11. Houssen YG, Gusachenko I, Schanne-Klein MC, Allain JM: Monitoring micrometer-scale collagen organization in rat-tail tendon upon mechanical strain using second harmonic microscopy. **J Biomech 44:**2047-2052

12. Lake SP, Cortes DH, Kadlowec JA, Soslowsky LJ, Elliott DM: Evaluation of affine fiber kinematics in human supraspinatus tendon using quantitative projection plot analysis. **Biomech Model Mechanobiol 11:**197-205

13. Lake SP, Miller KS, Elliott DM, Soslowsky LJ: Effect of fiber distribution and realignment on the nonlinear and inhomogeneous mechanical properties of human supraspinatus tendon under longitudinal tensile loading. **J Orthop Res 27:**1596-1602, 2009

14. Lake SP, Miller KS, Elliott DM, Soslowsky LJ: Tensile properties and fiber alignment of human supraspinatus tendon in the transverse direction demonstrate inhomogeneity, nonlinearity, and regional isotropy. **J Biomech 43:**727-732

15. Lokshin O, Lanir Y: Viscoelasticity and preconditioning of rat skin under uniaxial stretch: microstructural constitutive characterization. **J Biomech Eng 131:**031009, 2009

16. Peltz CD, Sarver JJ, Dourte LM, Wurgler-Hauri CC, Williams GR, Soslowsky LJ: Exercise following a short immobilization period is detrimental to tendon properties and joint mechanics in a rat rotator cuff injury model. **J Orthop Res 28:**841-845

17. Perry SM, Getz CL, Soslowsky LJ: After rotator cuff tears, the remaining (intact)

tendons are mechanically altered. **J Shoulder Elbow Surg 18:**52-57, 2009

18. Quinn KP, Winkelstein BA: Preconditioning is correlated with altered collagen fiber alignment in ligament. **J Biomech Eng 133:**064506, 2011

19. Schatzmann L, Brunner P, Staubli HU: Effect of cyclic preconditioning on the tensile properties of human quadriceps tendons and patellar ligaments. **Knee Surg Sports Traumatol Arthrosc 6 Suppl 1:**S56-61, 1998

20. Sellaro TL, Hildebrand D, Lu Q, Vyavahare N, Scott M, Sacks MS: Effects of collagen fiber orientation on the response of biologically derived soft tissue biomaterials to cyclic loading. **J Biomed Mater Res A 80:**194-205, 2007

21. Stouffer DC, Butler DL, Hosny D: The relationship between crimp pattern and mechanical response of human patellar tendon-bone units. **J Biomech Eng 107:**158-165, 1985

22. Sun W, Sacks M, Fulchiero G, Lovekamp J, Vyavahare N, Scott M: Response of heterograft heart valve biomaterials to moderate cyclic loading. **J Biomed Mater Res A 69:**658-669, 2004

23. Sverdlik A, Lanir Y: Time-dependent mechanical behavior of sheep digital tendons, including the effects of preconditioning. **J Biomech Eng 124:**78-84, 2002

24. Teramoto A, Luo ZP: Temporary tendon strengthening by preconditioning. **Clin Biomech (Bristol, Avon) 23:**619-622, 2008

25. Thomopoulos S, Williams GR, Gimbel JA, Favata M, Soslowsky LJ: Variation of biomechanical, structural, and compositional properties along the tendon to bone

insertion site. **J Orthop Res 21:**413-419, 2003

26. Thornton GM, Frank CB, Shrive NG: Ligament creep behavior can be predicted from stress relaxation by incorporating fiber recruitment. **Journal of Rheology 45:**493-507, 2001

27. Tower TT, Neidert MR, Tranquillo RT: Fiber alignment imaging during mechanical testing of soft tissues. **Ann Biomed Eng 30:**1221-1233, 2002

28. Venkatasubramanian RT, Grassl ED, Barocas VH, Lafontaine D, Bischof JC: Effects of freezing and cryopreservation on the mechanical properties of arteries. **Ann Biomed Eng 34:**823-832, 2006

29. Viidik A: Functional properties of collagenous tissues. **Int Rev Connect Tissue Res 6:**127-215, 1973

30. Viidik A: A rheological model for uncalcified parallel-fibred collagenous tissue. **J Biomech 1:**3-11, 1968

31. Viidik A: Tensile strength properties of Achilles tendon systems in trained and untrained rabbits. **Acta Orthop Scand 40:**261-272, 1969

32. Woo SL, Gomez MA, Seguchi Y, Endo CM, Akeson WH: Measurement of mechanical properties of ligament substance from a bone-ligament-bone preparation. **J Orthop Res 1:**22-29, 1983

33. Zar JH: **Biostatistical analysis, ed 4th.** Upper Saddle River, N.J.: Prentice Hall, 1999

Chapter 3. Collagen Fiber Re-Alignment, Mechanics and Correlations in a Mature Mouse Supraspinatus Tendon Model

A. Introduction

Collagen fiber re-alignment is one postulated mechanism of tendon structural response to load. Recently, work in a rat supraspinatus tendon (SST) model demonstrated inhomogeneous collagen fiber alignment and mechanical properties.[10] While collagen fiber re-alignment was found to increase throughout the mechanical test, a large shift in collagen fiber re-alignment was found during preconditioning.[10] A correlation between preconditioning and altered collagen fiber alignment has also been identified in ligament.[12] While preconditioning is commonly accepted to be an important component of mechanical testing protocols, the mechanisms of preconditioning are not well understood. Additionally, effects of increasing the number of cycles of preconditioning on collagen fiber re-alignment and experimentally measured mechanical properties has not yet been examined in tendon. A better understanding of the effects of preconditioning on tendon structural changes and mechanical properties are necessary to ensure that experimental results are consistent, repeatable and easily interpretable across studies.

While the rat model is a well-established model for examining clinical problems in the shoulder, the mouse model has advantages including being an established developmental model with a wide range of genetically modified animals available to

further elucidate structure-function relationships in tendon. Additionally, mice have similar anatomy to humans, are easy to handle and are associated with low husbandry costs. However, local collagen fiber alignment and mechanics have not yet been characterized in the mouse SST model. Therefore, the objective of this study was to locally measure: 1) collagen fiber re-alignment during preconditioning (with 5, 10 and 20 cycles) and tensile mechanical testing and 2) to compare local differences in collagen fiber alignment and corresponding mechanical properties to characterize tissue response to mechanical load in the mature mouse SST tendon. Further, this study will identify correlations between structure and mechanical properties and determine if collagen fiber re-alignment is affected by increasing the number of preconditioning cycles. We hypothesize that 1) tendons will demonstrate the largest shift in fiber re-alignment during preconditioning, but will also re-align during the toe- and linear-regions. Additionally, we hypothesize that 2) mechanical properties and initial collagen fiber alignment will be greater at the midsubstance location of the tendon compared to the tendon-to-bone insertion site and that 3) a correlation between mechanics and collagen fiber alignment will be present.

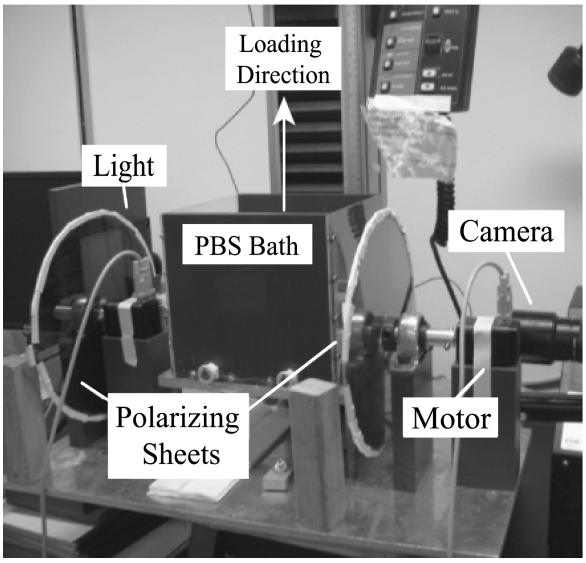

Figure 3.1 Angled side-view of the tendon tensile testing set-up showing polarized light and imaging system: light source, rotating cross-polarized sheets, stepper motors and camera.

B. Methods

B1. Sample Preparation

This study was approved by the University of Pennsylvania IACUC. Postnatal mice in a C57/BL/6 (Jackson Laboratory) were bred in house. All litters were reduced to 6 pups within 1 day of birth to reduce variance from litter size.[5] Pups were weaned 21 days after birth and separated by sex. Only females were used in this study and a sample was defined as a collective litter of 6 female pups from the same breeder pair. SSTs were removed from female postnatal mice at 90 days old. Three different mechanical testing preconditioning protocols (5, 10, 20 cycles) were randomly assigned (n=9 per protocol). Tendons from the same mouse were not used for the same mechanical testing protocol. SSTs were carefully removed under a dissection microscope for mechanical testing. Excess tissue was removed with the tendon still attached to the humeral head. Tendon cross-sectional area was measured using a custom built device consisting of LVDTs, a CCD laser, and translation stages. Stain lines were placed on the tendons to denote the tendon insertion site and midsubstance for

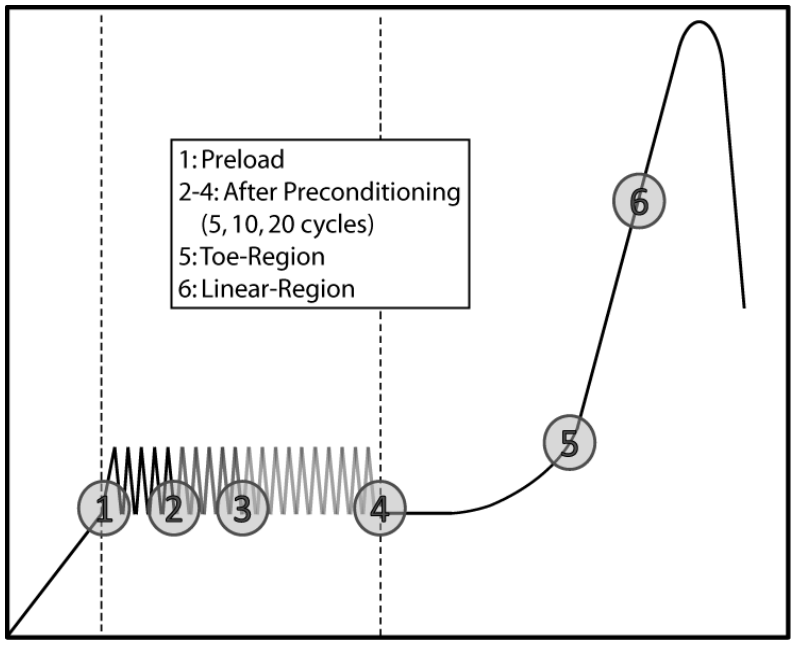

Figure 3.2 Schematic of the testing protocol with six points at which collagen fiber alignment was calculated for analysis highlighted.

alignment and mechanical analysis. The humeral head was trimmed to a small bone chip. Verhoeff's stain was used to mark the tendon insertion site and midsubstance and a 2.5 mm gauge length was denoted. Both ends of the tendon were secured with cyanoacrylate adhesive between two pieces of sandpaper. Tendons were secured in the grips and a grip holder was used to ensure that tendons remained unloaded during loading into the mechanical testing device.[2]

B2. Mechanical Testing

Samples were placed in a room temperature phosphate buffered saline (PBS) bath and loaded into a tensile testing system (Instron, Norwood, MA) integrated with a polarized light setup, consisting of a linear backlight (Dolan-Jenner, Boxborough, MA), 90°-offset rotating polarizer sheets (Edmund Optics, Barrington, NJ) on either side of the test sample, and a digital camera (Basler, Exton, PA) (Fig 3.1). A brief pilot study was performed to confirm that no changes in alignment or mechanical behavior were found in a room temperature PBS bath compared to a 37° bath. Prior to testing, the stepper motor encoder (Lin Engineering, Santa Clara, CA) was initialized by resetting the encoder value with the polarizer sheets set at a position corresponding to 0° of angular rotation. A 10 N load cell was used for all tests. The following protocol was utilized for all mechanical tests: preloaded to a nominal load of 0.02N, followed by preconditioning either 5, 10, or 20 cycles of preconditioning from 0.02-0.05N at a rate of 0.1%/second, followed by a 60 second hold. Finally, a ramp-to-failure was applied at a rate of 0.1%/second (Fig 3.2). Sets of 13 images were acquired every 20 seconds as the polarizers rotated through a 125° range for measurement of fiber alignment during loading. Images were taken every

5 seconds for optical strain analysis as described previously.[4]

B3. Data Analysis

Local strain was measured optically and stress was calculated as force divided by initial area. A structural fiber recruitment model was used to determine strains representing the toe- and linear-regions. The transition-region (intersection of the toe- and linear-region strains of the load-displacement curve) was modeled at 50% fiber recruitment and a point in the linear-region was modeled at 75% fiber recruitment.[9,11] Fiber alignment was calculated from image sets as previously described.[7] Briefly, images of the tendon surface were divided into rectangular areas. Pixel intensities were summed by area per image and plotted against angle of polarizer rotation. A sine wave was fit to the intensity angle to determine the angle corresponding to the minimum pixel intensity, which represents the average direction of the area's collagen fiber alignment.

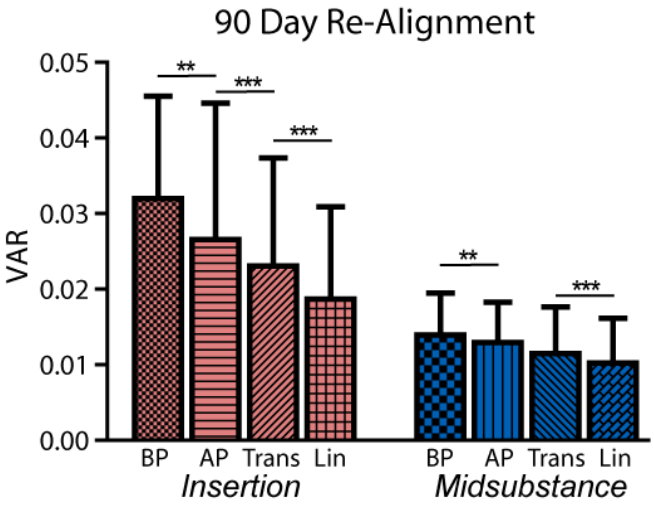

Figure 3.3 VAR values demonstrate that collagen fiber re-alignment occurred throughout the entire mechanical test (preconditioning, toe- and linear-region) at the insertion site and during preconditioning and linear-region at the midsubstance. Sig. *=p<0.025, **p<0.005, ***p<0.0005.

Circular variance, transition stress, transition strain, toe-region modulus, linear-region modulus and stiffness were determined. Circular variance (VAR), a measure of the spread of the distribution of collagen fiber alignment, was calculated for fiber

distributions before and after preconditioning (5, 10, 20 cycles), at the transition region (intersection of the toe- and linear-regions as determined by the structural fiber recruitment model: 50% recruitment at transition[11]), and at the linear-region (75% fiber recruitment). Fiber re-alignment during preconditioning was evaluated by comparing VAR values from before preconditioning (BP) to after preconditioning (AP) for each preconditioning protocol (Fig 3.2). Similar methods were used to determine fiber re-alignment during the toe- and linear-regions of the stress-strain curve. Additionally, circular variance and mean angle were evaluated at 3 regions across the width of the insertion site at the preload and linear-region points to further investigate the collagen fiber distribution at the insertion site location.

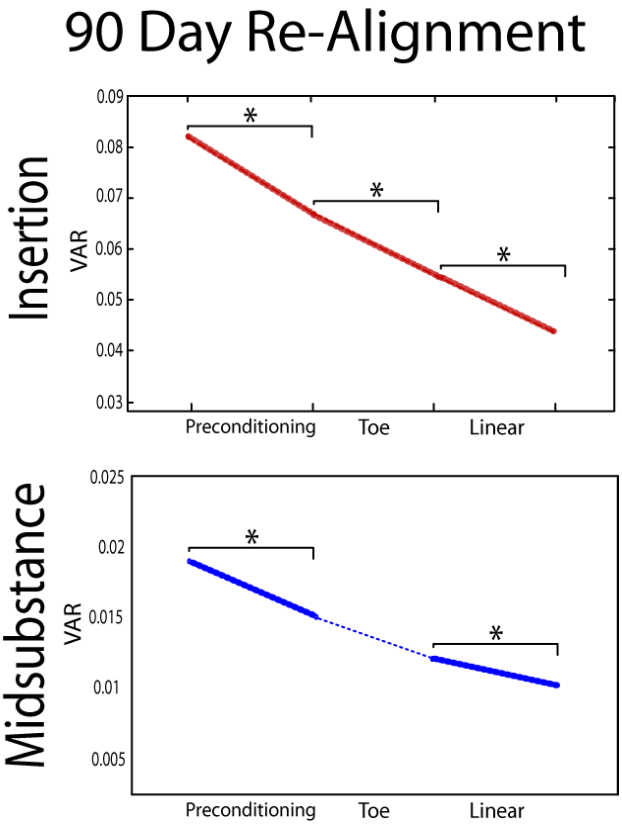

Figure 3.4 Circular variance (VAR) values for representative samples demonstrate that collagen fiber re-alignment occurred throughout the entire mechanical test (preconditioning, toe- and linear-region) at the insertion site and during preconditioning and linear-region at the midsubstance. *p<0.025.

B4. Statistical Analysis

For all parameters, two-way ANOVAs were used to evaluate interactions between 1) protocol and location. A Bonferroni correction was applied if the interaction was

significant. Post-hoc paired t-tests were used to evaluate local differences between mechanical properties and cross-sectional area and data is presented as mean ± standard deviation. Shapiro-Wilk tests indicated non-normally distributed data for VAR values. Therefore, nonparametric tests were used for evaluating fiber re-alignment. VAR data was analyzed as paired comparisons and is presented as median + interquartile range. Changes in fiber alignment (Friedman test) were compared for tendon location (midsubstance versus the insertion site) and for the mechanical test region (preconditioning, toe- and linear-region). Bonferroni corrections were applied for multiple comparisons. Spearman rank correlation coefficients were calculated to evaluate correlations between mechanical and alignment parameters.

C. Results

C1. Protocol

No differences in collagen fiber re-alignment or mechanics were found between protocols with varying number of preconditioning cycles. Therefore to increase power, data was pooled across the protocols for the remaining analyses.

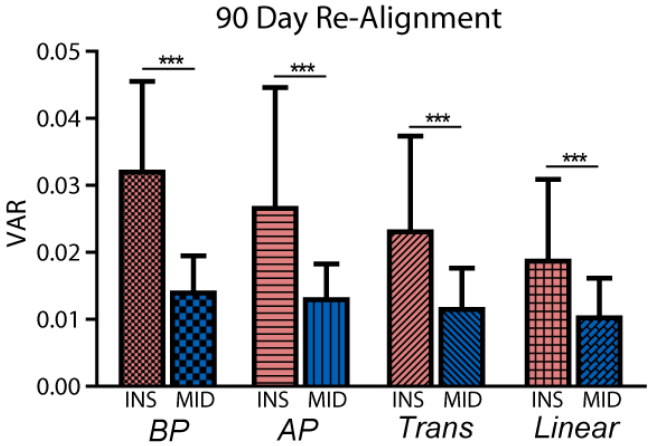

Figure 3.5 Circular variance values demonstrate that the insertion site location was more disorganized compared to the tendon midsubstance throughout the entire mechanical test. ***p<0.0005.

C2. Collagen Fiber Re-Alignment

At the insertion site, collagen fiber re-alignment occurred throughout the entire mechanical test (during

preconditioning and the toe- and linear-regions) (Figs 3.3 and 3.4). At the midsubstance location, collagen fiber re-alignment occurred during preconditioning and the linear-region of the mechanical test (Figs. 3.3 and 3.4). Locally, the insertion site was more disorganized than the tendon midsubstance throughout the entire mechanical test (Fig 3.5). No differences in collagen fiber alignment or mean angle were identified across regions along the width of the insertion site.

C3. Mechanical Properties

Locally, the insertion site cross-sectional area was larger than at the midsubstance location (Fig 3.6). Both toe- and linear-region moduli were larger at the midsubstance location compared to the insertion site (Figs 3.7 and 3.8 respectively). No difference in transition strain was identified (Fig 3.9).

C4. Correlations

Low negative correlations were found between before (r_s=-0.25, p=0.03) and after preconditioning (r_s=-0.25, p=0.04) VAR values and linear-region modulus. No significant correlations were found between before and after preconditioning VAR values and transition strain.

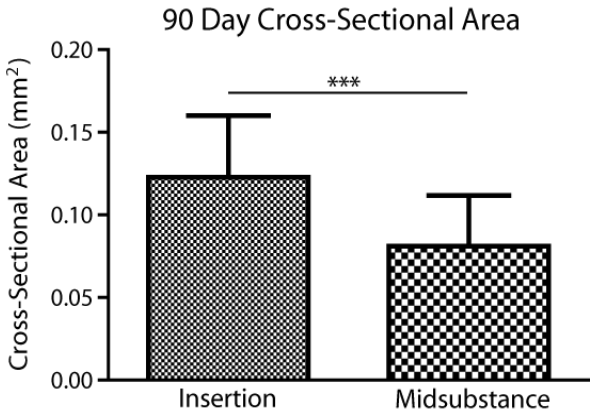

Figure 3.6 The insertion site cross-sectional area was larger than at the midsubstance location. ***p<0.0005.

D. Discussion

This study quantified local collagen fiber re-alignment throughout the mechanical

test and corresponding local mechanical properties in a mature mouse SST model. As expected, the insertion site re-aligns throughout the entire mechanical test (Figs 3.3 and 3.4). However, surprisingly, the midsubstance did not re-align during the toe-region (Figs 3.3 and 3.4). It is believed that the tendon-to-bone insertion site experiences complex multi-axial loads in vivo resulting in a more disorganized collagen fiber distribution.[7,14,15] A more disorganized collagen fiber distribution may require additional collagen fiber re-alignment at the insertion site compared to the midsubstance location. Therefore it is possible that the midsubstance location "pauses" recruiting fibers following preconditioning to allow collagen fibers to uncrimp during the toe-region and giving the insertion site additional time to recruit fibers before transitioning into the linear-region. Alternatively, it is possible that the fibers initially recruited in the midsubstance during preconditioning fail at the end of the toe-region. Assuming these fibers were initially aligned in the direction of load or required a minimal amount of re-orientation, the fibers would be tensioned almost immediately and may fail earlier in the ramp-to-fail. The early failure of those fibers would require the recruitment of additional fibers in the linear-region at the midsubstance location.

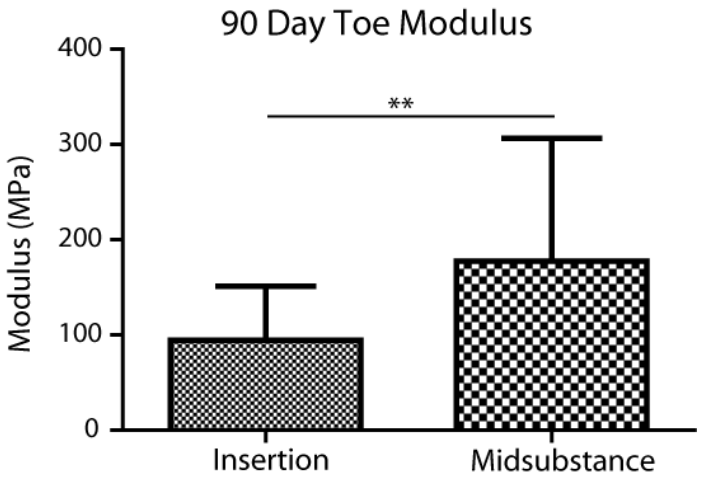

Figure 3.7 The toe-region modulus was lower at the insertion site compared to the midsubstance location. **p<0.005

Interestingly in this study, unlike the mature rat SST, the midsubstance and insertion site locations in the mouse SST were found to demonstrate different re-alignment behaviors (Figs 3.3 and 3.4). It is possible that the differences in re-alignment behavior provides support the idea that the midsubstance and insertion site experience different loading conditions in vivo which may initiate matrix remodeling resulting in different fiber network configurations including alterations in not only collagen fiber alignment, but collagen fiber cross-link formation as well as fiber-fiber and fiber-matrix interactions. These potential changes in the network of collagen fibers between the insertion site and midsubstance may affect their ability to respond to load simultaneously or in the same manner. Additionally, it is possible that the insertion site and midsubstance locations respond to load by different mechanisms. In vivo loads are thought to occur primarily in the toe-region which is thought to be explained by straightening of crimped collagen fibers and a reorientation of fibers to align fully in the direction of loading.[1,13] The results from this study suggest that the toe-region of the midsubstance may not be explained by collagen fiber re-alignment, while the re-alignment may contribute to the toe-region of the insertion site.

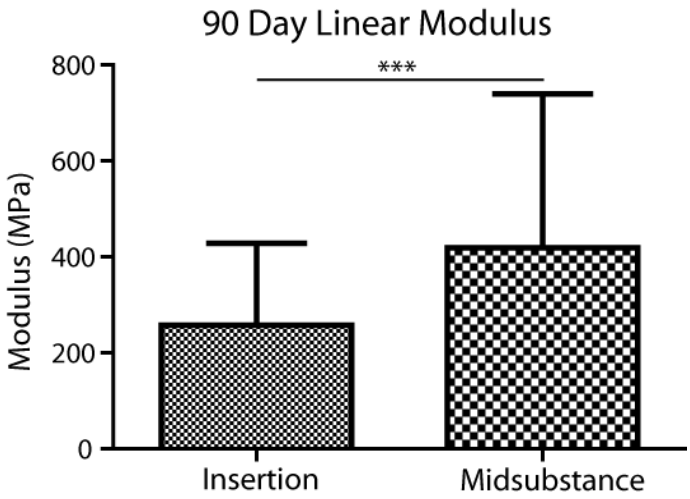

Figure 3.8 A lower linear-region was present at the insertion site compared to the midsubstance location. ***p<0.0005

As expected, mechanical properties were lower (Figs 3.7 and 3.8) and a more disorganized collagen fiber distribution was found at the insertion site compared to the midsubstance location in the mouse SST (Fig 3.5). The strong local differences in collagen fiber re-alignment, toe and linear moduli at the insertion site compared to the midsubstance location support the theory that the insertion site experiences complex, multi-axial loads. Additionally, the results from this study support previous work in both the rat and human SST.[7,8,10] Further, a low but significant correlation between collagen fiber alignment before (r_s=-0.25, p=0.03) and after preconditioning (r_s=-0.25, p=0.04) with linear modulus was identified. This result provides more information on tendon structure-function relationships and supports previous work in the human SST tendon.[7] Additionally, it indicates that collagen fiber distributions are an important predictor of mechanical properties and should be incorporated into constitutive models.[6]

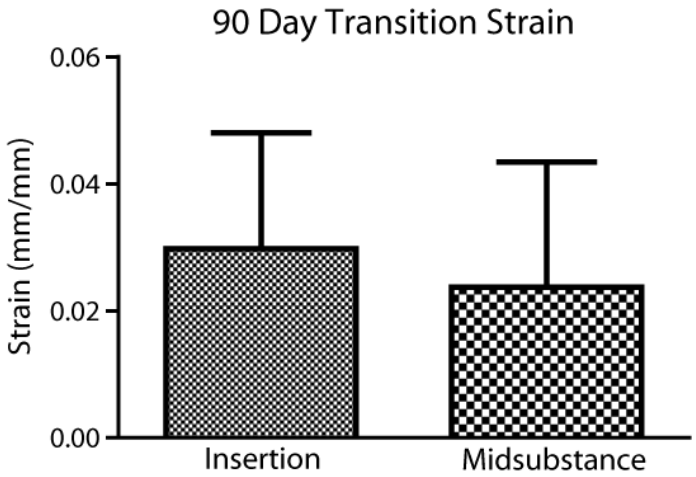

Figure 3.9 No significant differences in transition strain were identified.

In addition, this study did not identify significant changes in collagen fiber re-alignment behavior or mechanical properties with increasing number of preconditioning cycles. Both locations re-aligned during preconditioning indicating that fibers in mature tendons begin to respond almost immediately to the presence of mechanical load given

the very small loads and low number of cycles utilized in the protocols in this study. However, the shift in collagen fiber alignment found in this study during preconditioning supports previous work in the rat SST and in ligament suggesting that preconditioning is correlated to the re-alignment of collagen fibers.[10,12] Further, the results from this study suggest that tendons respond via collagen fiber re-alignment to the small loads seen during preconditioning regardless of the duration of the loading or the location of the tendon. Results support the concept that the network of mature collagen fibers at 90 days old are able to communicate quickly and efficiently across the entire tendon length in the presence of small external loads.[3] These results suggest that the re-alignment of collagen fibers in the direction of load may serve as one contributing mechanism to establishing a consistent history between tendon samples to achieve repeatable and consistent measurements of mechanical properties.

This study is not without limitations which must be understood. First, toe and linear-region VAR values for each age were determined using the average strain quantified from the individual sample fiber recruitment model results in order to make comparisons at one consistent strain value rather than individually determining an appropriate value to represent the toe- and linear-region for each individual sample and location. This was done to allow for consistent comparisons of collagen fiber re-alignment data with collagen fiber crimp frequency values to be discussed in Chapter 4 as well as to establish a consistent and repeatable method to be utilized in the subsequent chapter examining collagen fiber re-alignment and uncrimping throughout development (Chapters 5 and 6 respectively). However, the average values used in this study are

within the parameters to represent the toe- and linear-regions of each location and the use of average values improves consistency within this experiment in addition to allowing for future comparisons across studies. Secondly, the cross polarizer method used in this study can only measure fibers ±45° from the tendon long axis instead of the full 180° range of all possible fiber orientations. An angle value correction was applied based on the assumption that fibers must reorient toward the direction of loading as has been performed previously.[7,8] Finally, this study only examined an increase in the number of cycles of preconditioning as opposed to varying the magnitude of the loads or actual loading protocol of preconditioning itself. It is possible that these variables may alter collagen fiber re-alignment or subsequent mechanical properties following preconditioning. Future studies are needed to continue to elucidate the effect of preconditioning on measured mechanical properties in addition to tendon structural response to load. However despite this limitation, the results from this study provide additional insight into tendon structure-function relationships and the structural response of tendon to preconditioning.

In conclusion, this study demonstrated that the insertion site has a more disorganized collagen fiber distribution and lower mechanical properties compared to the midsubstance location in a mature mouse SST tendon model. Additionally, the study identified that while the insertion site re-aligns throughout the mechanical test, the midsubstance location only re-aligns during preconditioning and in the linear-region. Finally, this study identified a low but significant correlation between collagen fiber alignment and linear modulus. Future studies are necessary to examine the structural

response of tendon to preconditioning protocols of varying magnitude.

E. References

1. Abrahams M: Mechanical behaviour of tendon in vitro. A preliminary report. **Med Biol Eng 5:**433-443, 1967
2. Ansorge HL, Adams S, Birk DE, Soslowsky LJ: Mechanical, compositional, and structural properties of the post-natal mouse Achilles tendon. **Ann Biomed Eng 39:**1904-1913
3. Birk DE, Southern JF, Zycband EI, Fallon JT, Trelstad RL: Collagen fibril bundles: a branching assembly unit in tendon morphogenesis. **Development 107:**437-443, 1989
4. Derwin KA, Soslowsky LJ, Green WD, Elder SH: A new optical system for the determination of deformations and strains: calibration characteristics and experimental results. **J Biomech 27:**1277-1285, 1994
5. Festing MF: Design and statistical methods in studies using animal models of development. **ILAR J 47:**5-14, 2006
6. Lake SP, Cortes DH, Kadlowec JA, Soslowsky LJ, Elliott DM: Evaluation of affine fiber kinematics in human supraspinatus tendon using quantitative projection plot analysis. **Biomech Model Mechanobiol 11:**197-205
7. Lake SP, Miller KS, Elliott DM, Soslowsky LJ: Effect of fiber distribution and realignment on the nonlinear and inhomogeneous mechanical properties of human supraspinatus tendon under longitudinal tensile loading. **J Orthop Res 27:**1596-1602, 2009
8. Lake SP, Miller KS, Elliott DM, Soslowsky LJ: Tensile properties and fiber

alignment of human supraspinatus tendon in the transverse direction demonstrate inhomogeneity, nonlinearity, and regional isotropy. **J Biomech 43:**727-732

9. Miller KS, Connizzo BK, Soslowsky LJ: Collagen Fiber Re-Alignment in a Neonatal Developmental Mouse Supraspinatus Tendon Model. **Ann Biomed Eng**, 2012

10. Miller KS, Edelstein, L., Connizzo, B. K., and Soslowsky, L. J... Effect of Preconditioning and Stress Relaxation on Local Collagen Fiber Re-Alignment: Inhomogeneous Properties of Rat Supraspinatus Tendon. **Journal of Biomechanical Engineering In press**, 2012

11. Peltz CD, Sarver JJ, Dourte LM, Wurgler-Hauri CC, Williams GR, Soslowsky LJ: Exercise following a short immobilization period is detrimental to tendon properties and joint mechanics in a rat rotator cuff injury model. **J Orthop Res 28:**841-845

12. Quinn KP, Winkelstein BA: Preconditioning is correlated with altered collagen fiber alignment in ligament. **J Biomech Eng 133:**064506

13. Screen HR, Lee DA, Bader DL, Shelton JC: An investigation into the effects of the hierarchical structure of tendon fascicles on micromechanical properties. **Proc Inst Mech Eng H 218:**109-119, 2004

14. Thomopoulos S, Williams GR, Gimbel JA, Favata M, Soslowsky LJ: Variation of biomechanical, structural, and compositional properties along the tendon to bone insertion site. **J Orthop Res 21:**413-419, 2003

15. Thomopoulos S, Williams GR, Soslowsky LJ: Tendon to bone healing:

differences in biomechanical, structural, and compositional properties due to a range of activity levels. **J Biomech Eng 125:**106-113, 2003

Chapter 4. Collagen Fiber Crimp Behavior in a Mature Mouse Model

A. Introduction

In this chapter, a new quantitative method for analyzing collagen fiber crimp frequency will be presented and validated using a previously established semi-quantitative method. The quantitative method will then be utilized to quantify local collagen fiber crimp frequency throughout a mechanical testing protocol and in response to multiple preconditioning protocols in a mature mouse SST model. Crimp morphology is believed to be related to tendon mechanical behavior. The uncrimping of collagen fibers is thought to explain the toe-region of the mechanical test,[9,23,29] providing a potential explanation for tendon nonlinear behavior. Collagen fiber crimp has been extensively characterized at slack or nonspecific loading conditions;[4-7] however, few studies have examined crimp throughout a mechanical testing protocol at specific, quantifiable loads. Preconditioning is widely accepted as an important component of mechanical testing protocols, which provides tendons with a consistent loading history. However, the mechanisms of preconditioning are not well understood. A recent study in rat tail tendon fascicles showed that preconditioning was accompanied by a decrease in the crimp period and a shift of the toe-region of the stress-strain curve to higher strains.[11] However, the effect of the number of preconditioning cycles on collagen fiber crimp has not been examined.

It has been speculated that the collagen fiber crimp behavior may vary by

location. In Chapter 3, the mature mouse supraspinatus tendon (SST) demonstrated a more disorganized collagen fiber distribution and a lower linear modulus at the insertion site compared to the midsubstance location. In addition, studies in ligament have shown a preferential uncrimping of the central third of the ligament as well as near the bone.[2] However, local collagen fiber crimp frequency has not been quantified and the potential dependence of collagen fiber crimp behavior on tendon location has also not been examined. Additionally, it is not known how changing the boundary conditions and the residual stress of the tendon from the in vivo state to the excised mechanical testing set-up affects collagen crimp behavior. To obtain an appropriate reference position for quantifying changes in crimp frequency throughout tensile mechanical testing, the tendon must still be connected to the bony insertion as well as the muscle-tendon junction.[4] For the SST model, the tendon must still be attached to the humeral head and the supraspinatus muscle must remain tethered to the scapula.

Therefore, the objective of this study was to quantify local changes in collagen fiber crimp frequency throughout a mechanical testing protocol in a mature mouse SST model to determine 1) where collagen fiber uncrimping occurs throughout the mechanical test; 2) if collagen fiber crimp behavior is affected by increasing the number of preconditioning cycles; and 3) if crimp behavior varies by location. We hypothesize that: 1) collagen fiber uncrimping will be confined to the toe-region of the mechanical test; 2) increasing the number of preconditioning cycles will decrease crimp frequency; and 3) the insertion site will demonstrate a higher frequency of crimp compared to the midsubstance location.

B. Methods

B1. Sample Preparation

Postnatal mice in a C57/BL/6 (Jackson Laboratory) background were bred on site at the University of Pennsylvania in an IACUC approved study. All litters were reduced to six pups within 1 day of birth to reduce variance from litter size.[3] Pups were weaned at 21 days after birth and separated by sex. To reduce variation, only female mice were used in this study. In order to compare changes in crimp frequency throughout a mechanical test, 6 mice from the same breeder pair were defined as a single sample and mechanical testing points were randomly assigned to shoulders within each litter. SSTs from female mice were removed at 90 days old (N=9 for each mechanical testing point). Under a stereomicroscope, SSTs were dissected out and excess tissue was removed with the tendon still attached to the humeral head. As described in Chapter 3, the humeral head was trimmed to a small bone chip and then both ends of the tendon were secured between pieces of sandpaper with cyanoacrylate adhesive. A gauge length of 2.5mm was used for all specimens. Tendons were secured in the grips and a grip holder was used to protect the tendons during handling and loading into the testing device.[1]

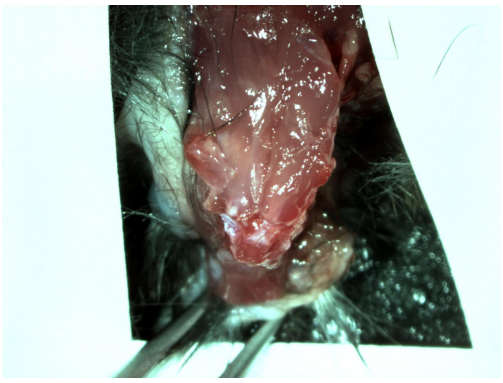

Figure 4.1 Bone-tendon-muscle unit of the supraspinatus visualized under a stereomicroscope.

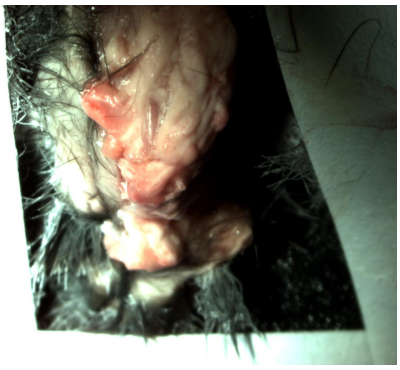

Figure 4.2 Bone-tendon-muscle unit of the supraspinatus after flash freezing.

B2. Reference Configuration Dissection Protocol

An additional sample from each breeder pair was prepared to serve as a reference configuration for the mechanical testing points. The reference configuration samples were flash frozen while still attached to the muscle and humeral head to provide an "in situ" reference configuration for comparative analysis. All dissections were performed under a stereomicroscope. Mice were placed on their sides and secured to the table using masking tape. After the shoulder joint was exposed, the shoulder was externally rotated to visualize the joint. The arm was secured with tape to maintain a consistent position throughout the dissection process.

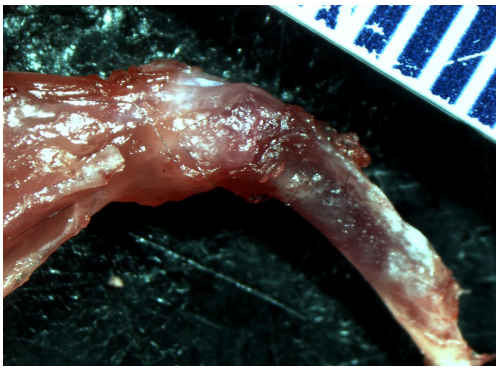

Figure 4.3 Excised flash-frozen bone-tendon-muscle complex.

Throughout the project, care was taken to secure shoulders at a consistent angle. Trapezius and deltoid muscles were removed to expose the acromioclavicular and scapulohumeral joints. The AC ligament was cut and the clavicle was peeled back to expose the SST and subscapularis tendons (Fig 4.1). The acromion was removed to visualize the infraspinatus tendon. The infraspinatus and subscapularis tendons were sharply detached at their insertion sites. The entire remaining shoulder joint was thoroughly sprayed with flash freezing spray (Fig 4.2). With the joint frozen, the humeral shaft was sharply detached from the body near the elbow joint and any remaining attachments to the scapulohumeral joint were sharply dissected (Fig 4.3). The joint was quickly positioned in a freezing tray, embedded in tissue freezing medium and doused with liquid nitrogen. In graphical representation this point is referred to as

the "in situ" or IS point.

B3. Mechanical Testing

Following sample preparation, all samples were placed in a tank and loaded into a tensile testing system (Instron, Norwood, MA). Samples sprayed with phosphate buffered saline throughout the testing process to maintain a consistent hydration level and a 10 N load cell was used for all tests. Collagen fiber crimp was assessed at 6 different points throughout the mechanical test: at the preload (0.02N), after 5, 10 and 20 cycles of preconditioning (0.02N to 0.05N) and at the toe- and linear-regions (Fig 4.4). A structural fiber recruitment model was used to determine strains to represent the toe- and linear-regions.[19] The toe-region was modeled at 50% fiber recruitment and the linear-region was modeled at 75% fiber recruitment.[19] Tendons were snap-frozen (sprayed for 20 seconds with flash freezing spray (Decon Laboratories, King of Prussia, PA)) while mounted in the testing device immediately following the designated tensile loading protocol to obtain a "snapshot" of crimp at the desired testing point.[26] Samples were sharply detached at the insertion site and top grip and immediately embedded in tissue freezing medium (Triangle Biomedical Sciences, Durham, NC). All samples were cut into 8 μm sections and stained with Picrosirius Red and Hematoxylin.

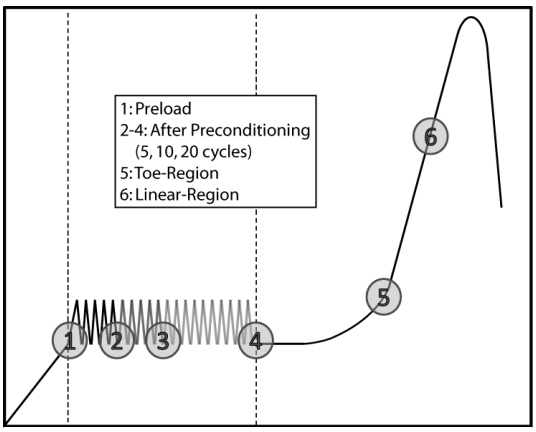

Figure 4.4 Schematic of the mechanical testing protocol. Crimp was assessed at 6 points throughout the tensile mechanical test.

B4. Data Analysis

For each sample, sections were analyzed at the midsubstance and insertion site locations and 2 slides were imaged for each sample using both a new quantitative and previously established semi-quantitative methods (Fig 4.5).[26] Sections were examined using polarized light microscopy and custom software in a blinded manner.

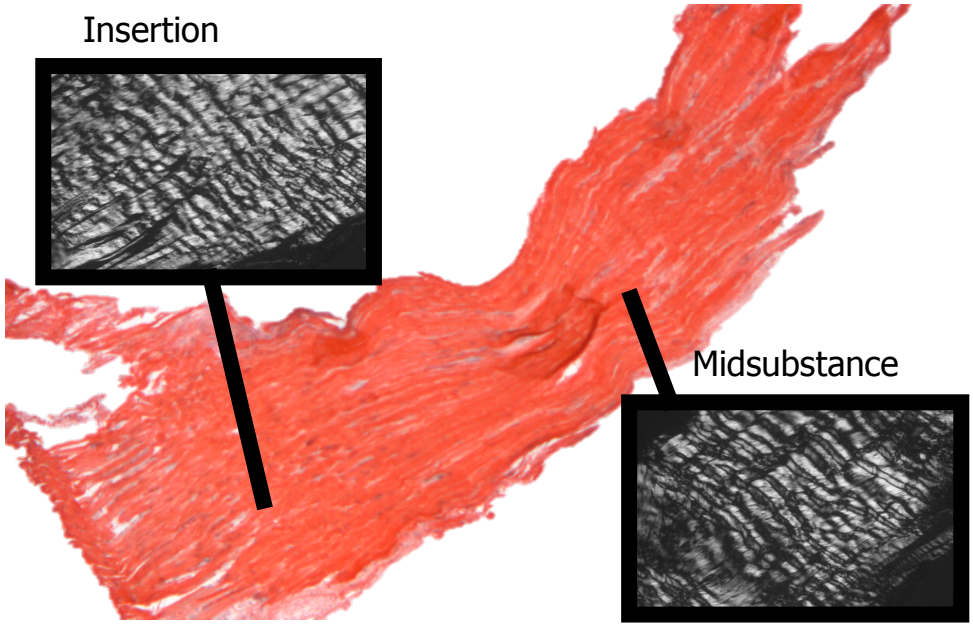

Figure 4.5 Data was analyzed at the midsubstance and insertion site locations.

a. Quantitative Analysis Software Development

In order to quantify collagen fiber crimp frequency throughout mechanical testing, custom software (Matlab, Natwick, MA) was developed. After selecting a sample for analysis, the user is prompted to select a quadrilateral region along the

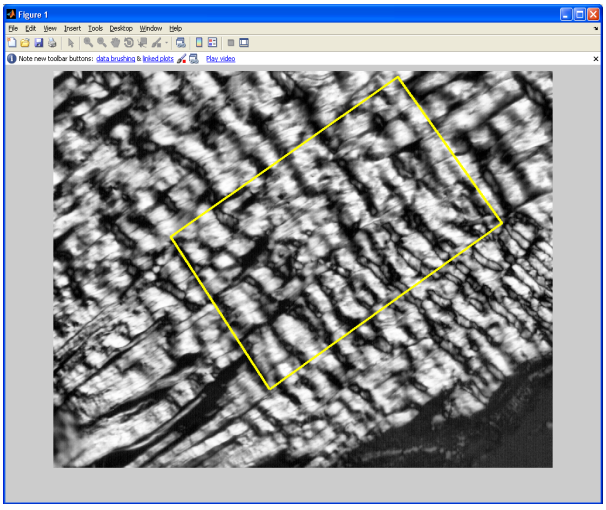

Figure 4.6 A blinded user selects a quadrilateral region along the fiber direction.

fiber direction (Fig 4.6). Next, the user is prompted to select which images from that sample to analyze. A pilot study examined the effect of the angle of the polarizer on the polarized light microscope with crimp frequency results. This study found no significant differences in crimp frequency after analyzing samples at various angles. Therefore, for this dissertation, all images will be analyzed at 75°. Since the pilot study did not identify significant differences in crimp frequency measurements with varying angle, choosing a single angle for the analysis is appropriate and any angle chosen, as long as consistent, would be sufficient for the quantitative analysis. However, in order to validate the quantitative analysis, a previously established semi-quantitative method will be used on the same regions selected for the quantitative. As described in the following section, the semi-quantitative method requires histology grading by blinded investigators. Changing the angle of the polarizers results in a fluctuation of the contrast and intensity fluctuation of the dark and light bands that indicate collagen fiber crimp. In order to

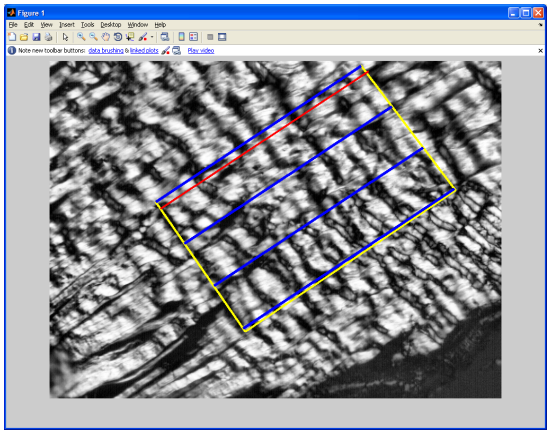

Figure 4.7 A blinded user draws a line along the long axis of the tendon in the primary fiber direction (red line). The program then divides the selected quadrilateral region into 3 equal sub-region (blue lines).

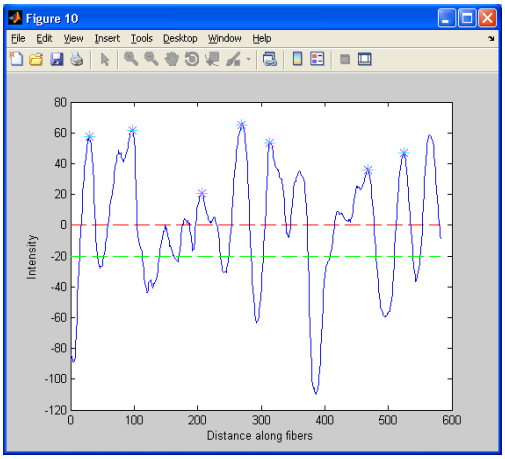

Figure 4.8 For each sub-region, the user selects peaks that cross both the red (mean pixel intensity) and green (deviation of 20 pixels from the mean intensity) lines.

consistently and repeatedly grade the samples, the angle of the highest contrast was chosen for the ease of the blinded graders. Next, the user is asked to draw a line parallel to the tendon long-axis in the primary fiber direction (Fig 4.7). The program then determines the pixel intensity variations along the length of the fiber direction for the selected region. After normalizing the image, average crimp frequency in the fiber direction is determine by pixel fluctuations. The user-selected region is divided in 3 equal sub-regions (Fig 4.7). At each sub-region, the pixel intensities are plotted along the length of the tendon. The pixel intensities are normalized to the mean pixel intensity at that sub-region. Additionally, a line representing a deviation of 20 pixels from the mean is also shown. Users are then prompted to select peaks that both cross the mean intensity threshold and fluctuate by a minimum of 20 pixels from the mean intensity (Fig 4.8). A pilot study was performed examining a variety of inclusion criteria. A deviation of 20 pixels from the mean was determined to be the most consistent and repeatable criteria between users.

b. Software Validation

To validate custom software, preload, toe, and linear-region samples were analyzed for percent crimp area by a previously established semi-quantitative method.[26] A quadrilateral shaped region was selected for each sample for the quantitative analysis was graded by 2 blind graders to determine percent crimped area. Briefly, for each region selected, a grid was drawn over the selection, dividing it into 6 sub-regions. Each sub-region was given a grade of I-III as defined previously.[26] Samples were classified as Type I (substantial crimp), Type II (intermediate crimp), or Type III (minimal crimp).[26]

Representative images for Type I-III crimp were identified for the SST based on the criteria previously established (Fig 4.9).[26] Grader scores were compiled and total percent crimped area was calculated for each sample at each location.[26] Quantitative data was transformed to a I-III scale to compare to the semi-quantitative grading results. To determine intrauser reliability, one researcher repeated the quantitative analysis 3 times for 5 samples. To determine inter-user reliability, two independent researchers performed the quantitative analysis on a subset of samples and their results were compared.

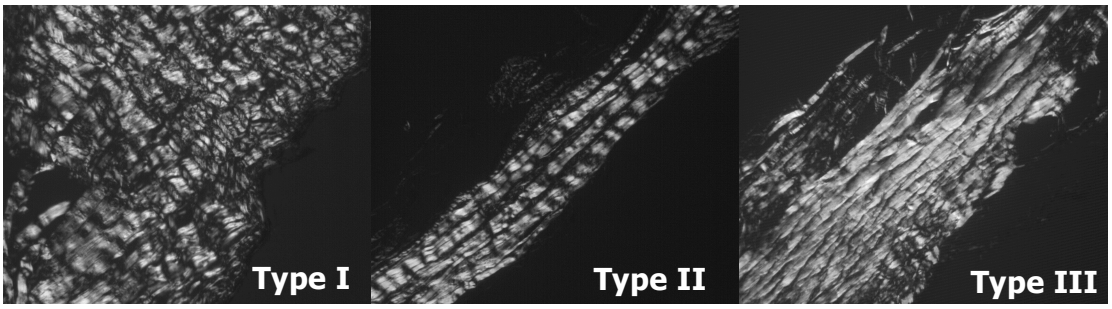

Figure 4.9 Representative samples of type I (left), type II (middle) and type (III) crimp in a SST. Image sizes 670μm x 880μm.

c. Quantitative Analysis

Custom software was used to quantify collagen fiber frequency at the insertion site and midsubstance locations. Briefly, at each selected region, the pixel intensity variation was determined along the length of the tendon in the fiber direction. After normalizing the image, average crimp frequency in the fiber direction was determined by pixel fluctuations. For each location analyzed, the results from the 2 slides were averaged and crimp frequency is reported.

B5. Statistical Analysis

a. Software Validation

Intra-class correlation coefficients (ICC) were used to determine the proportion of variance due to the repeater-user and between-user variability. A high ICC indicates that there is little variation between the frequencies of each sample determined by the users. A Bland-Altman analysis was used to examine consistency between quantitative and semi-quantitative methods.

b. Crimp Frequency

To compare changes in crimp frequency throughout the mechanical testing protocol for each litter, imputation by predictive mean matching was performed.[14,15,30] A 2-way (region of test and location) repeated-measures ANOVA was used and a Bonferroni correction was applied if the interactions were significant. Post-hoc t-tests were used to evaluate changes in crimp frequency and corrections for multiple statistical comparisons were made for each hypothesis.

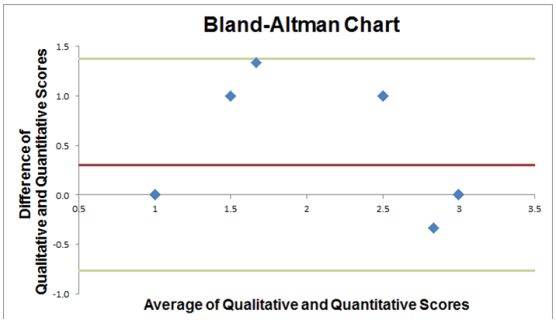

Figure 4.10 Bland-Altman measure of correlation showed random distribution of points, indicating no bias.

To address hypothesis 1, post-hoc paired t-tests were used to compare changes in crimp frequency throughout adjacent points in the mechanical test. For example, the preload and after 5 cycles of preconditioning were compared to determine if a change in crimp frequency occurred during the 5 cycles of preconditioning. Similar methods were used to identify changes in crimp frequency during 10 and 20 cycles in addition to the toe- and linear-regions of the ramp-to-failure. Additionally,

paired t-tests with a Bonferroni correction were made to evaluate changes during the toe-region with each preconditioning protocol. For this hypothesis, significance was set at $p<0.0.16$.

For hypothesis 2, paired t-tests with Bonferroni corrections were made to evaluate changes during each of the preconditioning protocols compared to the preload. Significance was set at $p<0.016$. For hypothesis 3, paired t-tests were used to compare local changes between the insertion site and midsubstance locations.

C. Results

ICC indicated that frequency measurements were consistent and repeatable (0.92 for intra-user and 0.86 inter-user). Bland-Altman plots demonstrated a normal distribution of error between the quantitative and semi-quantitative methods (Fig 4.10). The repeated measures 2-way ANOVA identified that the effect of time (throughout the mechanical test) was significant but that the effect of location was not significant. No significant interaction between time and location was

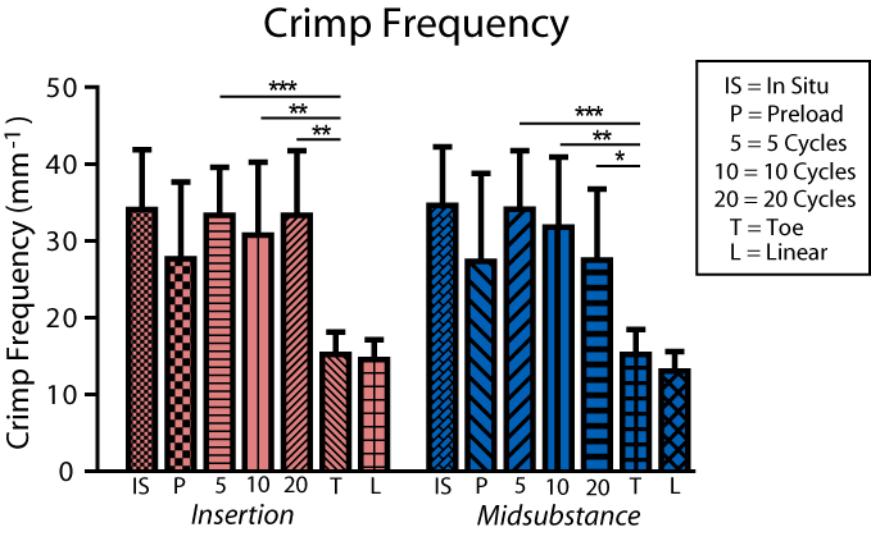

Figure 4.11 Crimp frequency throughout the mechanical test demonstrates a decrease in crimp frequency during the toe-region regardless of the preconditioning protocol or location. Sig=*p<0.016, **p<0.0003, ***p<0.0003.

identified.

Statistical corrections for multiple comparisons were performed by hypothesis. For hypothesis 1, significance was set at $p<0.016$. Significance decreases in crimp frequency were identified at the toe-region with all preconditioning protocols, at both insertion site and midsubstance locations (Fig 4.11). No significant changes in crimp frequency were identified at additional points throughout the mechanical test.

For hypothesis 2, significance was set at $p<0.016$. No significant changes were

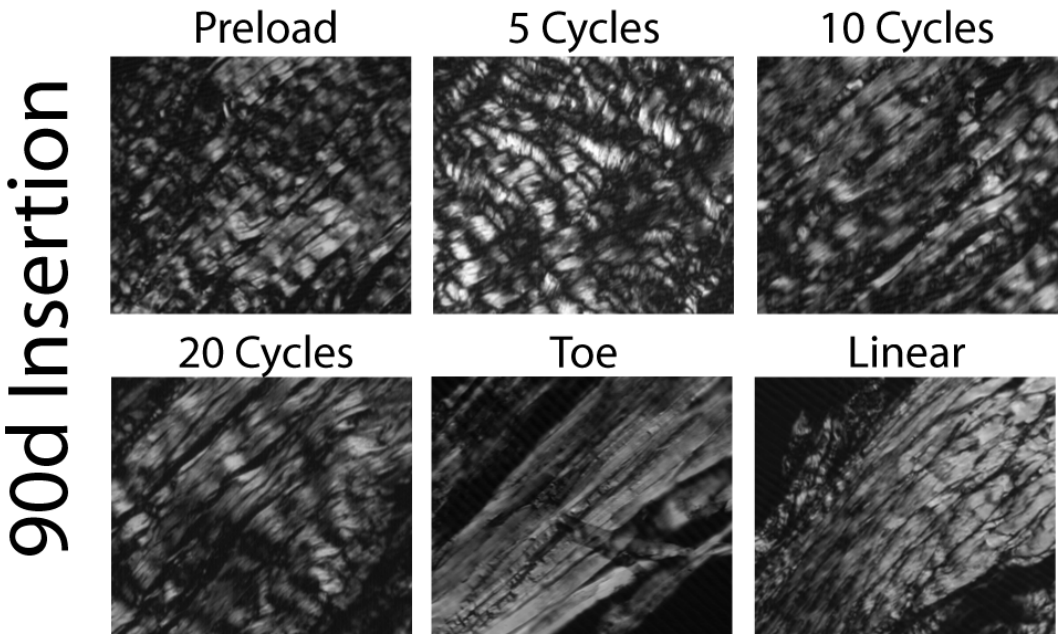

Figure 4.12 Representative histology throughout the test at the insertion site location. Image sizes 250μm x 100μm.

identified with increasing number of preconditioning cycles (Fig 4.11). Histology and average values of crimp frequency throughout the test are reported and demonstrate a mild decrease in crimp frequency with increasing number of preconditioning cycles (Figs 4.12 and 4.13).

D. Discussion

In this chapter, a new, quantitative analysis of collagen fiber crimp frequency was validated with a previously established method.[26] The new custom-software provides the opportunity to obtain quantified crimp frequency values at specific known loads throughout a mechanical testing protocol and this software is an important tool to better understand how crimp structure contributes to mechanical properties and how it is effected by disease, aging, injury, etc.. In chapter 6, the new quantitative method will be utilized to examine how collagen fiber crimp behavior changes throughout postnatal development.

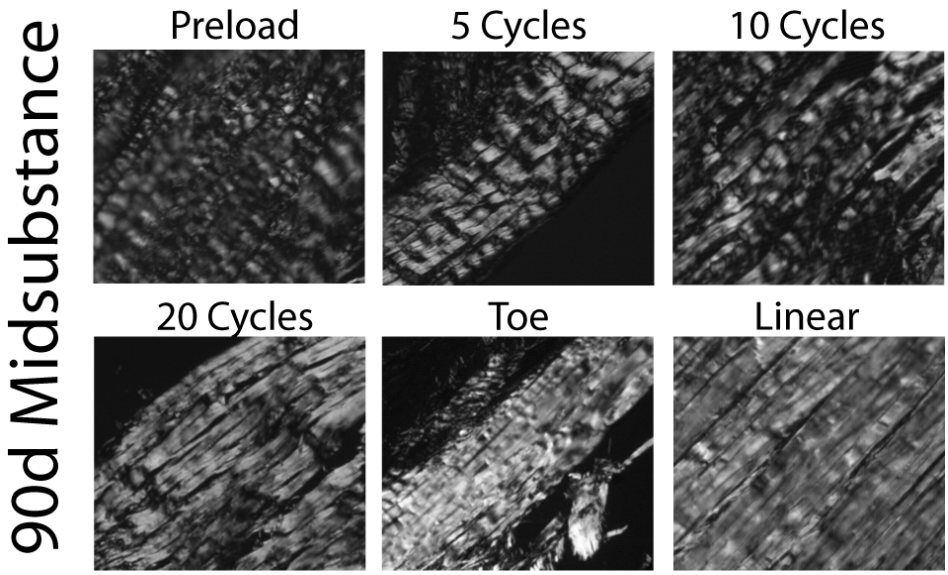

Figure 4.13 Representative histology throughout the test at the midsubstance location. Image sizes 250μm x 100μm.

Additionally, this study identified that the uncrimping of collagen fibers was confined to the toe-region of the mechanical test at both the insertion site and midsubstance locations in mature mouse tendon. Significant decreases in crimp frequency were identified in the toe-region regardless of the preconditioning protocol that

was applied. The results from this study support previous speculation that the uncrimping of collagen fibers may explain the toe-region of the stress-strain curve and contribute to the nonlinear behavior of tendons.[9,11,21-23,27,28]

In addition, this study found no significant differences between crimp frequency at the preload compared to after any of the applied preconditioning protocols (5, 10 or 20 cycles). This suggests that the uncrimping of collagen fibers occurs in the toe-region regardless of the number of preconditioning cycles. However, histology and the reported average values of crimp frequency across all litters indicate that, while not statistically significant, decreases in crimp frequency with increasing number of preconditioning cycles may be present (Figs 4.12 and 4.13). In Chapter 3, we identified that significant collagen fiber re-alignment occurred during preconditioning, regardless of the number of cycles, at both the insertion site and midsubstance locations, supporting previous work suggesting that collagen fiber re-alignment is one possible mechanism of preconditioning.[17,20] The results from this study and Chapter 3 suggest that in response to mechanical load, collagen fibers first re-align in the direction of load and then uncrimp. Histology and reported average values of crimp frequency for all litters (Figs 4.12 and 4.13) suggest that, while not significant, groups of collagen fibers may begin to uncrimp during preconditioning at the midsubstance location. In Chapter 3, we determined that the mouse SST, like the rat and human SST, demonstrates a more highly aligned distribution of collagen fibers at the midsubstance location compared to the insertion site.[12,17] It is possible that some fiber populations at the midsubstance location may begin to uncrimp during preconditioning after the initial re-alignment of those fibers.

Meanwhile, collagen fiber populations at the insertion site are still primarily re-aligning towards the direction of loading to compensate for the more disorganized collagen fiber distribution. In this study, the entire tendon was flash frozen at 5 and 8% strains to represent points in the toe- and linear-regions. While these are appropriate strains to represent each of the corresponding regions, it is possible that the insertion site and midsubstance locations are at different stages of the toe-region, which may provide explanation for these differences in crimp behavior.

Surprisingly, no differences in crimp frequency were identified between the insertion site and midsubstance locations. In Chapter 3, the insertion site was found to have a lower modulus, more disorganized collagen fiber distribution and higher cross-sectional area compared to the midsubstance location. Additionally, the two locations demonstrated different patterns of collagen fiber re-alignment behavior. The more disorganized collagen fiber distribution and lower tensile modulus values have been speculated to be caused by multi-axial loads seen at the insertion site.[12,13,16,17,24,25] The results from this study suggest that crimp frequency may not be affected by the multi-axial loads experienced at the insertion site. Crimp may form regardless of the external mechanical loading environment or it is also possible that crimp formation occurs in response to tensile loading as opposed to compressive or multi-axial loading. The origin of crimp formation is currently unknown. However, the formation of crimp has been speculated to be dependent on one or more of the following factors: mechanical impulses from the contraction of fibroblasts,[8,10] mechanical properties of the collagen fibril and interfibrillar matrix,[10] the formation of elastin fibers,[18] blood circulation,[18] fetal limb

movements,[18] or a passive mechanical mechanism of fiber buckling following shrinkage of the matrix.[8]

Further, no significant differences were identified between crimp frequency at the reference configuration and after the preload (Fig 4.12). The reference configuration, or "in situ" condition, was flash-frozen while still attached to the supraspinatus muscle and humeral head. The lack of significant differences identified between the reference configuration and the preload indicate that the crimp frequency behavior demonstrated throughout the mechanical test may be applicable to the crimp behavior in vivo. This study suggests that the uncrimping of collagen fibers may be an in vivo structural response to mechanical load, not solely an artifact of ex vivo mechanical testing and changing the residual stress experienced by tendon.

This study is not without limitations which must be understood. First, the structural fiber recruitment model was utilized to determine average strain values for the tendon samples using the stress-strain curves from Chapter 3. While the average values are within the parameters to represent the toe- and linear-regions of both the insertion site and midsubstance locations, it is possible that the locations were at different "points" in the toe-region. However, the chosen method improves consistency within this experiment and allowed for comparisons with future experiments, in addition to drawing conclusions across the experimental groups examined in Chapter 3. In addition, this study examined collagen fiber crimp behavior throughout one mechanical testing protocol. Future studies are necessary to determine the effects of collagen fiber crimp behavior in response to different loading protocols and at additional strains in the toe- and

linear-regions at both locations. Further, histology from this project was stained in multiple batches, though the analysis methods performed were consistent and repeatable. Care was taken to ensure that the quantitative software normalized each image by the average pixel intensity and established exclusion criteria based on the standard deviation of pixel fluctuations to exclude artifact and only include fluctuations representing collagen fiber crimp. This method minimizes the potential effect of different batches of stain on the histology analyses. Finally, while the reference configuration samples in this study were flash frozen while still attached to the humerus and supraspinatus muscle, adjacent structures were removed. The supraspinatus tendon is located deep within the shoulder joint, therefore to ensure that the tendon was flash frozen during dissection, the deltoid and additional adjacent structures, such as the infraspinatus and subscapularis, were removed in this study. The removal of these structures may have changed the load experienced by the supraspinatus tendon and may have affected crimp frequency. Future studies are needed to further examine the native crimp frequency and collagen fiber distribution of the supraspinatus tendon at its native state in the body.

In conclusion, this Chapter describes a new quantitative technique for examining collagen fiber crimp frequency at specific, quantifiable points throughout a mechanical test. In addition, local crimp frequency behavior was quantified in a mature mouse SST model. The results from this chapter will serve as baseline values for future comparisons throughout postnatal development to be presented in Chapter 6. Additionally, the information in this chapter as well as Chapter 3 provide the foundational work for examining structural changes in response to load in a mature mouse SST model. Future

work in genetically modified animals or injury models can utilize the data presented in these chapters for baseline comparisons to elucidate the affect of certain genes, diseases or injury on structural behavior.

E. References

1. Ansorge HL, Adams S, Birk DE, Soslowsky LJ: Mechanical, compositional, and structural properties of the post-natal mouse Achilles tendon. **Ann Biomed Eng 39:**1904-1913
2. Boorman RS, Norman T, Matsen FA, 3rd, Clark JM: Using a freeze substitution fixation technique and histological crimp analysis for characterizing regions of strain in ligaments loaded in situ. **J Orthop Res 24:**793-799, 2006
3. Festing MF: Design and statistical methods in studies using animal models of development. **ILAR J 47:**5-14, 2006
4. Franchi M, Fini M, Quaranta M, De Pasquale V, Raspanti M, Giavaresi G, et al: Crimp morphology in relaxed and stretched rat Achilles tendon. **J Anat 210:**1-7, 2007
5. Franchi M, Ottani V, Stagni R, Ruggeri A: Tendon and ligament fibrillar crimps give rise to left-handed helices of collagen fibrils in both planar and helical crimps. **J Anat 216:**301-309
6. Franchi M, Quaranta M, Macciocca M, Leonardi L, Ottani V, Bianchini P, et al: Collagen fibre arrangement and functional crimping pattern of the medial collateral ligament in the rat knee. **Knee Surg Sports Traumatol Arthrosc 18:**1671-1678
7. Franchi M, Raspanti M, Dell'Orbo C, Quaranta M, De Pasquale V, Ottani V, et al: Different crimp patterns in collagen fibrils relate to the subfibrillar arrangement. **Connect Tissue Res 49:**85-91, 2008

8. Gathercole LJ, Keller A: Crimp morphology in the fibre-forming collagens. **Matrix 11:**214-234, 1991

9. Hansen KA, Weiss JA, Barton JK: Recruitment of tendon crimp with applied tensile strain. **J Biomech Eng 124:**72-77, 2002

10. Herchenhan A, Kalson NS, Holmes DF, Hill P, Kadler KE, Margetts L: Tenocyte contraction induces crimp formation in tendon-like tissue. **Biomech Model Mechanobiol**

11. Houssen YG, Gusachenko I, Schanne-Klein MC, Allain JM: Monitoring micrometer-scale collagen organization in rat-tail tendon upon mechanical strain using second harmonic microscopy. **J Biomech 44:**2047-2052

12. Lake SP, Miller KS, Elliott DM, Soslowsky LJ: Effect of fiber distribution and realignment on the nonlinear and inhomogeneous mechanical properties of human supraspinatus tendon under longitudinal tensile loading. **J Orthop Res 27:**1596-1602, 2009

13. Lake SP, Miller KS, Elliott DM, Soslowsky LJ: Tensile properties and fiber alignment of human supraspinatus tendon in the transverse direction demonstrate inhomogeneity, nonlinearity, and regional isotropy. **J Biomech 43:**727-732

14. Landerman LR, Land KC, Pieper CF: An empirical evaluation of the predictive mean matching method for imputing missing values. **Sociological Methods & Research 26:**3-33, 1997

15. Little RJA: Missing-Data Adjustments in Large Surveys. **Journal of Business & Economic Statistics 6:**287-296, 1988

16. Miller KS, Connizzo BK, Soslowsky LJ: Collagen Fiber Re-Alignment in a Neonatal Developmental Mouse Supraspinatus Tendon Model. **Ann Biomed Eng**, 2012

17. Miller KS, Edelstein, L., Connizzo, B. K., and Soslowsky, L. J... Effect of Preconditioning and Stress Relaxation on Local Collagen Fiber Re-Alignment: Inhomogeneous Properties of Rat Supraspinatus Tendon. **Journal of Biomechanical Engineering In press**, 2012

18. Oryan A, Shoushtari AH: Histology and ultrastructure of the developing superficial digital flexor tendon in rabbits. **Anat Histol Embryol 37:**134-140, 2008

19. Peltz CD, Sarver JJ, Dourte LM, Wurgler-Hauri CC, Williams GR, Soslowsky LJ: Exercise following a short immobilization period is detrimental to tendon properties and joint mechanics in a rat rotator cuff injury model. **J Orthop Res 28:**841-845

20. Quinn KP, Winkelstein BA: Preconditioning is correlated with altered collagen fiber alignment in ligament. **J Biomech Eng 133:**064506

21. Rigby BJ: Effect of Cyclic Extension on the Physical Properties of Tendon Collagen and Its Possible Relation to Biological Ageing of Collagen. **Nature 202:**1072-1074, 1964

22. Rigby BJ, Hirai N, Spikes JD, Eyring H: The Mechanical Properties of Rat Tail Tendon. **J Gen Physiol 43:**265-283, 1959

23. Screen HR, Lee DA, Bader DL, Shelton JC: An investigation into the effects of

the hierarchical structure of tendon fascicles on micromechanical properties. **Proc Inst Mech Eng H 218:**109-119, 2004

24. Thomopoulos S, Williams GR, Gimbel JA, Favata M, Soslowsky LJ: Variation of biomechanical, structural, and compositional properties along the tendon to bone insertion site. **J Orthop Res 21:**413-419, 2003

25. Thomopoulos S, Williams GR, Soslowsky LJ: Tendon to bone healing: differences in biomechanical, structural, and compositional properties due to a range of activity levels. **J Biomech Eng 125:**106-113, 2003

26. Thornton GM, Shrive NG, Frank CB: Ligament creep recruits fibres at low stresses and can lead to modulus-reducing fibre damage at higher creep stresses: a study in rabbit medial collateral ligament model. **J Orthop Res 20:**967-974, 2002

27. Viidik A: Simultaneous mechanical and light microscopic studies of collagen fibers. **Z Anat Entwicklungsgesch 136:**204-212, 1972

28. Woo SL: Mechanical properties of tendons and ligaments. I. Quasi-static and nonlinear viscoelastic properties. **Biorheology 19:**385-396, 1982

29. Woo SL, Debski RE, Zeminski J, Abramowitch SD, Saw SS, Fenwick JA: Injury and repair of ligaments and tendons. **Annu Rev Biomed Eng 2:**83-118, 2000

30. Yuan Y: Multiple Imputation Using SAS Software. **Journal of Statistical Software 45:**1-25, 2011

Chapter 5. Collagen Fiber Re-Alignment, Mechanics and Correlations in a Postnatal Developmental Mouse Supraspinatus Tendon Model

A. Introduction

This chapter will quantify local collagen fiber re-alignment and corresponding mechanical properties throughout postnatal development in a mouse supraspinatus tendon model at ages 4, 10 and 28 days. This chapter will compare collagen fiber alignment and mechanical properties throughout development with those at the mature time point of 90 days described in Chapter 2. Additionally, this chapter will examine correlations between fiber alignment and mechanical properties to further elucidate structure-function relationships throughout postnatal development.

One proposed mechanism of tendon structural response to mechanical load is collagen fiber re-alignment. Changes in collagen fiber re-alignment have been shown to vary by tendon location in both the human and rat supraspinatus tendon (SST).[15,18] In a recent study, the tendon-to-bone insertion site in the rat SST demonstrated a more disorganized collagen distribution than the midsubstance throughout the entire mechanical testing protocol.[18] Postnatal tendons, with immature collagen fibrils, may respond to load in a much different manner and at a different time scale than collagen fibers with mature fiber-fiber and fiber-matrix connections. However, collagen fiber re-alignment has not yet been examined throughout postnatal development.

The development of tendon hierarchical structure during fibrillogenesis can be marked by at least three stages, [5,7,33] which have been previously documented in the mouse model.[2,33] Initially during development, collagen molecules assemble to form immature fibril intermediates (4 days old) which assemble end-to-end during linear fibril growth (10 days old). In addition, the distribution of collagen fibril diameter size changes throughout development.[19-22] During early development, the distribution is tight consisting mainly of small diameter fibrils. Throughout development, the distribution increases as fibrils coalesce laterally to form large diameter fibrils. At four days old, a normal distribution of small diameter fibrils was observed and fibril intermediates had begun their initial assembly. By ten days old, the transition from fibril assembly to growth begins and fibril diameters are heterogeneous; large diameter fibrils are present at this stage in addition to smaller diameter fibrils. By thirty days old, a broad distribution of fibril diameters is present with large diameter fibrils being characteristic. While changes in tendon structure throughout development are thought to correlate with increasing stiffness of tendon during maturation, the ability of collagen fibers to re-align in the direction of loading throughout mechanical testing has not been examined in developmental tendon.[29] It is currently unknown if the changing structure seen throughout development affects where collagen fiber re-alignment will occur during the mechanical testing process.

Additionally, the mature SST has demonstrated local differences between the tendon insertion site and midsubstance locations. The tendon insertion site is characterized by a more disorganized collagen fiber distribution and lower linear

modulus than the tendon midsubstance.[14,18,32] Mature tendon-to-bone insertion sites are marked by 4 distinct zones.[32] It has been suggested that the continuous gradation in tissue composition and structure found at the insertion site is necessary to aid in efficient load transfer between tendon and bone as well as to minimize stress concentrations.[3,4,32] A mature fibrocartilaginous insertion site is not formed until 21 days post-natal in the mouse SST, therefore local changes between the insertion site and tendon midsubstance are only expected after 21 days postnatal development.[13] Additionally, it is unknown if tendon will structurally respond to load as a continuous unit before the insertion site is fully developed or if the tendon will be able to successfully transmit loads between the tendon and bone before the insertion site is fully developed. Further, changes in collagen fiber re-alignment and a shift in the mean angle of collagen fibers have been identified in mature rat SST during preconditioning.[18] Collagen fiber re-alignment is postulated to be a mechanism of preconditioning,[18,25,30] however, the effect of the number of preconditioning cycles on collagen fiber re-alignment has not yet been examined.

While there is currently a basic knowledge of compositional and structural changes during development, the mechanical properties of tendon throughout development are not usually measured due to their fragile size and nature.[33] Recent work in our laboratory demonstrated the ability to mechanically test developing mouse Achilles tendon utilizing custom-made fixtures that protect the tendon prior to tensile loading.[1] However, tendon properties are known to vary by location and function and the mechanical properties of developmental supraspinatus tendon have not yet been

examined.

Therefore, the objective of this study was to determine developmental changes in local mechanical and structural behavior in order to address how tendon structurally responds to load as well as to examine tendon inhomogeneity throughout development in a mouse SST model. Additionally, this study will evaluate if collagen fiber re-alignment is dependent on the specific preconditioning protocol (5, 10 or 20 cycles). We hypothesized that: toe- and linear-region moduli will increase throughout development; local differences between midsubstance and insertion site moduli will be detectable at late postnatal development; during late postnatal development, tendons will demonstrate the largest shift in fiber re-alignment during preconditioning while early postnatal development tendons will experience fiber re-alignment during the toe region and with 20 cycles of preconditioning; local differences between midsubstance and insertion site fiber alignment will be detectable in late postnatal development tendon; and that a significant correlation exists between mechanical and organizational properties.

B. Methods

B1. Sample Preparation

This study was approved by the University of Pennsylvania IACUC. Postnatal mice in a C57/BL/6 (Jackson Laboratory) background were bred in house. All litters were reduced to 6 pups within one day of birth to reduce variance from litter size.[11] Pups were weaned at 21 days after birth and separated by sex. Supraspinatus tendons were harvested from male and female postnatal mice at 4, 10, and 28 days old. Three

different mechanical testing preconditioning protocols (5, 10, 20 cycles) were randomly assigned (n=9-11 per age per protocol). Tendons from the same mouse were not used for the same mechanical testing protocol. Supraspinatus tendons were carefully removed under a dissection microscope for mechanical testing. Excess tissue was removed with the tendon still attached to the humeral head. Tendon cross-sectional

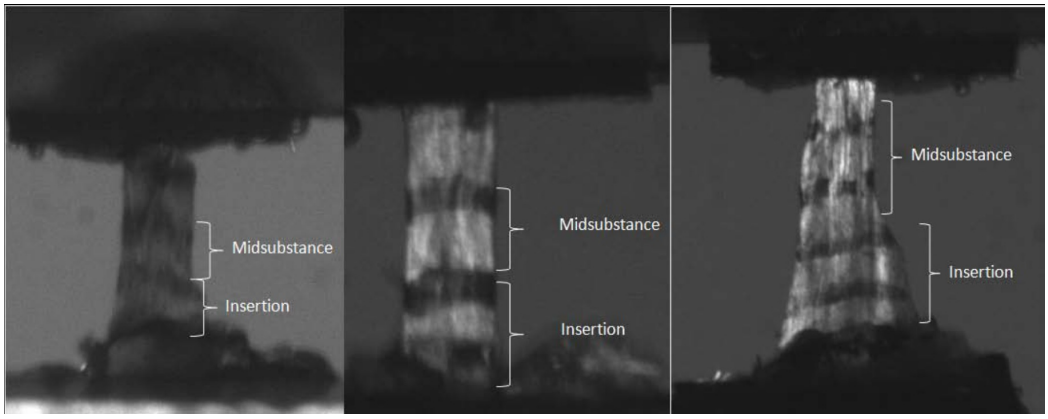

Figure 5.1 Representative SSTs for mechanical testing and polarized light analysis (left to right, 4, 10 and 28 days old). Stain lines denoted insertion site and midsubstance locations. Grip to grip and stain line to stain line gauge lengths were as follows (grip:stain): 4 and 10 days old (1.5mm:0.5mm), 28 days old (2.5 mm: 1mm).

area was measured using a custom built device consisting of LVDTs, a CCD laser, and translation stages.[10] Stain lines were placed on the tendons to denote the tendon insertion site and midsubstance to track strain optically[8] and denote areas for alignment analysis. The humeral head was trimmed to a small bone chip and then both ends of the tendon were secured between pieces of sandpaper with a cyanoacrylate adhesive. Verhoeff's stain was used to mark the tendons as previously described in many studies (e.g. Ansorge 2011).[1] The stain was gently applied using 100μm thread saturated with

Verhoeff's stain to mark the top layer of collagen fibers. Pilot studies performed with and without stain measured similar grip-to-grip mechanical properties indicating that the staining did not damage the postnatal tendons. Grip to grip and stain line to stain line gauge lengths were as follows (grip:stain): 4 and 10 days old (1.5 mm: 0.5 mm), 28 days old (2.5 mm:1 mm) (Fig 5.1). Tendons were secured in the grips and a grip holder was used to ensure that the tendons remained unloaded during handling and mounting for mechanical testing (Fig 5.2).[1]

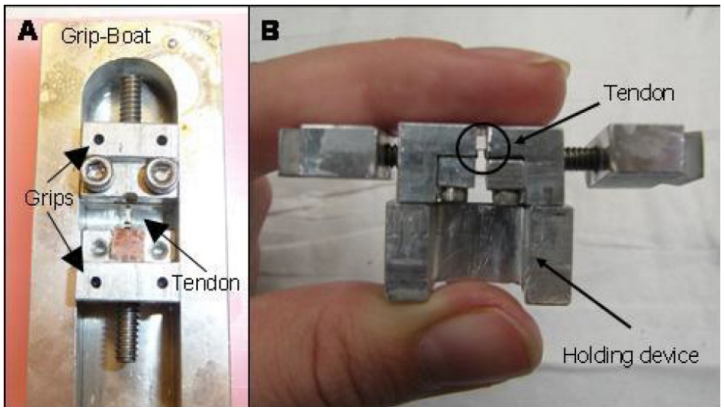

Figure 5.2 A: Custom designed grip-boat with grips. B: Custom designed grip-holder, indicated by the arrow, with a tendon loaded between the grips, indicated with a circle. The grip-holder ensured that the tendon remained unloaded prior to mounting in the Instron testing device. [1]

B2. Mechanical Testing

Samples were placed in a room temperature phosphate buffered saline (PBS) bath and loaded in a tensile testing system (Instron, Norwood, MA) integrated with a polarized light setup, consisting of a linear backlight (Dolan-Jenner, Boxborough, MA), 90°-offset

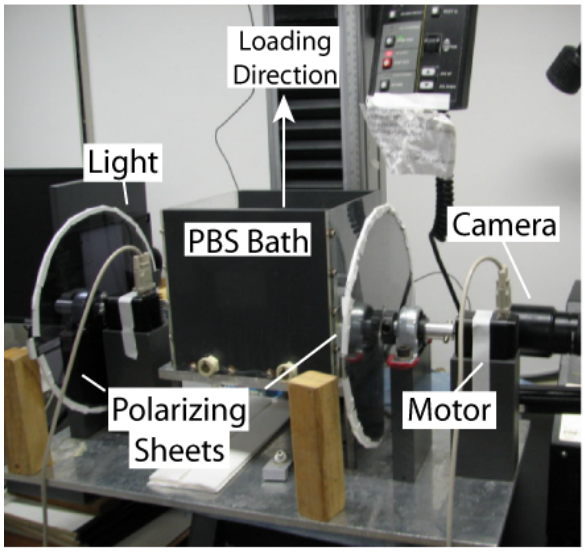

Figure 5.3 Angled side-view of the tendon tensile testing setup showing polarized light and imaging system: light source, rotating cross-polarized sheets, stepper motors, and camera.

rotating polarizer sheets (Edmund Optics, Barrington, NJ) on either side of the test sample, and a digital camera (Basler, Exton, PA) (Fig 5.3).[14] A small pilot study confirmed that collagen fiber re-alignment and mechanical properties were not different when tendons were tested in a room temperature PBS bath compared to a 37° temperature bath. Prior to testing, the stepper motor encoder (Lin Engineering, Santa Clara, CA) was initialized by resetting the encoder value with the polarizer sheets set at a position corresponding to 0º of angular rotation. A 10N load cell was used for all tests. Each supraspinatus tendon underwent the following mechanical testing protocol: preloaded to a nominal load (0.005N for 4 and 10 day tendons, 0.02N for 28 day tendons), preconditioned for either 5, 10 or 20 cycles (0.005-0.008N for 4-10 days old, 0.02-0.04N for 28 days old) at a rate of 0.1%/second and held for 60 seconds (Fig 5.4). Finally, a ramp to failure was performed at a rate of 0.1%/second. Sets of 13 images were acquired every 20 seconds as the polarizers rotated through a 125° range for measurement of fiber alignment during loading. A small pilot study determined that no significant collagen fiber re-alignment occurred during the 60 second hold following

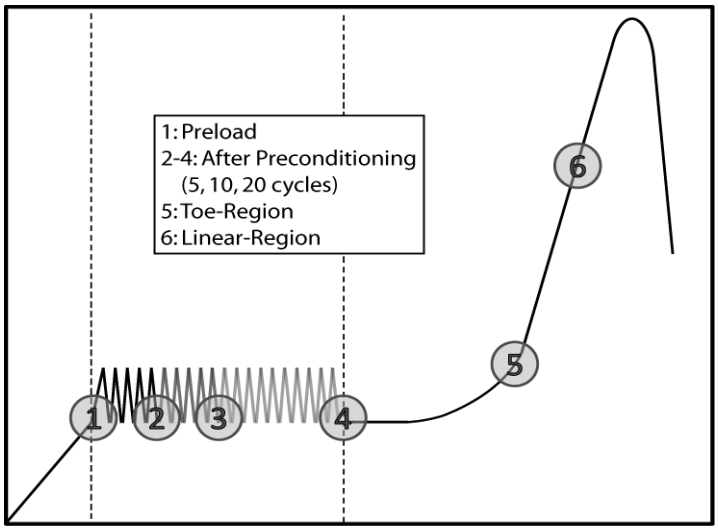

Figure 5.4 A schematic of the testing protocol with six points at which collagen fiber alignment data was evaluated**.**

preconditioning before the ramp-to-failure. Images were taken every 5 seconds for optical strain analysis as described previously.[8]

B3. Data Analysis

The following parameters were measured: transition stress (stress at the intersection of the toe- and linear-regions of the load-displacement curve), transition strain (strain measured at the transition point), local optical toe- and linear-moduli, cross-sectional area, and the spread of the local collagen fiber distribution at several points throughout the mechanical testing process. Local strain was measured optically and stress was calculated as force divided by initial area. A structural fiber recruitment model was used to determine the transition point for each age group (intersection of the toe- and linear-regions of the load-displacement curve).[23] The transition-region was modeled at 50% fiber recruitment and a point in the linear-region was modeled at 75% fiber recruitment utilizing the load-displacement curves. Fiber alignment was calculated from the image sets as previously described.[14,15] Briefly, images of the tendon surface were divided into rectangular areas. Care was taken to maintain a consistent resolution across all age groups for alignment analysis. Pixel intensities were summed by area per image and plotted against angle of polarizer rotation. A sine wave was fitted to the intensity-angle to determine the angle corresponding to the minimum pixel intensity, which represents the average direction of the area's collagen fiber alignment.

Circular variance, transition stress, transition strain, toe-region modulus, and the linear-region stiffness and modulus were determined. Circular variance (VAR), a measure of the distribution of collagen fiber alignment, was calculated for fiber

distributions before and after preconditioning (5, 10, 20 cycles), at the transition region (intersection of toe- and linear-regions: determined using a structural fiber recruitment model at 50% fiber recruitment),[23] and the linear-region strain (at 75% fiber recruitment). Fiber re-alignment during preconditioning was evaluated by comparing VAR values from before preconditioning (BP) and after preconditioning (AP) for each preconditioning protocol. Similar methods were used to determine fiber re-alignment during the toe- and linear-regions of the stress-strain curve.

B4. Statistical Analysis

For all parameters, two-way ANOVAs were used to evaluate interactions between 1) protocol and location and 2) age and location. A one-way ANOVA was used when the interaction was not significant followed by post-hoc tests. In addition, multiple comparisons were evaluated with Bonferroni corrections. Mechanical parameters were evaluated using parametric statistics and the data is presented as mean ± standard deviation (SD). Changes in parameters were compared for tendon location (midsubstance vs. insertion) and tendon age. Alternatively, Shapiro-Wilk tests indicated non-normally distributed data for VAR values and as a result, non-parametric statistical tests were used for evaluating fiber re-alignment. VAR data was analyzed as paired comparisons and is presented as median ± interquartile range. Changes in fiber alignment (Friedman test) were compared for tendon location (midsubstance vs. insertion) and for the mechanical test region (preconditioning, toe- and linear-region). Finally, the Spearman rank correlation coefficients were calculated to evaluate correlations between mechanical and

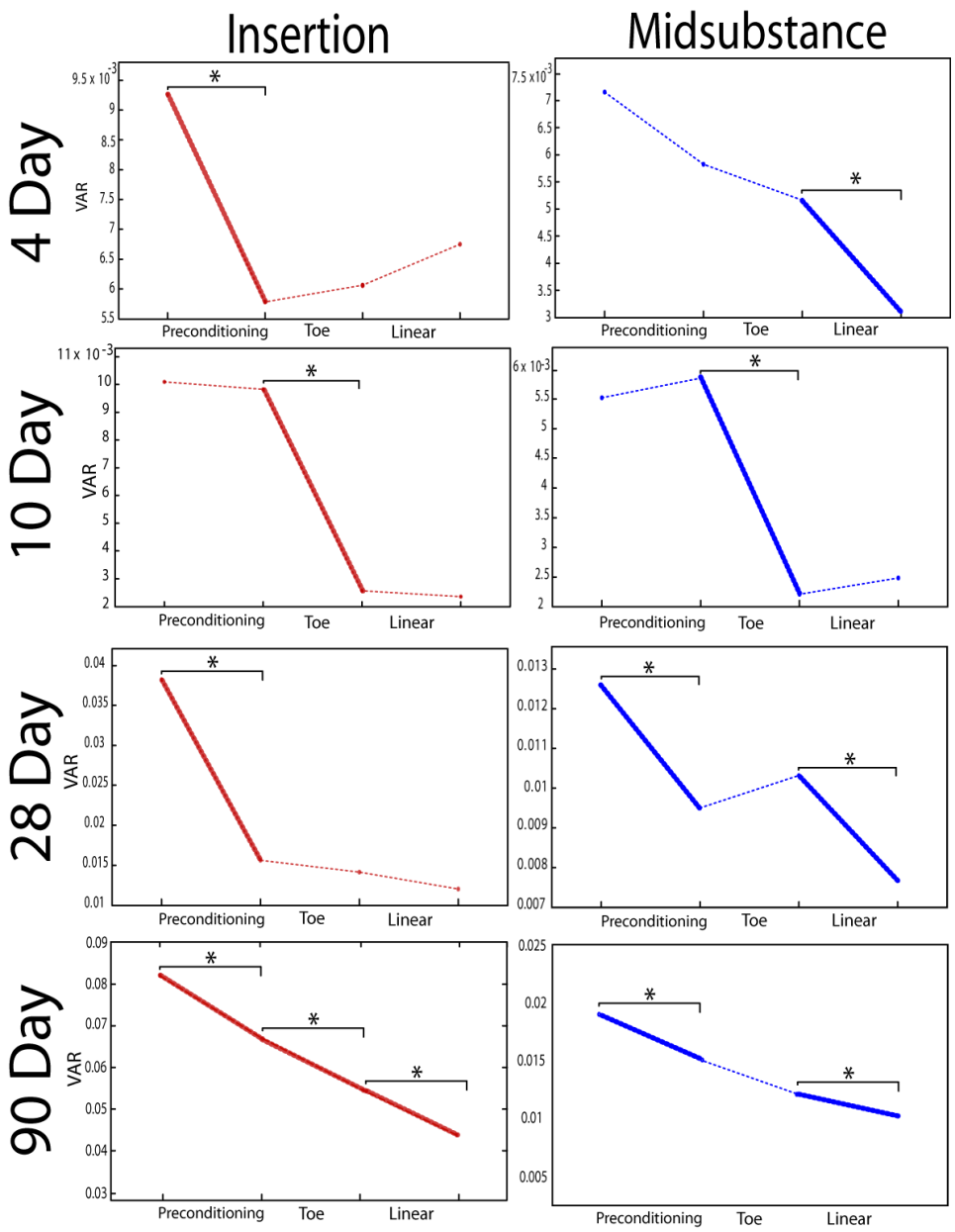

Figure 5.5 Circular variance (VAR) values for representative samples demonstrate that re-alignment (decrease in VAR) occurred during preconditioning for 4 days (top) insertion site, at the linear-region for 4 day midsubstance, at the toe-region for both 10 day (middle) locations, and during preconditioning for both 28 day (bottom) locations. * = $p<0.01$.

alignment parameters.

C. Results

C1. Protocol

No differences in collagen fiber re-alignment or mechanics were found between protocols with varying number of preconditioning cycles. Therefore to increase power, data was pooled across the protocols for the remaining analyses.

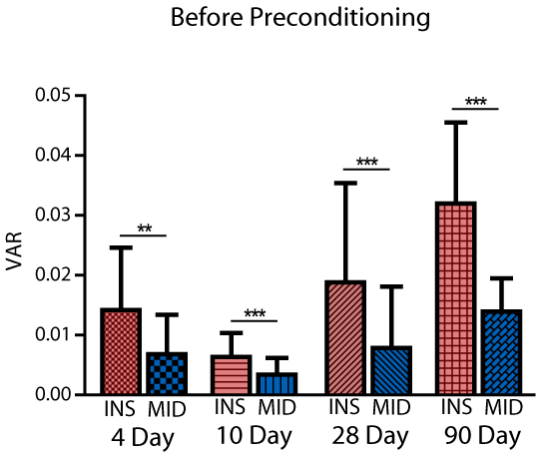

Figure 5.6 Circular variance (VAR) values demonstrate that the insertion site location was more disorganized (higher VAR) than the midsubstance location at all ages before preconditioning. **p<0.005, ***p<0.0005.

C2. Re-Alignment

Region of Test	Age			
	4 days	10 days	28 days	90 days
Before	0.0084*	0.0002*	0.0009*	<0.0001*
After	0.15	0.0008*	0.0003*	<0.0001*
Transition	0.32	0.031	0.0008*	<0.0001*
Linear	0.15	0.0006*	0.0005*	<0.0001*

Table 5.1 *Indicates significant difference at p<0.025, compares distributions at the insertion site and midsubstance locations throughout the mechanical test.

At 4 days old, the midsubstance location re-aligned in the linear-region while the insertion site re-alignment occurred during preconditioning (Fig 5.5). At 10 days old, both the midsubstance and insertion site locations re-aligned in the toe-region of the stress-strain curve. At 28 days old, collagen fiber re-alignment occurred during preconditioning for both locations as well as during the linear-region for the midsubstance. Locally, the insertion site of the tendon was more disorganized than the

midsubstance only before preconditioning in 4 day old tendons (Fig 5.6). The insertion site was more disorganized than the tendon midsubstance at all mechanical testing points, except at the 10 day transition point, in 10 and 28 day old tendons (Fig 5.6 (before preconditioning) and Table 5.1).

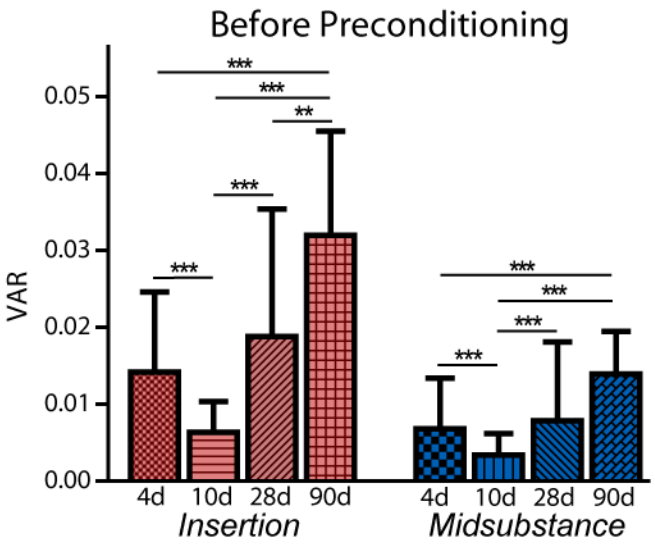

Figure 5.7 Circular variance (VAR) values throughout developmental age demonstrate that collagen fiber alignment increases (decreases in VAR) from 4 to 10 days. After 10 days, collagen fiber alignment decreases with developmental age at both locations. *p<0.016, **p<0.003, ***p<0.0003.

Collagen fiber alignment before preconditioning increased (decrease in VAR) from 4 to 10 days at both locations (Fig 5.7, data presented as median+interquartile range). A decrease in collagen fiber alignment (increase in VAR) was found between 4 and 90 day tendons at both locations. Collagen fiber alignment decreased from 10 to 28 days and from 10 to 90 days at both locations. A decrease in alignment was also found between 28 and 90 days at the insertion site.

C3. Mechanics

Local differences in toe modulus were found at 4 days and 28 days old with the midsubstance location having a higher modulus than the insertion site (Fig 5.8). Additionally, there was an increase in toe modulus from 4 to 90 days at the insertion site and from 4 to 28 and 4 to 90 days at the midsubstance location (Fig 5.9 & Table

5.2). Additionally, an increase in toe modulus was found at the midsubstance location from 10 to 28 days and from 10 to 90 days. Toe modulus also increased from 28 to 90 days at the insertion site location (Fig. 5.9).

Surprisingly, the linear modulus was greater at the tendon midsubstance than at the insertion site for all age groups (4, 10 and 28 days) (Fig 5.10). Additionally, there was an increase in linear modulus at the insertion site location at all ages compared to 4 days (Fig 5.11). 90 day midsubstance linear modulus was also higher than the 4 day midsubstance. Additionally, linear modulus was higher at 90 days compared to 28 days at both locations (Fig 5.11).

The transition stress for the insertion site location decreased from 4 days to 28

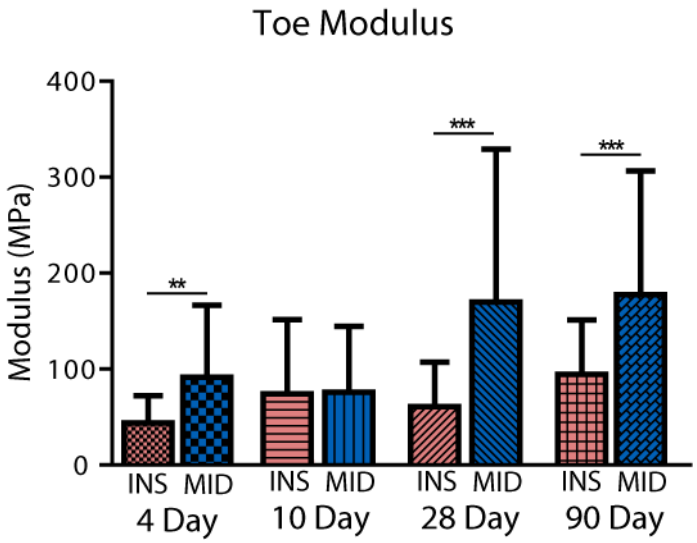

Figure 5.8 A lower toe modulus is present at the insertion site compared to the midsubstance location at 4, 28 and 90 days.*p<0.025, **p<0.005, ***p<0.0005.

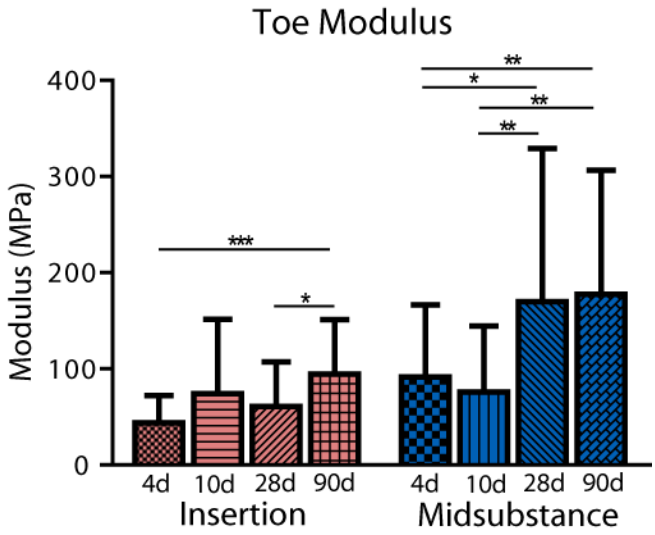

Figure 5.9 Toe modulus increases throughout development from 4 and 28 days compared to 90 days at the insertion site and from 4 and 10 days compared to 28 and 90 days at the midsubstance location. *p<0.016, **p<0.003, ***p<0.0003.

days (Table 5.2). The transition strain at the insertion site was higher than at the midsubstance location at 4 days old (Fig 5.12). Additionally, the transition strain was larger at the 4 day insertion site location compared to all time points and at the midsubstance location compared to 28 days (Fig 5.13). At the midsubstance location, transition strain was larger at the 10 days compared to 28 days as well as at 28 days compared to 90 days (Figs 5.13 and 5.14).

Stiffness increased with age across all time points at both locations, with the exception of at the midsubstance location between 10 and 28 days. Cross sectional-area was larger at the insertion site location than the midsubstance at 28 days old (Fig 5.15). Increases in cross-sectional area with age were present at all time points at both locations (Fig 5.16 & Table 5.2).

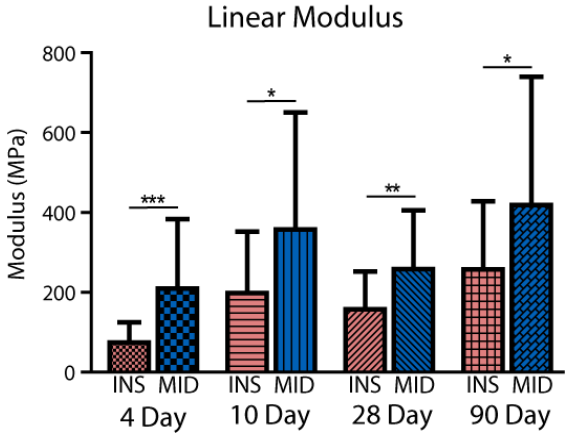

Figure 5.10 A lower linear modulus is present at the insertion site compared to the midsubstance location at all time points. *p<0.025, **p<0.005, ***p<0.0005.

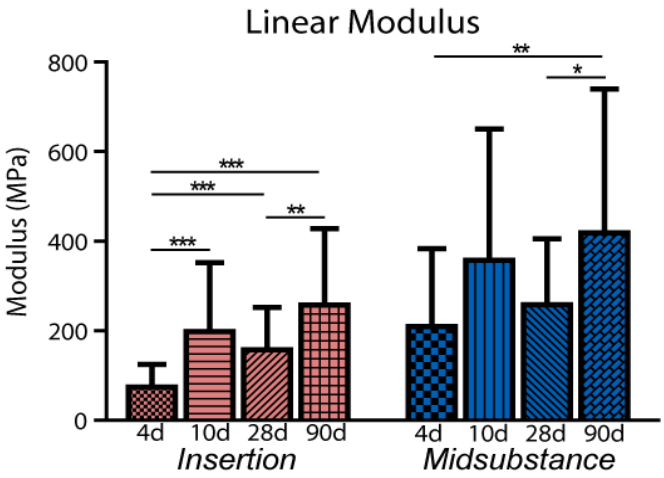

Figure 5.11 An increase in linear modulus is seen between 4 and 10, 28, and 90 days at the insertion site and between 4 and 90 days at the midsubstance location. Additionally, 90 day linear modulus values were higher at 90 days compared to 28 at both locations. *p<0.016, **p<0.003, ***p<0.0003.

C4. Correlation

A negative and significant correlation was found between collagen fiber alignment and mechanics for both the before (r_s=-0.24, p=0.001) and after preconditioning (r_s=-0.20, p=0.007) VAR values and linear-region modulus for 4, 10, and 28 day data. The strongest correlation between alignment values before and after preconditioning and linear modulus was found at 28 days: before (r_s=-0.42, p=0.0008) and after preconditioning (r_s=-0.42, p=0.001). The 90 day and 28 day data together resulted in low correlations but significant negative correlations for late development between alignment before and after preconditioning and linear modulus: before (r_s=-0.24, p=0.006) and after preconditioning (r_s=-0.22, p=0.01).

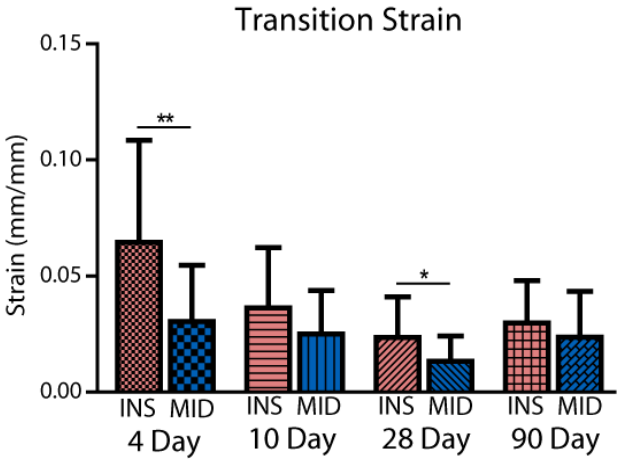

Figure 5.12 A higher strain was required to transition to the linear-region at the insertion site compared to the midsubstance location at 4 and 28 days. *p<0.025, **p<0.005, ***<0.0005.

A positive and significant correlation was found between collagen fiber alignment and transition

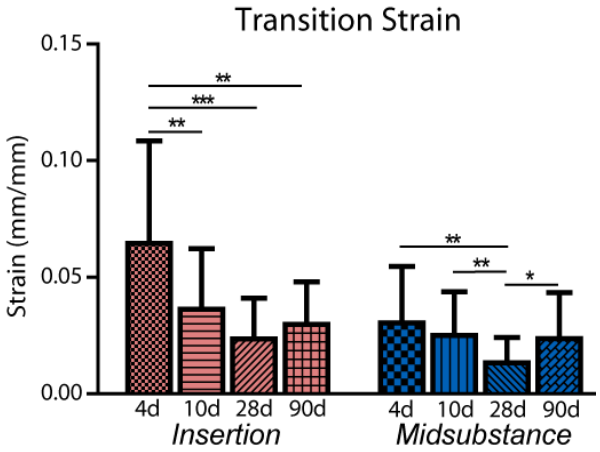

Figure 5.13 Transition strain decreases with age at the insertion site from 10 to 28 days at the midsubstance. *p<0.016, **p<0.003, ***p<0.0003.

strain for both the before (4 days: r_s=0.45, p=0.0008; 10 days: r_s=0.37, p=0.004)) and after preconditioning (4 days: r_s=0.38, p=0.005; 10 days: r_s=0.31, p=0.01) VAR values at 4 and 10 days old.

Combining the 4 and 10 day data gives a moderate correlation between collagen fiber alignment before preconditioning and transition strain for early development (r_s=0.47, p<0.0001).

D. Discussion

This study quantified mechanical properties throughout postnatal development in the mouse SST. As expected, mechanical properties increased throughout development. Specifically, increases in the toe- and linear-moduli (Fig 5.9 and Fig 5.11) as well as cross-sectional area (Fig 5.16) were seen throughout development. The results in the developmental SST support similar findings from previous work in the midsubstance of the mouse Achilles tendon.[1] Both the SST and Achilles tendon demonstrated an increase in linear modulus from 4 to 10 days but no significant differences between 10 and 28 days (Fig 5.11). Additionally, a decrease in transition strain was noted from 10 to

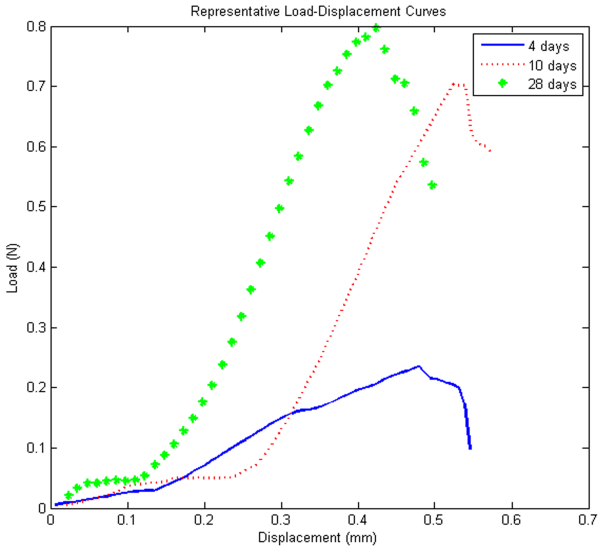

Figure 5.14 A representative load-displacement curve from each age group (4, 10 and 28 days) is shown demonstrating the decrease in transition strain between 28 and 10 day tendons.

28 days at the midsubstance location in the SST and Achilles tendon.[1] Transition strain also decreased with all time points at the insertion site in the present study (Fig 5.13 and 5.14). The large transition strain found at early developmental ages suggests that the structural changes that occur during the toe-region of the mechanical test may take longer in developmental tendon. The toe-region of the mechanical test is thought to be explained by uncrimping of collagen fibers. It has been speculated that early developmental tendons possess a higher frequency of collagen fiber crimp potentially explaining the elongated toe-region.[9] Additionally, it is possible that the immature collagen fibril network (lack of long, continuous collagen fibrils, established collagen cross-links, proteoglycan bridges and branches between collagen fibrils)[6] limit effective communication between neighboring fibrils, resulting in a slower response to mechanical load through both collagen fiber re-alignment and uncrimping throughout development. Tendons have a complex hierarchical structure where procollagen molecules assemble to form collagen fibrils, which form fibers, which form fascicles, which form tendon. In this study, tendon level mechanics and fascicle level structural changes are quantified. However, local fascicle level structural changes are reported which represent the

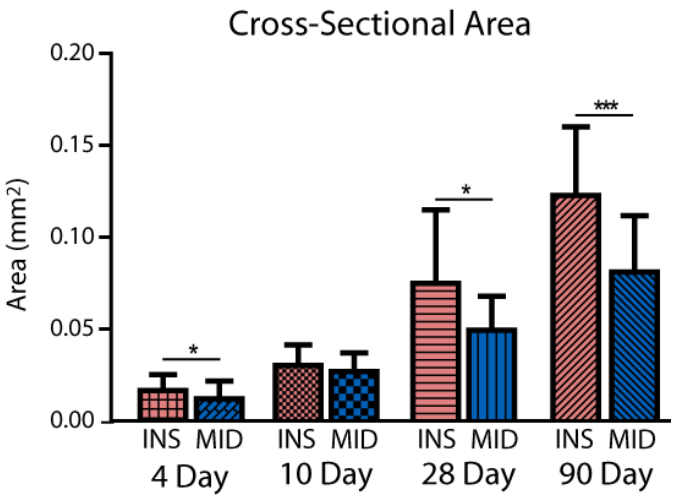

Figure 5.15 Locally, the insertion site demonstrated a higher cross-sectional area than the midsubstance at 28 and 90 days. *p<0.025, **p<0.005, ***p<0.0005.

structural behavior on the scale of collagen fibers. Therefore, we will be reporting local collagen fiber re-alignment. Additionally, throughout this discussion, previously documented changes in collagen fibril structure will be used to interpret observed results in collagen fiber re-alignment and mechanical properties. However it is currently not known how collagen fibril level structure influences structural changes at the collagen fiber level or tendon level mechanics and merits further study as the transition of load and mechanical properties from fibril to fiber level structure is unclear.

Interestingly, this study shows that significant collagen fiber re-alignment occurs at different points in the mechanical loading protocol, indicating that the tendon's ability to structurally respond to load through re-orientation of collagen fibers in the direction of load is dependent on developmental age and more importantly, level of tissue organization or maturity. As hypothesized, fiber re-alignment occurred during preconditioning at both locations in 28 day tendon (Fig 5.5). However, no changes in fiber alignment were demonstrated during the toe-region at 28 days for either location. In Chapter 3, collagen fiber re-alignment occurred throughout the entire mechanical test at the insertion site of 90 day tendons (Fig 5.5). Additionally, 90 day tendons are more

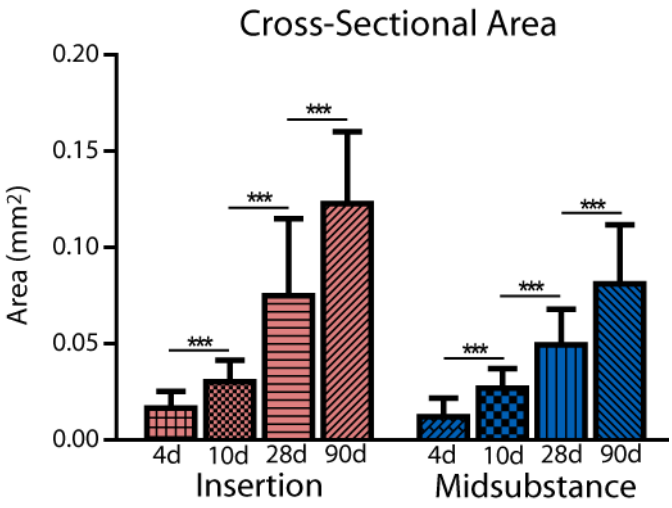

Figure 5.16 Increases in cross-sectional area with age were found at both locations for all comparisons. *p<0.016, **p<0.003, ***p<0.0003.

disorganized at the insertion site compared to 28 day tendons (Fig 5.7). These results suggest that the 90 day tendons have continued to remodel and lay down a more heterogeneous fiber population in response to the multi-axial loads experienced at the tendon-to-bone insertion site. In the linear-region, however, re-alignment was found to occur at the midsubstance location but not at the insertion site, paralleling the response of the 90 day midsubstance (Fig 5.5). These results show that the 28 day tendon responded structurally at the first sign of load, despite the magnitude of load for the preconditioning protocols, and demonstrated similar behavior to the mature rat SST.[18]

At 10 days, collagen fiber re-alignment occurred during the toe-region of the mechanical test at both locations (Fig 5.5). Interestingly, the re-alignment behavior at 4 days was location-dependent. The midsubstance of the tendon re-aligned in the linear-region and the insertion site re-aligned during preconditioning (Fig 5.5). These results suggest that early developmental tendons require either higher loads or a longer exposure to load before responding structurally. The delay in structural response could potentially be explained by the immature networks of collagen fibrils that have been previously demonstrated at 4 and 10 days in mouse tendon.[33] Four day mouse tendons have been shown to consist of disconnected collagen fibril intermediates, while at 10 days collagen fibrils have linearly fused but still consist primarily of small diameter fibrils.[33] While it is currently not known how the fibril level structure relates to fiber level behavior, the results from the present study at 4 days suggest that the ability of a collagen fiber network composed of small collagen fibril intermediates may be insufficient to communicate and

Age (Days)	Location	Initial Area (mm^2)	Toe Modulus (MPa)	Linear Modulus (MPa)	Transition Strain (mm/mm)
4	Insertion	0.016 ± 0.01^{bcd}	43.7 ± 28.6^{ad}	74.1 ± 50.8^{abcd}	0.064 ± 0.04^{abcd}
10		0.030 ± 0.01^{acd}	74.0 ± 77.6	198.5 ± 153.9^{a}	0.036 ± 0.26
28		0.075 ± 0.04^{ad}	60.8 ± 46.3^{ad}	157 ± 94.6^{ad}	0.024 ± 0.02
90		0.12 ± 0.04^{a}	98.9 ± 60.3^{a}	257.4 ± 170.7^{a}	0.031 ± 0.02
4	Midsub	0.012 ± 0.01^{bcd}	91.6 ± 74.9^{cd}	209.7 ± 174.2^{d}	0.03 ± 0.02^{c}
10		0.027 ± 0.01^{cd}	75.8 ± 68.7^{cd}	357.5 ± 292.9	0.025 ± 0.02^{c}
28		0.049 ± 0.02^{d}	170.0 ± 159.2	258.3 ± 147.3^{d}	0.013 ± 0.01^{d}
90		0.081 ± 0.03	177.4 ± 129.2	477.5 ± 398.1	0.34 ± 0.25

Table 5.2 Data represented as mean ± st dev. [a]Significant comparisons between midsubstance (abbreviated "midsub") and insertion site location; [b]Significantly different from 10 days, [c]Significantly different from 28 days, [d]Significantly different from 90 days. Significance set at $p<0.016$.

transmit load. It is possible that fibers are unable to communicate to each other due to the lack of a developed collagen fibril network and collagen-matrix interactions that may help transmit and support load between the insertion site and tendon midsubstance. Changes in collagen cross-links, crimp morphology and proteoglycan content in tendon are thought to be related to the mechanical properties of tendon in transmitting tensional

forces.[12] In particular, the lack of mature collagen fibril cross-links or proteoglycan bridges between adjacent fibers may prevent the transmission of tensile forces between adjacent collagen fibrils or fibers, resulting in a longer toe-region and lack of communication between the insertion site and tendon midsubstance during early postnatal development. Additionally, while linear fusions are present in collagen fibrils at 10 days postnatal, the fibril network is still underdeveloped. However, long, continuous collagen fibrils are one proposed mechanism by which tendons transmit load.[24] While the exact mechanism of load transfer is still under debate, the present study supports this, suggesting that elongated collagen fibrils may allow the tendon to uniformly respond to load at the fiber level as seen in the 10 day uniform re-alignment during the toe-region. Linear growth of collagen fibrils has been suggested to be integral in the development of mechanical stability and has been correlated to increases in ultimate tensile strength and elastic modulus.[29] The increases in collagen fibril length could be a consequence of fibril fusion and crosslink formation enabling for quicker communication and transmission of loads between collagen fibrils, which may result in a shorter transition region and increased modulus values at higher hierarchical scales. Additionally, a higher strain was necessary to transition from the toe- to linear-region of the stress-strain curve at 10 days compared to 28 days (Figs 5.13 and 5.14). This indicates that although the collagen fibrils are linearly growing, the collagen fibers still require longer exposure to loads, or higher loads, to reach the linear-region of the mechanical test.

Local differences in mechanical properties, collagen fiber distribution and collagen fiber re-alignment behavior were examined throughout postnatal development. At 4

days, differences in collagen fiber distribution and collagen fiber re-alignment behavior suggest that the insertion site and tendon midsubstance develop at different rates. The lack of organized and mature tissue at the insertion site is a potential explanation for the local differences seen at 4 days old. Previous work has shown that at 3 days old the tendon insertion site is composed primarily of type II collagen as opposed to the 4-zone insertion seen in mature tendon.[13] Additionally, as previously discussed, the collagen fibril network at 4 days has been demonstrated to be small, disconnected fibril intermediates that may affect the ability of collagen fibers to communicate or transmit load from one tendon location to another.[6] It is possible that the mechanical properties measured in 4 day tendon (particularly at the insertion site location) are primarily representative of the tendon extracellular matrix (as opposed to primarily the disconnected collagen fibrils) (Fig 5.14).

In addition to demonstrating different local re-alignment behaviors, 4 day old tendons were more disorganized at the insertion site compared to the tendon midsubstance only before preconditioning. Remarkably, following re-alignment during preconditioning at the insertion site, differences in collagen fiber distribution were no longer detectable between the midsubstance and insertion (Table 5.1). Collagen fibers at midsubstance location may be more developed as indicated by their higher linear modulus and more organized collagen distribution compared to the insertion site. The 4 day tendon midsubstance behaves as expected with a delayed re-alignment response compared to mature SST and 10 day tendon (Fig 5.5). These results suggest that the midsubstance collagen fibril and fiber networks are more developed than the insertion site and can

gradually recruit fibers in the direction of load (as represented by the long transition-region seen at 4 days), while the insertion site is composed primarily of a disconnected group of fibril intermediates affecting it collagen fiber structural behavior. One possible explanation for this is that the tendon midsubstance may experience tension from the surrounding muscle throughout development.[28] Previous work has noted that the development of functionally distinct fibrocartilages occurs at different rates in the rat Achilles and quadriceps tendons.[26,27] It is possible that the local differences seen in mechanics and alignment behavior can be explained by the midsubstance and insertion site developing at different rates. The insertion site might need to be more developed before successfully transmitting loads or providing communication between the midsubstance and insertion site locations.

Local differences in linear modulus and collagen fiber distribution were found at 10 days (Figs. 5.11 and 5.6). Weaker mechanical properties and more disorganized collagen fiber distributions were found at the insertion site compared to the midsubstance location. However, while differences were present in mechanics and collagen fiber distributions, the two locations demonstrated similar collagen fiber re-alignment behavior (Fig 5.5) and no differences in toe-region modulus (Fig 5.8). The insertion site may be more developed at 10 days compared to 4 days, allowing for communication and load transmission. Previous studies have shown that the transition zone and layers of fibrocartilage near the insertion site were evident, regardless of mechanical stimuli, at 7 days postnatal.[31] Additionally, type X collagen and mineralized fibrocartilage have been found at the insertion site location in 14 day old tendon.[31] Ten day tendons may be

beginning to experience complex loads commonly occurring in mature animals at the tendon-to-bone insertion site, as demonstrated by the more disorganized collagen fiber distribution and lower modulus compared to the midsubstance location.

Additionally, local differences in mechanical and organizational properties were found at 28 days. Decreased modulus and more disorganized collagen fiber distributions were present at the insertion site compared to the midsubstance location. Previous work demonstrated that by 21 days, the characteristic 4 zone insertion site is fully developed.[13] Additionally, it has been demonstrated that mechanical stimuli are necessary to form the transitional fibrocartilaginous insertion site.[31] These previous studies, together with the strong local differences shown in the present study for mechanical properties and fiber distribution, suggest that the insertion site experiences complex multi-axial loads at 28 days old which continue throughout maturity. Similar to the 90 day animals in Chapter 3, a difference in re-alignment behavior was found at 28 days between the insertion site and midsubstance locations (Fig 5.5). Previous work examining mature rat SST and subscapularis tendon found identical re-alignment behavior between the insertion site and midsubstance.[16,18] The 28 day tendon midsubstance was found to re-align in the linear-region of the mechanical test in addition to during preconditioning in this study, paralleling the behavior of the 90 day midsubstance (Fig 5.5). It is possible, that the differences in re-alignment behavior are unique to mouse SST. Postnatal mouse tendons are not considered mature until 3-4 months old, therefore one potential explanation for the discrepancy between collagen fiber re-alignment behavior seen at the 28 day insertion site compared to the 90 day insertion site is that the collagen fiber-fiber interactions (such

as proteoglycan bridges), collagen fibril cross-links and fiber-matrix interactions are not yet fully mature. Additional cross-links and fiber-matrix interactions will provide a more complex, interconnected network of fibrils, increasing mechanical strength and the potential for load transmission across the tendon. Further, collagen fibrils have been shown to branch and weave in and out of adjacent collagen fibers as they develop, forming additional connections with other collagen fibers which may increase the ability for load transmission across the tendon.[6] While a fully mature network is expected to allow the fibers to communicate and transmit load to other fibers at a fast rate and to respond to load quicker, the additional bonds formed between the collagen fibrils, fibers and the other components of the extracellular matrix will also provide additional resistance for the fibers to rotate toward the direction of loading. It is possible that a larger number of fibers rotate initially during preconditioning in the 28 day tendons, while collagen fibers from mature tendons may continue to recruit and re-align in the direction of load throughout the remainder of the mechanical test. Another potential explanation is that the tendon is beginning to fail at the insertion site and that collagen fibers are damaged or broken therefore preventing the tendon from demonstrating additional re-alignment following preconditioning. SSTs at 90 days failed at higher loads and it is expected that the collagen fibers comprising the 90 day tendons fail at higher loads compared to the 28 day fibers. It is possible that the 28 day tendons did not demonstrate significant re-alignment in the toe- and linear-regions as while some populations of fibers re-aligned in the direction of loading, those initially recruited fibers were catastrophically failing.

This study also determined that a low (r_s=-0.24) but significant (p=0.001) correlation exists between mechanical and organizational properties for the 4, 10 and 28 day data. A negative correlation was identified between linear modulus and the before preconditioning and after preconditioning circular variance values, suggesting that increased alignment (decr VAR) is correlated with increased mechanical properties. This finding further supports previous work in the human SST that found a negative correlation between linear modulus and VAR values.[15] Interestingly, the strongest correlation between alignment values before and after preconditioning was found at 28 days: before (r_s=-0.42, p=0.0008) and after preconditioning (r_s=-0.42, p=0.001) while a low but significant correlation was found between before and after preconditioning values and linear modulus at 90 days. This suggests that additional cross-link formations between fibril, fiber-fiber, and fiber-matrix connections that form during late development may contribute to a more disorganized, but more connected collagen fibril and fiber networks. After re-aligning in the direction of loading, the connected collagen fibril network may be contributing to the increase in tendon's linear modulus noted between 28 and 90 days at both locations (Fig 5.11).

Additionally, a positive and significant correlation was found between collagen fiber alignment and transition strain for both the before (4 days: r_s=0.45, p=0.0008; 10 days: r_s=0.37, p=0.004)) and after preconditioning (4 days: r_s=0.38, p=0.005; 10 days: r_s=0.31, p=0.01) VAR values at 4 and 10 days old. A more disorganized collagen fiber distribution and higher strain before transition to the linear-region was noted at the 4 day insertion site compared to the midsubstance location. The correlation between collagen

fiber alignment and transition strain at 4 days further supports the concept that the insertion site and tendon midsubstance develop separately and at separate rates as the more highly aligned midsubstance can respond to load in a quicker manner and time scale than its less developed insertion site counterpart. Combining the 4 and 10 day data gives a moderate correlation between collagen fiber alignment before preconditioning and transition strain for early development (r_s=0.47, $p<0.0001$). Four day tendons demonstrated a more disorganized collagen fiber distribution and required a higher transition strain than the 10 day samples at both locations. This correlation further supports the idea presented earlier in this chapter that the disorganized, small group of fibril intermediates comprising the 4 day tendon may be influencing the ability of collagen fibers to recognize and respond to mechanical load, while the 10 day tendons' fibrils have begun to fuse linearly and may allow for more effective communicate between collagen fibers.[17]

This study is not without assumptions which must be understood. First, toe- and linear-region VAR values for each age group were determined using the average strain quantified from the individual sample fiber recruitment model results in order to make comparisons at one consistent strain value per developmental age rather than individually determining an appropriate value to represent the toe- and linear-region for each individual sample and at each location. We are confident that the average values are within the parameters to represent the toe- and linear-regions of each age group and that the chosen method improves consistency within this experiment in addition to allowing for comparisons with future experiments examining additional mechanisms of structural

changes. Secondly, the crossed polarizer method used in this study can only measure fibers ±45º from the tendon long axis instead of the full 180º range that would contain all possible fiber orientations. An angle value correction was applied based on the assumption that fibers must reorient toward the direction of loading as has been performed previously.[15] Finally, collagen fibril diameter has not been examined in the mouse supraspinatus tendon at all ages throughout development. The ages chosen for this study were based on results from the mouse Achilles tendon and results may vary by tendon. However, a broad range was utilized that likely spans the relevant ages.

In conclusion, this study demonstrated that tendon collagen fiber re-alignment may be dependent upon developmental age and that collagen fibril development may affect the tendon's ability to structurally respond to load on a higher hierarchical level. Additionally, the study identified a negative correlation between linear modulus and collagen fiber distribution before and after preconditioning across all developmental time points (4, 10 and 28 days). Additionally, a correlation was identified between collagen fiber distribution before preconditioning and transition strain at early developmental time points (4 and 10 day). Further, this study provides valuable insights regarding the development of the supraspinatus tendon insertion site in the mouse. Chapter 6 studies will investigate local changes in collagen fiber crimp throughout development to determine if crimp behavior can further explain the observed changes in transition strain and re-alignment. Additionally, further work is necessary to examine collagen fibril development in the mouse SST and the influence of fibril level changes on higher hierarchical scales as well as to examine mechanical properties on smaller hierarchical

scales.

E. References

1. Ansorge HL, Adams S, Birk DE, Soslowsky LJ: Mechanical, compositional, and structural properties of the post-natal mouse Achilles tendon. **Ann Biomed Eng 39:**1904-1913
2. Ansorge HL, Meng X, Zhang G, Veit G, Sun M, Klement JF, et al: Type XIV collagen regulates fibrillogenesis: premature collagen fibril growth and tissue dysfunction in null mice. **J Biol Chem 284:**8427-8438, 2009
3. Benjamin M, Kumai T, Milz S, Boszczyk BM, Boszczyk AA, Ralphs JR: The skeletal attachment of tendons--tendon "entheses". **Comp Biochem Physiol A Mol Integr Physiol 133:**931-945, 2002
4. Benjamin M, Newell RL, Evans EJ, Ralphs JR, Pemberton DJ: The structure of the insertions of the tendons of biceps brachii, triceps and brachialis in elderly dissecting room cadavers. **J Anat 180 (Pt 2):**327-332, 1992
5. Birk DE, Nurminskaya MV, Zycband EI: Collagen fibrillogenesis in situ: fibril segments undergo post-depositional modifications resulting in linear and lateral growth during matrix development. **Dev Dyn 202:**229-243, 1995
6. Birk DE, Southern JF, Zycband EI, Fallon JT, Trelstad RL: Collagen fibril bundles: a branching assembly unit in tendon morphogenesis. **Development 107:**437-443, 1989
7. Birk DE, Zycband EI, Woodruff S, Winkelmann DA, Trelstad RL: Collagen fibrillogenesis in situ: fibril segments become long fibrils as the developing tendon matures. **Dev Dyn 208:**291-298, 1997

8. Derwin KA, Soslowsky LJ, Green WD, Elder SH: A new optical system for the determination of deformations and strains: calibration characteristics and experimental results. **J Biomech 27:**1277-1285, 1994

9. Diamant J, Keller A, Baer E, Litt M, Arridge RG: Collagen; ultrastructure and its relation to mechanical properties as a function of ageing. **Proc R Soc Lond B Biol Sci 180:**293-315, 1972

10. Favata M: Scarless Healing in the Fetus: Implications and Strategies for Postnatal Tendon Repair **Ph.D. thesis. University of Pennsylvania.**, 2006

11. Festing MF: Design and statistical methods in studies using animal models of development. **ILAR J 47:**5-14, 2006

12. Franchi M, Trire A, Quaranta M, Orsini E, Ottani V: Collagen structure of tendon relates to function. **ScientificWorldJournal 7:**404-420, 2007

13. Galatz L, Rothermich S, VanderPloeg K, Petersen B, Sandell L, Thomopoulos S: Development of the supraspinatus tendon-to-bone insertion: localized expression of extracellular matrix and growth factor genes. **J Orthop Res 25:**1621-1628, 2007

14. Lake SP, Miller KS, Elliott DM, Soslowsky LJ: Effect of fiber distribution and realignment on the nonlinear and inhomogeneous mechanical properties of human supraspinatus tendon under longitudinal tensile loading. **J Orthop Res 27:**1596-1602, 2009

15. Lake SP, Miller KS, Elliott DM, Soslowsky LJ: Tensile properties and fiber alignment of human supraspinatus tendon in the transverse direction demonstrate

inhomogeneity, nonlinearity, and regional isotropy. **J Biomech 43:**727-732

16. Miller K. S. SJT, N. A. Trasolini, L. J. Soslowsky: The Upper Band of the Subscapularis Tendon in the Rat has Inferior Mechanical Properties. **Transactions of the Orthopaedic Research Society**, 2011

17. Miller KS, Connizzo BK, Soslowsky LJ: Collagen Fiber Re-Alignment in a Neonatal Developmental Mouse Supraspinatus Tendon Model. **Ann Biomed Eng**, 2012

18. Miller KS, Edelstein, L., L. J. Soslowsky: Effect of preconditioning on collagen fiber recruitment: inhomogeneous properties of the rat supraspinatus tendon. **Proceeding of the ASME 2010 Summer Bioengineering Conference**, 2010

19. Moore MJ, De Beaux A: A quantitative ultrastructural study of rat tendon from birth to maturity. **J Anat 153:**163-169, 1987

20. Nakagawa Y, Majima T, Nagashima K: Effect of ageing on ultrastructure of slow and fast skeletal muscle tendon in rabbit Achilles tendons. **Acta Physiol Scand 152:**307-313, 1994

21. Oryan A, Shoushtari AH: Histology and ultrastructure of the developing superficial digital flexor tendon in rabbits. **Anat Histol Embryol 37:**134-140, 2008

22. Parry DA, Craig AS, Barnes GR: Tendon and ligament from the horse: an ultrastructural study of collagen fibrils and elastic fibres as a function of age. **Proc R Soc Lond B Biol Sci 203:**293-303, 1978

23. Peltz CD, Sarver JJ, Dourte LM, Wurgler-Hauri CC, Williams GR, Soslowsky LJ:

Exercise following a short immobilization period is detrimental to tendon properties and joint mechanics in a rat rotator cuff injury model. **J Orthop Res 28:**841-845

24. Provenzano PP, Vanderby R, Jr.: Collagen fibril morphology and organization: implications for force transmission in ligament and tendon. **Matrix Biol 25:**71-84, 2006

25. Quinn KP, Winkelstein BA: Preconditioning is correlated with altered collagen fiber alignment in ligament. **J Biomech Eng 133:**064506, 2011

26. Ralphs JR, Tyers RN, Benjamin M: Development of functionally distinct fibrocartilages at two sites in the quadriceps tendon of the rat: the suprapatella and the attachment to the patella. **Anat Embryol (Berl) 185:**181-187, 1992

27. Rufai A, Benjamin M, Ralphs JR: Development and ageing of phenotypically distinct fibrocartilages associated with the rat Achilles tendon. **Anat Embryol (Berl) 186:**611-618, 1992

28. Schweitzer R, Zelzer E, Volk T: Connecting muscles to tendons: tendons and musculoskeletal development in flies and vertebrates. **Development 137:**2807-2817

29. Silver FH, Freeman JW, Seehra GP: Collagen self-assembly and the development of tendon mechanical properties. **J Biomech 36:**1529-1553, 2003

30. Sverdlik A, Lanir Y: Time-dependent mechanical behavior of sheep digital tendons, including the effects of preconditioning. **J Biomech Eng 124:**78-84, 2002

31. Thomopoulos S, Kim HM, Rothermich SY, Biederstadt C, Das R, Galatz LM: Decreased muscle loading delays maturation of the tendon enthesis during postnatal development. **J Orthop Res 25:**1154-1163, 2007

32. Thomopoulos S, Williams GR, Gimbel JA, Favata M, Soslowsky LJ: Variation of biomechanical, structural, and compositional properties along the tendon to bone insertion site. **J Orthop Res 21:**413-419, 2003

33. Zhang G, Young BB, Ezura Y, Favata M, Soslowsky LJ, Chakravarti S, et al: Development of tendon structure and function: regulation of collagen fibrillogenesis. **J Musculoskelet Neuronal Interact 5:**5-21, 2005

Chapter 6. Examining Differences in Local Collagen Fiber Crimp Frequency Throughout Mechanical Testing in a Developmental Mouse Supraspinatus Tendon Model

A. Introduction

This chapter will quantify local collagen fiber crimp frequency throughout postnatal development in a mouse supraspinatus tendon model at ages 4, 10 and 28 days. This chapter will utilize the software and techniques described in Chapter 4 to examine changes in collagen fiber crimp frequency throughout a tensile mechanical testing protocol. Additionally, this chapter will examine changes in crimp frequency with developmental age and compare the results with the mature time point (90 days) examined in Chapter 4.

Consistently and repeatedly characterizing the mechanical response of soft tissues can be challenging given their time and history dependence.[6,36] While it is commonly accepted that preconditioning is an important component of mechanical testing protocols, the mechanisms of preconditioning are poorly understood. Recent studies have identified correlations between collagen fiber re-alignment and preconditioning.[23,26] Additionally, a recent study in rat tail tendon fascicle showed that preconditioning was accompanied by a decrease in the crimp period and a shift of the toe-region of the stress-strain curve to higher strains.[16] Crimp morphology is believed to be related to tendon mechanical behavior. While crimp has been extensively studied at slack or nondescript load

conditions,[10-13,17] few studies have examined crimp at specific, quantifiable loads. Additionally, the effect of number of preconditioning cycles on collagen fiber crimp frequency has not yet been examined throughout postnatal development. Further research is necessary to examine the effect of preconditioning on tendon structural response to load and to determine how the structure of tendon affects its mechanical properties. Additional information on the effect of preconditioning will improve the repeatability and consistency of experimental results and aid interpretation of results across studies.

In addition, the effect of developing structure on the tendon's ability to respond to mechanical load through the uncrimping of collagen fibers has not yet been examined. In Chapter 5, we demonstrated that where collagen fiber re-alignment occurred throughout the mechanical testing protocol may depend on developmental age and the maturity of the collagen fiber matrix.[22] It is possible that the ability of collagen fibers to uncrimp in response to mechanical load may also depend on the tendon's underlying structure and may affect tendon mechanical properties. Studies have speculated that collagen fiber crimp behavior changes throughout development.[7,14,31] However, the ability of collagen fibers to uncrimp in response to load has not been extensively studied throughout postnatal development nor has it been examined in the supraspinatus tendon (SST). A higher collagen fiber crimp frequency at younger ages may explain the elongated toe-region seen throughout postnatal development[1,22] as increased crimp has been shown to affect the toe-region of the stress-strain curve.[17]

Additionally, it has been suggested that collagen fiber crimp patterns vary by

location.[5,32] In Chapters 3 and 5 we showed that compared to the tendon midsubstance, the supraspinatus tendon-to-bone insertion site experiences higher strains, demonstrates a more disorganized collagen fiber distribution, weaker mechanics and changes in fiber re-alignment behavior.[18,22,23,33] Studies in ligament have also shown a "preferential" uncrimping of the central third of the ligament as well as near the bone. This suggests that the insertion site and midsubstance locations in the SST may display differences in crimp behavior,[5] although neither local collagen fiber crimp frequency nor the potential dependence of collagen fiber uncrimping on location have yet been quantified. Finally, it is not known how changing the boundary conditions and the residual stress of the tendon from the in vivo state to the excised uniaxial, tensile mechanical testing set-up affects collagen fiber crimp behavior.

Therefore, the objective of this study was to quantify local changes in collagen fiber crimp frequency in a developmental mouse SST model throughout a mechanical testing protocol to determine 1) where fiber uncrimping occurs throughout the mechanical test, 2) if collagen fiber crimp behavior is dependent on the number of preconditioning cycles, 3) if local collagen fiber crimp frequency changes with developmental age and 4) if collagen fiber crimp behavior is dependent on tendon location. We hypothesize that 1) Collagen fiber uncrimping will occur primarily in the toe-region of the mechanical test regardless of age; 2) Collagen fiber crimp frequency will decrease with increased number of preconditioning cycles; 3) Crimp frequency will decrease with developmental age; 4) The insertion site will demonstrate an increased crimp frequency compared to the tendon midsubstance.

B. Methods

B1. Sample Preparation

This study was approved by the University of Pennsylvania IACUC. Postnatal mice in a C57/BL/6 (Jackson Laboratory) background were bred on site. All litters were reduced to six pups within 1 day of birth to reduce variance from litter size,[9] Pups were weaned at 21 days after birth and separated by sex. In order to compare changes in crimp frequency throughout the mechanical test, a litter was defined as a single sample[1] and mechanical testing points were randomly assigned to shoulders within each litter. SSTs from male and female postnatal mice were removed at 4, 10 and 28 days old (N= 9-11 for each age and mechanical testing point). Under a stereomicroscope, SSTs were dissected out and excess tissue was removed with the tendon still attached to the humeral head. As described previously in Chapter 5, the humeral head was trimmed to a small bone chip and then both ends of the tendon were secured with cyanoacrylate adhesive between pieces of sandpaper,[22] grip-to-grip gauge length of the samples was 1.5 mm for 4 and 10 days old and 2.5 mm for 28 days old.[22] Tendons were secured in the grips and a grip holder was used to ensure the tendons were not loaded or damaged during handling.[1,22]

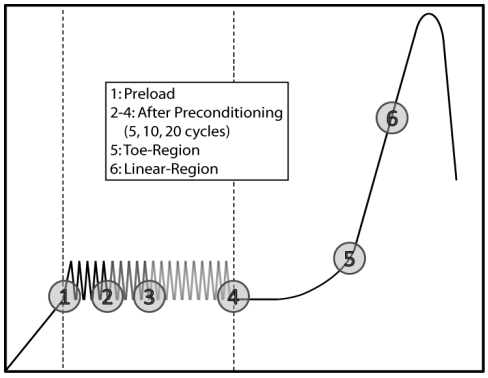

Figure 6.1 A schematic of the testing protocol with 6 points at which crimp was assessed.

B2. Reference Configuration Dissection Protocol

An additional sample from each litter was prepared to serve as a reference configuration for the mechanical testing points. The reference configuration samples

were flash frozen while still attached to the supraspinatus muscle and humeral head to provide an "in situ" reference configuration for comparative analysis. All dissections were performed under a stereomicroscope. Mice were placed on their sides and secured to the table using masking tape. After the shoulder joint was exposed, the shoulder was externally rotated to visualize the joint. The arm was secured with tape to maintain a consistent position throughout the dissection process. During dissections, care was taken to secure the shoulders at a consistent angle across samples. Next, the trapezius and deltoid muscles were removed to expose the acromioclavicular and scapulohumeral joints. The AC ligament was then cut and the clavicle was peeled back to expose the SST and subscapularis tendon. The acromion was removed to visualize the infraspinatus tendon. The infraspinatus and subscapularis tendons were then sharply detached at their respective insertion sites. Then, the entire remaining shoulder joint was sprayed with flash freezing spray. The humeral shaft was then sharply detached from the body near the elbow while any remaining attachments to the frozen joint were sharply dissected. The joint was quickly positioned in a freezing tray, embedded in tissue freezing medium and doused with liquid nitrogen. In graphical representation, the reference point will be referred to as the "in situ" or IS point.

B3. Mechanical Testing and Histology

Samples were placed in a tank and loaded into a tensile testing system (Instron, Norwood, MA). Samples were kept moist with phosphate buffered saline spray throughout the testing process and a 10 N load cell was used for all tests. Collagen fiber crimp was assessed at 6 different points during the mechanical test: at the preload (0.005

N for 4 and 10 day tendons, 0.02N for 28 day tendons), after 5, 10, 20 cycles of preconditioning (0.005-0.008N for 4 and 10 day tendons and 0.002-0.04N for 28 day tendons) and at the toe- and linear-regions (Fig 6.1).[22] Preconditioning was performed at load control but represented average strains of 0.5 and 1% for 4 days, 1 and 2% for 10 days and 28 days at an average rate of 0.07 Hz. Strains representing the toe- and linear-regions were determined using a structural fiber recruitment model at 50% fiber recruitment to represent the transition strain (intersection of toe- and linear-regions) and 75% to represent the linear region as described in previous studies.[22,24] Immediately following the designated tensile loading protocol, tendons were snap-frozen (sprayed for 20 seconds with flash freezing spray (Decon Laboratories, King of Prussia, PA)) while mounted in the testing device to obtain a "snapshot" of crimp at the desired point in the mechanical test.[34] Samples were sharply detached at the insertion site and top grip and quickly embedded in tissue freezing medium (Triangle Biomedical Sciences, Durham, NC). All samples were cut into 8 μm sections and were stained with Picrosirius Red and Hematoxylin.

B4. Data Analysis

For each sample, 2 sections were analyzed at the midsubstance and insertion sites for 10 and 28 days and at one location (encompassing the majority of the tendon) at 4 days due to the decreased size of collagen fibers and resolution limitations during analysis (Fig 6.2). Sections were examined using polarized light microscopy and custom software in a blinded manner. The custom software (Matlab, Natwick, MA) developed in Chapter 4 was used to quantitatively analyze collagen crimp frequency. Briefly, blinded users

selected a region for analysis and the pixel intensity variation was determined along the length of the collagen fibers. After normalizing the image, average crimp frequency was determined by pixel fluctuations. For each location analyzed, the results from the 2 sections selected were averaged and crimp frequency in mm^{-1} is reported.

B5. Statistical Analysis

Imputation, using the predictive-mean matching method, was performed to represent missing crimp frequency values within each litter.[19,20,38] A 3-way (region of test, location and age) repeated measures ANOVA was used and a Bonferroni correction was applied if interactions were significant. Post-hoc t-tests were used to evaluate changes in crimp frequency and corrections for multiple statistical comparisons were made for each hypothesis. To address hypothesis 1, post-hoc paired t-tests were used to compare to

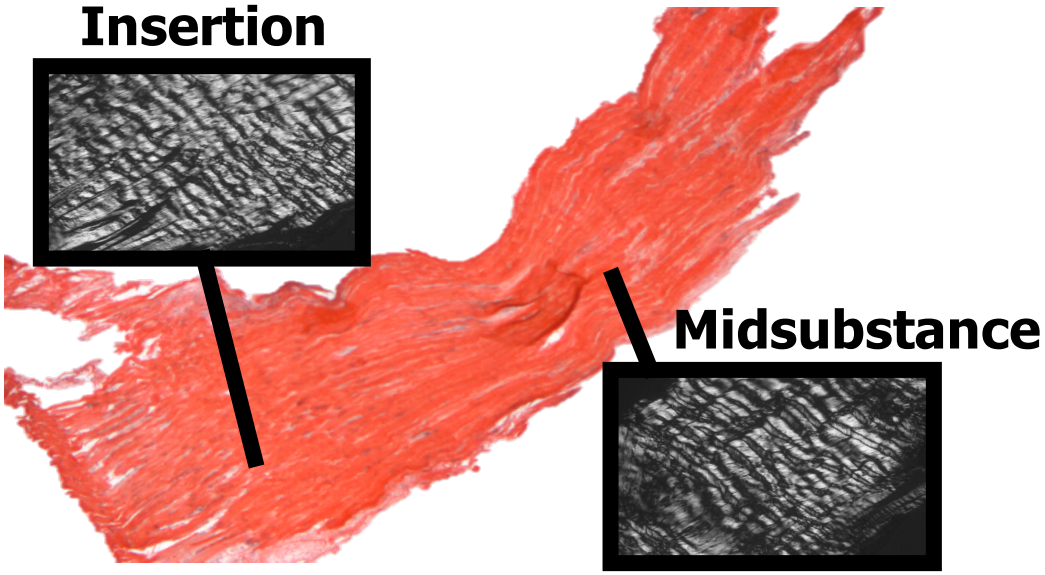

Figure 6.2 Picrosirius Red and polarized light images were acquired at the insertion site and midsubstance locations of each sample for 10 and 28 days.

changes in crimp frequency throughout adjacent points in the mechanical test. For example, preload and 5 cycles of preconditioning data were examined to determine if

uncrimping occurred during the 5 cycles of preconditioning. Similar methods were used to identify changes in crimp frequency during 10 and 20 cycles in addition to at the toe- and linear-regions of the ramp-to-failure. Additionally, paired t-tests with a Bonferroni correction were applied to evaluate changes during the toe-region with each preconditioning protocol. The crimp frequency at the in situ reference configuration was also compared to the preload value. To address hypothesis 2, paired t-tests with a Bonferroni correction were made to evaluate changes during each of the preconditioning protocols compared to the preload. To address hypothesis 3, post-hoc t-tests were used to compare local changes in crimp frequency with developmental age. Crimp frequency is presented as mean ± standard deviation.

C. Results

The repeated measures 3-way ANOVA identified that the effects of time and age were significant. The ANOVA demonstrated that no changes in crimp frequency were identified between locations. No interactions between time, age or location were found to be significant. Results, as well as statistical corrections for multiple comparisons, are presented by hypothesis. A table of p-values is also provided for completeness and to aid in interpretation of these results (Tables 6.1,

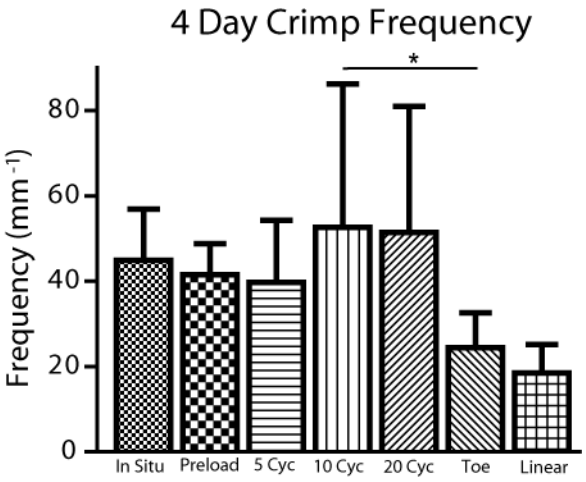

Figure 6.3 Crimp frequency at 4 days old demonstrates that crimp frequency decreases during the toe-region following 10 cycles of preconditioning. *=p<0.016.

6.2 and 6.3).

To address hypothesis 1**,** comparisons between adjacent points throughout the test were made. Additional comparisons between points analyzed after 5 cycles and 10 cycles of preconditioning compared to the toe-region were also made. For this hypothesis, significance was set at $p<0.016$. At 4 and 10 days old, the uncrimping of collagen fibers was confined to the toe-region of the mechanical test (4 days: Fig 6.3, 10 days: Fig 6.4 and Table 6.1). A significant decrease in crimp frequency was found following 10 cycles of preconditioning compared to the toe-region at 4 days (Fig 6.3 and Table 6.1). At 10 days, significant decreases in crimp frequency were identified at the toe-region compared to all preconditioning protocols at both locations (Fig 6.4 and Table 6.1). At 28 days, significant decreases in collagen fiber crimp frequency were present between 5 and 10 cycles of preconditioning and during the toe-region of the mechanical test at the insertion site (Fig 6.5 and Table 6.1). Significant decreases in collagen fiber crimp frequency were found during the toe-region at the midsubstance for all

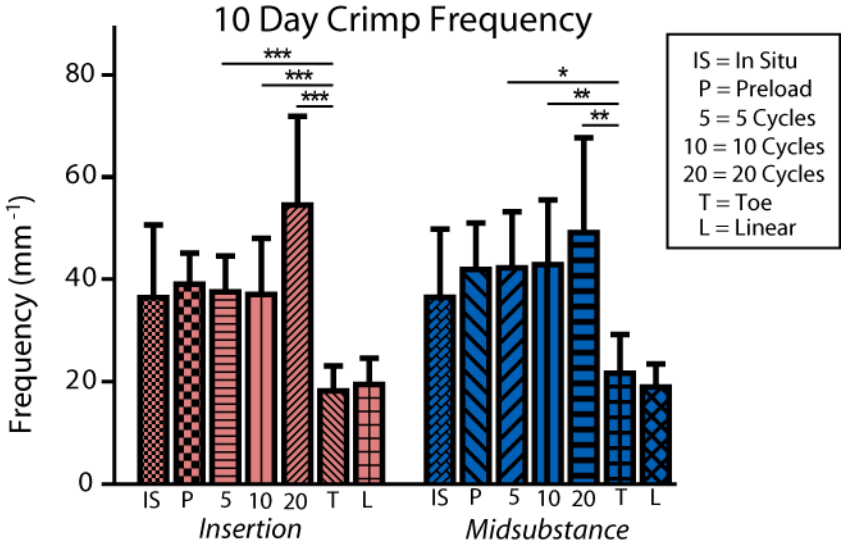

Figure 6.4 Crimp frequency at 10 days old demonstrates that crimp frequency decreases during the toe-region regardless of the mechanical testing protocol**.** *p<0.016, **p<0.003, ***p<0.0003.

preconditioning protocols (Fig 6.5 and Table 6.1). Average changes in crimp frequency throughout the mechanical test for the 28 day insertion site and midsubstance location were (ins:mid): between preload and 5 cycles (-4:-11), 5 cycles and 10 cycles (3:8), 10 and 20 cycles (5:9), 20 cycles and the toe-region (6:12), toe- and linear-regions (5:2).

To address hypothesis 2, collagen fiber crimp frequency was examined at the preload compared to each preconditioning protocol. For this hypothesis, significance was set at $p<0.016$. At 4 and 10 days, the increasing number of preconditioning cycles did not affect collagen fiber crimp behavior (Table 6.2). At both locations at 28 days, an increase in crimp frequency was identified during 10 cycles of preconditioning compared to the preload (Fig 6.5 and Table 6.2). Additionally, while not defined as significant after correction, ($p=0.02$ for both comparisons) an increase in crimp frequency was found during 5 cycles of preconditioning compared to the preload while a decrease in crimp frequency was found after 20 cycles (Fig.6.6 and Table 6.2). Average changes in crimp frequency after

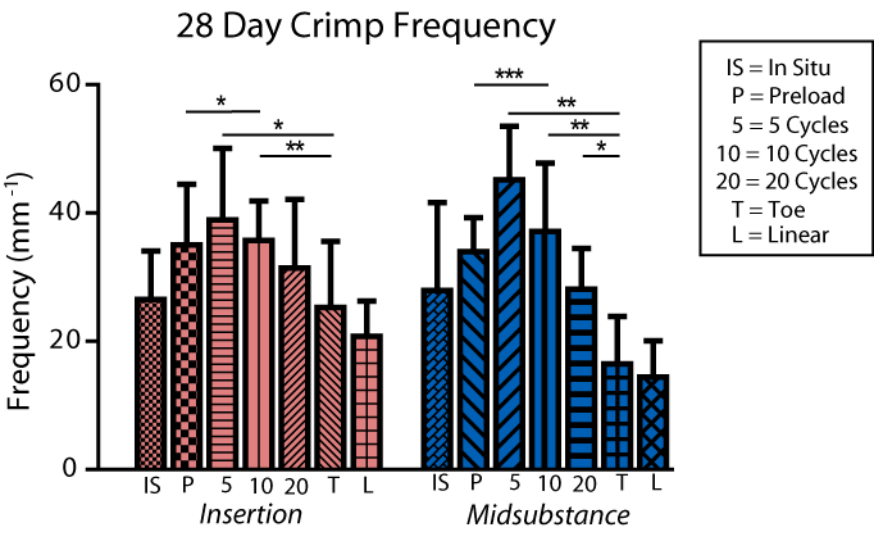

Figure 6.5 Crimp frequency demonstrates that crimp frequency decreases during the toe-region and increases from the preload to 10 cycles of preconditioning at both locations. *p<0.016, **p<0.003, ***p<0.0003.

preconditioning compared to the preload for the 28 day insertion site and midsubstance location were (ins:mid): between preload and 5 cycles (-4, -11), preload and 10 cycles (-1, -3), and preload and 20 cycles (4, 4).

Age and Location	Preload vs. 5 cycles	5 vs. 10 cycles	10 vs. 20 cycles	5 cycles vs. Toe	10 cycles vs. Toe	20 cycles vs. Toe	Toe vs. Linear
4 days	0.7	0.09	0.3	0.03	0.01*	0.02	0.1
10 day Ins	0.3	0.4	0.08	<0.0001*	<0.0001*	<0.0001*	0.5
10 day Mid	0.8	0.4	0.6	0.007*	0.002*	0.0005*	0.4
28 day Ins	0.1	0.6	0.4	0.01*	0.0003*	0.2	0.4

Table 6.1 P-values for changes in crimp frequency for adjacent points throughout the mechanical testing protocol. * Indicates significant difference at $p<0.016$, compares distributions at 4 days and at 10 and 28 days at the insertion site and midsubstance locations throughout the mechanical test. Also examines changes between all points after preconditioning and the toe-region.

To address hypothesis 3**,** a significant decrease in crimp frequency was found between 10 and 90 days at both locations ($p=0.008$ and $p=0.01$ for the insertion site and midsubstance respectively, Table 6.3). However, no significant changes in crimp frequency were identified between 10 and 28 days or 28 and 90 days with the quantitative

analysis. Unfortunately, due to resolution limitations, comparisons were not made with the 4 day time points. However, histology indicates that the 4 days tendons demonstrated a smaller, less developed hierarchical structure compared to the 10 and 28 day tendons (Fig 6.7).

To address hypothesis 4, no changes in crimp frequency with location were found at either 10 or 28 days. Due to resolution limitations, only 1 region was analyzed at 4 days.

Age and Location	Preload vs. 5 cycles	Preload vs. 10 cycles	Preload vs. 20 cycles
4 days	0.7	0.3	0.4
10 day Ins	0.3	0.5	0.07
10 day Mid	0.8	0.7	0.4
28 day Ins	0.1	0.01*	0.1
28 day Mid	0.02	0.0002*	0.02

Table 6.2 P-values for changes in crimp frequency with increasing number of preconditioning cycles compared to the preload. * Indicates significant difference at $p<0.016$, compares distributions at 4 days and at 10 and 28 days at the insertion site and midsubstance locations with increasing number of preconditioning cycles compared to the preload.

Comparison	Insertion	Midsubstance
10 vs. 28	0.2	0.09
10 vs. 90	0.008	0.01
28 vs. 90	0.1	0.09

Table 6.3 P-values for examining differences in crimp frequency with increasing developmental age. * Indicates significant difference at $p<0.025$, compares crimp frequency values at the preload with each developmental age at each location (no comparisons made with 4 day time point).

D. Discussion

In this chapter, collagen fiber crimp frequency was quantified throughout a mechanical testing protocol in a postnatal developmental mouse SST model. As expected, the majority of collagen fiber uncrimping was confined to the toe-region for all ages, supporting the concept that the uncrimping of collagen fibers occurs during the toe-region of a mechanical test. Tendons from 10 day old mice were found to function as a continuous unit, with the insertion site and midsubstance locations demonstrating similar crimp responses to mechanical load. In Chapter 5, the insertion site and midsubstance locations of 10 day tendons were shown to exhibit similar collagen fiber re-alignment behavior in response to load.[22] These results support the concept that tendon fibrils have linearly fused by 10 days to form long, continuous fibrils which may allow fibers to transmit load along the length of the tendon.[2,4,22,25,39] Interestingly, at 28 days, the insertion site and midsubstance locations demonstrated slightly different crimp behaviors. At the 28 day insertion site, significant decreases in collagen fiber crimp frequency were present between 5 and 10 cycles of preconditioning and the toe-region, while no significant decrease in crimp frequency were found between 20 cycles of preconditioning and the toe-region ($p=0.2$) (Figs 6.5 and 6.6). At the 28 day midsubstance, significant decreases in collagen fiber crimp frequency were found during the toe-region for all preconditioning protocols (Fig 6.5 and Table 6.1). Overall, these findings support the results presented in Chapter 4 as well as speculation that the uncrimping of collagen fibers may explain the toe-region of the mechanical test.[15,16,27-29,35,37]

While similar crimp behavior was found during the toe-region at all ages, it should be noted that the actual strain levels at which the samples were flash-frozen for each age were different. A structural fiber recruitment model was used to determine toe- and linear-region strains.[22,24] Grip-to-grip strains representing the toe- and linear-regions

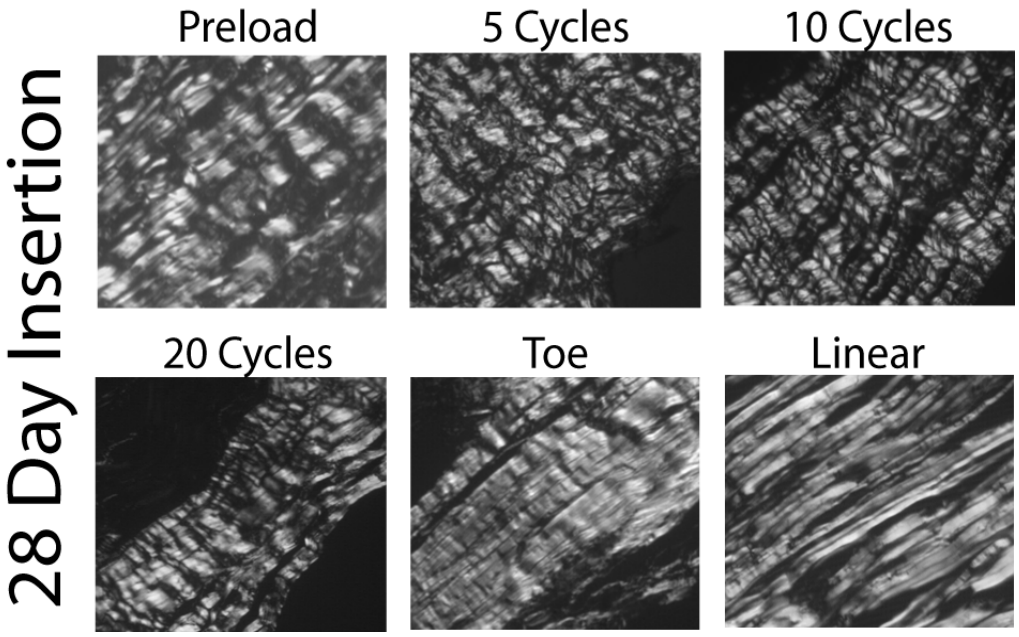

Figure 6.6 Representative images from the 28 day insertion site throughout the mechanical test demonstrate an increase in crimp frequency between the preload and after 10 cycles of preconditioning and a decrease in crimp frequency between after 5 and 10 cycles of preconditioning and the toe-region. Image sizes 250μm x 100μm.

calculated from the structural model were as follows: 17 and 22% for 4 days, 22 and 29% strain for 10 days and 5 and 7% strain for 28 days (5 and 8% for 90 days in Chapter 4). While the overall crimp behavior demonstrated at each age was similar, the early developmental tendons may require a prolonged exposure to load and higher strains in order to uncrimp and transition to the linear-region. This supports previous speculation that 4 and 10 day tendons demonstrate a delayed structural response to mechanical load

explained by the immature networks of collagen fibrils present at early postnatal development and their organization into immature fibril networks.[3 22,39] Additionally, a previous study in rat tail tendon defined linear region strains as higher than 6%[16] indicating that the 28 day collagen fibril network may be approaching maturity. Further supporting this, the structural fiber recruitment model suggested similar strains to represent the toe- and linear-regions at 28 and 90 days. Further, the extent of the toe-region is believed to be dependent on crimp angle and tendon function.[29]

Interestingly, results from this study at 28 days suggest collagen fiber crimp

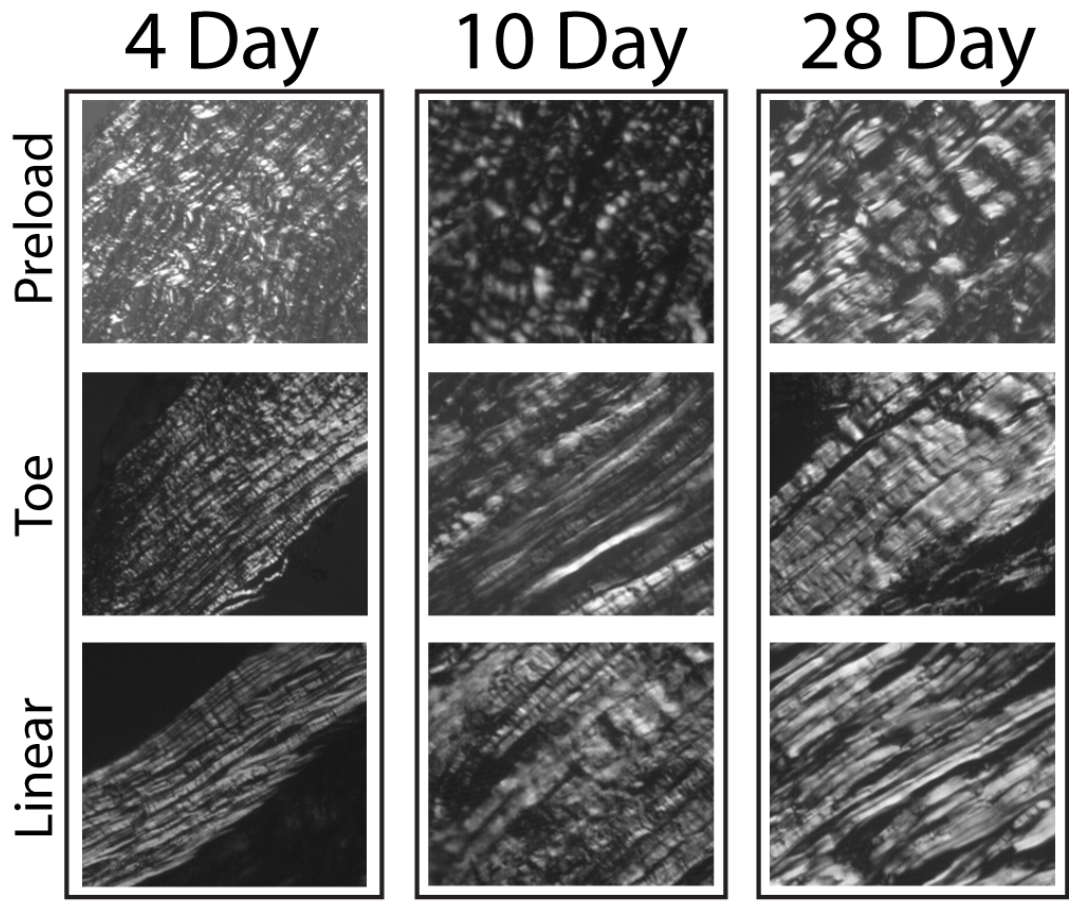

Figure 6.7 Representative images for 4, 10 and 28 days at the preload, toe- and linear-region. Histology demonstrates the smaller collagen fibrils and scale of crimp present at 4 days compared to 28 days. Image sizes 250μm x 100μm.

frequency following preconditioning may be dependent upon the number of cycles applied. Determining a reference configuration before measuring mechanical properties is very important for consistent mechanical testing and interpretation of experimental results. Additionally, it has been suggested that the chosen reference configuration and protocol may have strong implications for the transition strain and nonlinear region properties.[15] While increasing the number of preconditioning cycles did not affect collagen fiber crimp behavior at 4 and 10 days, significant increases in collagen fiber crimp frequency were found following 10 cycles of preconditioning compared to the preload at both locations at 28 days (Fig 6.5). In addition, while not significant after Bonferroni correction for multiple comparisons, an increase in crimp frequency was found after 5 cycles of preconditioning compared to the preload, while a decrease in crimp frequency was found after 20 cycles at the midsubstance location (Table 6.2). These results suggest that the preconditioning protocol applied may affect collagen fiber crimp behavior and therefore may influence mechanical properties measured later in the mechanical testing process. While significant changes in crimp frequency were not identified between the preload and varying cycles of preconditioning in Chapter 4, the 90 day histology data presented may provide support for concept that crimp frequency decreases with increasing number of preconditioning cycles. A previous study in rat tail tendon fascicles found an increase in crimp each time a new strain was reached, which they termed preconditioning.[16] They suggest that preconditioning may be associated with a change in the stress-free configuration explained primarily by the sliding of microstructures inside the fascicle leading to a shift in the toe-region of the stress-strain

curve.[16] In support, the current study also identified an increase in collagen fiber crimp frequency following 5 and 10 cycles of preconditioning compared to the preload. However, this study also identified a pattern of decreasing crimp frequency with increasing number of preconditioning cycles at the same load (Fig 6.5 and Table 6.2). This indicates that crimp behavior in response to mechanical load may possess viscoelastic and elastic components which merit further study. Additionally, the literature is currently unclear on whether the effects of preconditioning are reversible and further studies are necessary to examine the effect and subsequent recovery of structural changes during preconditioning.[16,28] It has been suggested that relaxation and recovery are governed by separate mechanisms and may involve a different time and length scale depending on the tissue age, function and applied protocol.[8,16] Additionally, previous studies suggest that collagen fiber re-alignment is also correlated with preconditioning.[23,26] These results indicate that collagen fiber uncrimping may also be affected by preconditioning and may be correlated with other structural changes seen during preconditioning.[16,21,28] Further, in Chapter 5 the ability of fibers to re-align in the direction of load was suggested to be dependent on the maturity of the collagen fiber matrix. The results from this study suggest that changes in crimp frequency may also be dependent on matrix maturity, as no changes in crimp frequency during preconditioning were detected at 4 or 10 days old, while either significant changes or potential patterns of change with average crimp frequency were identified at late development and at maturity. It is possible that a more mature and interconnected collagen fiber matrix allows tendons to re-align faster subsequently causing collagen fibers to uncrimp earlier in the

mechanical testing process.

This study also examined changes in crimp frequency with developmental age. No significant changes in crimp frequency were found between 10 and 28 days old or 28 and 90 days old (Table 6.3). Unfortunately, given the small scale of crimp at 4 days we were not able to compare crimp frequency between 4 days and later developmental time points due to resolution limitations. However, in agreement with previous work, histology suggests that 4 day tendon crimp exists on a much smaller scale in that it is compromised of an immature fiber network composed of collagen fibrils with small fibril diameters, which may result in the smaller diameter fibers noted in the histology (Fig 6.7).[2,4,22,39] Additionally, a significant decrease in crimp frequency was identified between 10 and 90 days at both locations (Table 6.3). This supports previous literature which suggests that collagen fiber crimp frequency decreases with age while total number of crimp stays constant.[7,14,31] The results from this study suggest the decreases in collagen fiber crimp frequency occur primarily in early development, as no significant changes were identified during late development. In addition, the lack of changes between 10 and 28 days and 28 and 90 days suggests the decrease in transition strain previously reported between 10 and 28 days may be explained by other factors such as increases in fiber-fiber and fiber-matrix connections throughout maturity.[22] Previous studies also suggest the uncrimping of collagen fibers may not be the only mechanism driving the toe-region; re-alignment of collagen fibers, fascicle rotation and fiber recruitment may account for the differences in transition strain noted with developmental age.[29] In addition, previous work in our laboratory suggests that 4 and 10 day tendons

require a longer exposure to mechanical load before structurally responding through the re-alignment of collagen fibrils, which may explain the longer toe-region demonstrated throughout development.[22]

Finally, while no differences in crimp frequency were found in this study between locations, differences in crimp behavior were identified at 28 days. Comparing average changes in crimp frequency for each set of paired data demonstrated that the midsubstance and insertion site locations displayed similar patterns of crimp behavior but the effect of preconditioning on collagen fiber crimp frequency was more pronounced at the midsubstance location. This is further supported by the patterns demonstrated at 90 days in Chapter 4, suggesting that crimp behavior at the midsubstance location may be more sensitive to changes in load or that the midsubstance location is able to respond to mechanical load by uncrimping collagen fibers faster possibly explained by the more highly aligned collagen fiber distribution.

Interestingly, no decrease in collagen fiber crimp frequency was found between 20 cycles and the toe-region at the insertion site ($p=0.2$), suggesting that collagen fiber crimp steadily decreased with an increasing number of preconditioning cycles (Fig 6.5 and Table 6.2). Significant decreases in crimp frequency were also found at the toe-region compared to all post-preconditioning time points at the midsubstance location (Fig 6.5). This result is supported by the average changes in crimp frequency per paired sample. Changes in crimp frequency were smaller at the insertion site compared to the midsubstance which indicates the overall response to load may be decreased at the insertion site. Supporting this, in Chapter 4, changes in crimp frequency were also larger

at the midsubstance location compared to the insertion site. Previous work in heart valve soft tissue biomaterials found that loading perpendicular to the preferred collagen fiber orientation resulted in fiber reorientation but not fiber uncrimping.[30] While tendon is primarily composed of collagen fibers aligned in the direction of loading, the insertion site displays a more disorganized collagen fiber distribution.[18,22,33] It is possible that this modest display of collagen fiber uncrimping at the insertion site could be explained by the more disorganized collagen fiber distribution, where the fiber must first reorient in the direction of loading before uncrimping. Additionally, previous studies suggest that changes in collagen fiber crimp frequency are nonuniform along the length of the tendon and some have indicated a preferential uncrimping near the bone.[15,32]

This study is not without limitations. First, the small size of the collagen network at the 4 day time point did not allow for quantitative comparisons across ages or location within the 4 days. All images were taken using a 20x objective to allow for comparisons of equal resolution across groups, however given the small fiber size at 4 days old, the fluctuations in pixel intensity were very close together and may have been oversampled in the analysis process. For this reason, comparisons were not made between 4 day tendons and additional time points. However, comparisons were made across 4 day points throughout the mechanical test because the same bias existed across all groups. Therefore, we are confident in our analysis of 4 day tendon behavior throughout the mechanical test, which was also confirmed by semi-quantitative analysis (data not shown). Additionally, the histology strongly supports the theory that 4 day tendons are composed primarily of small collagen fibril intermediates.

Secondly, the histology from this project was stained in multiple batches, though analysis methods performed were consistent and repeatable. Care was taken to ensure that the custom quantitative software normalized each image by the average pixel intensity and established exclusion criteria based on standard deviation of pixel fluctuations to exclude artifact and only include fluctuations representing collagen fiber crimp. This method minimizes the potential effect of different batches of stain on the histological analyses. In addition, this study examined collagen fiber crimp behavior throughout one mechanical testing protocol. Future studies are necessary to further examine the effects of collagen fiber crimp behavior in response to different preconditioning protocols and different magnitudes of preconditioning. Additionally, future studies are needed to examine additional points throughout the ramp-to-failure test, which will enable examination of earlier loads in the toe-region to further document the progress of local fiber uncrimping with increasing age. Finally, this study did not examine the ability of collagen fibers to return to initial collagen fiber crimp frequency. However, this study provides valuable insight into tendon structural response to load in the presence of preconditioning cycles. Future studies are needed to examine the conditions necessary for collagen fiber crimp to "recover" or return to a specified reference state.

In this chapter, we utilized the technique described in Chapter 4 to examine changes in local collagen fiber crimp frequency throughout mechanical testing in a postnatal developmental mouse SST model. Results confirm that uncrimping of collagen fibers contributes to the toe-region of the mechanical test. Results also indicate that other

factors, such as collagen fibril cross-links, proteoglycan bridges between fibers and maturity of the collagen matrix may also contribute its nonlinear behavior. Additionally, this study identified changes in collagen fiber crimp frequency with increasing number of preconditioning cycles, supporting our speculation in Chapter 4. The potential changes in crimp behavior identified with increasing number of cycles during precondition may have implications on the measurement of mechanical properties and identifying a proper reference configuration.

E. References

1. Ansorge HL, Adams S, Birk DE, Soslowsky LJ: Mechanical, compositional, and structural properties of the post-natal mouse Achilles tendon. **Ann Biomed Eng 39:**1904-1913
2. Birk DE, Nurminskaya MV, Zycband EI: Collagen fibrillogenesis in situ: fibril segments undergo post-depositional modifications resulting in linear and lateral growth during matrix development. **Dev Dyn 202:**229-243, 1995
3. Birk DE, Southern JF, Zycband EI, Fallon JT, Trelstad RL: Collagen fibril bundles: a branching assembly unit in tendon morphogenesis. **Development 107:**437-443, 1989
4. Birk DE, Zycband EI, Woodruff S, Winkelmann DA, Trelstad RL: Collagen fibrillogenesis in situ: fibril segments become long fibrils as the developing tendon matures. **Dev Dyn 208:**291-298, 1997
5. Boorman RS, Norman T, Matsen FA, 3rd, Clark JM: Using a freeze substitution fixation technique and histological crimp analysis for characterizing regions of strain in ligaments loaded in situ. **J Orthop Res 24:**793-799, 2006
6. Cheng S, Clarke EC, Bilston LE: The effects of preconditioning strain on measured tissue properties. **J Biomech 42:**1360-1362, 2009
7. Diamant J, Keller A, Baer E, Litt M, Arridge RG: Collagen; ultrastructure and its relation to mechanical properties as a function of ageing. **Proc R Soc Lond B Biol Sci 180:**293-315, 1972
8. Duenwald SE, Vanderby R, Jr., Lakes RS: Stress relaxation and recovery in

tendon and ligament: experiment and modeling. **Biorheology 47:**1-14

9. Festing MF: Design and statistical methods in studies using animal models of development. **ILAR J 47:**5-14, 2006

10. Franchi M, Fini M, Quaranta M, De Pasquale V, Raspanti M, Giavaresi G, et al: Crimp morphology in relaxed and stretched rat Achilles tendon. **J Anat 210:**1-7, 2007

11. Franchi M, Ottani V, Stagni R, Ruggeri A: Tendon and ligament fibrillar crimps give rise to left-handed helices of collagen fibrils in both planar and helical crimps. **J Anat 216:**301-309

12. Franchi M, Quaranta M, Macciocca M, Leonardi L, Ottani V, Bianchini P, et al: Collagen fibre arrangement and functional crimping pattern of the medial collateral ligament in the rat knee. **Knee Surg Sports Traumatol Arthrosc 18:**1671-1678

13. Franchi M, Raspanti M, Dell'Orbo C, Quaranta M, De Pasquale V, Ottani V, et al: Different crimp patterns in collagen fibrils relate to the subfibrillar arrangement. **Connect Tissue Res 49:**85-91, 2008

14. Gathercole LJ, Keller A: Crimp morphology in the fibre-forming collagens. **Matrix 11:**214-234, 1991

15. Hansen KA, Weiss JA, Barton JK: Recruitment of tendon crimp with applied tensile strain. **J Biomech Eng 124:**72-77, 2002

16. Houssen YG, Gusachenko I, Schanne-Klein MC, Allain JM: Monitoring micrometer-scale collagen organization in rat-tail tendon upon mechanical strain

using second harmonic microscopy. **J Biomech 44:**2047-2052

17. Hurschler C, Provenzano PP, Vanderby R, Jr.: Scanning electron microscopic characterization of healing and normal rat ligament microstructure under slack and loaded conditions. **Connect Tissue Res 44:**59-68, 2003

18. Lake SP, Miller KS, Elliott DM, Soslowsky LJ: Effect of fiber distribution and realignment on the nonlinear and inhomogeneous mechanical properties of human supraspinatus tendon under longitudinal tensile loading. **J Orthop Res 27:**1596-1602, 2009

19. Landerman LR, Land KC, Pieper CF: An empirical evaluation of the predictive mean matching method for imputing missing values. **Sociological Methods & Research 26:**3-33, 1997

20. Little RJA: Missing-Data Adjustments in Large Surveys. **Journal of Business & Economic Statistics 6:**287-296, 1988

21. Lokshin O, Lanir Y: Viscoelasticity and preconditioning of rat skin under uniaxial stretch: microstructural constitutive characterization. **J Biomech Eng 131:**031009, 2009

22. Miller KS, Connizzo BK, Soslowsky LJ: Collagen Fiber Re-Alignment in a Neonatal Developmental Mouse Supraspinatus Tendon Model. **Ann Biomed Eng**, 2012

23. Miller KS, Edelstein, L., Connizzo, B. K., and Soslowsky, L. J... Effect of Preconditioning and Stress Relaxation on Local Collagen Fiber Re-Alignment: Inhomogeneous Properties of Rat Supraspinatus Tendon. **Journal of**

Biomechanical Engineering In press, 2012

24. Peltz CD, Sarver JJ, Dourte LM, Wurgler-Hauri CC, Williams GR, Soslowsky LJ: Exercise following a short immobilization period is detrimental to tendon properties and joint mechanics in a rat rotator cuff injury model. **J Orthop Res 28:**841-845

25. Provenzano PP, Vanderby R, Jr.: Collagen fibril morphology and organization: implications for force transmission in ligament and tendon. **Matrix Biol 25:**71-84, 2006

26. Quinn KP, Winkelstein BA: Preconditioning is correlated with altered collagen fiber alignment in ligament. **J Biomech Eng 133:**064506

27. Rigby BJ: Effect of Cyclic Extension on the Physical Properties of Tendon Collagen and Its Possible Relation to Biological Ageing of Collagen. **Nature 202:**1072-1074, 1964

28. Rigby BJ, Hirai N, Spikes JD, Eyring H: The Mechanical Properties of Rat Tail Tendon. **J Gen Physiol 43:**265-283, 1959

29. Screen HR, Lee DA, Bader DL, Shelton JC: An investigation into the effects of the hierarchical structure of tendon fascicles on micromechanical properties. **Proc Inst Mech Eng H 218:**109-119, 2004

30. Sellaro TL, Hildebrand D, Lu Q, Vyavahare N, Scott M, Sacks MS: Effects of collagen fiber orientation on the response of biologically derived soft tissue biomaterials to cyclic loading. **J Biomed Mater Res A 80:**194-205, 2007

31. Shah JS, Palacios E, Palacios L: Development of crimp morphology and cellular

changes in chick tendons. **Dev Biol 94:**499-504, 1982

32. Stouffer DC, Butler DL, Hosny D: The relationship between crimp pattern and mechanical response of human patellar tendon-bone units. **J Biomech Eng 107:**158-165, 1985

33. Thomopoulos S, Williams GR, Gimbel JA, Favata M, Soslowsky LJ: Variation of biomechanical, structural, and compositional properties along the tendon to bone insertion site. **J Orthop Res 21:**413-419, 2003

34. Thornton GM, Shrive NG, Frank CB: Ligament creep recruits fibres at low stresses and can lead to modulus-reducing fibre damage at higher creep stresses: a study in rabbit medial collateral ligament model. **J Orthop Res 20:**967-974, 2002

35. Viidik A: Simultaneous mechanical and light microscopic studies of collagen fibers. **Z Anat Entwicklungsgesch 136:**204-212, 1972

36. Woo SL: Mechanical properties of tendons and ligaments. I. Quasi-static and nonlinear viscoelastic properties. **Biorheology 19:**385-396, 1982

37. Woo SL, Debski RE, Zeminski J, Abramowitch SD, Saw SS, Fenwick JA: Injury and repair of ligaments and tendons. **Annu Rev Biomed Eng 2:**83-118, 2000

38. Yuan Y: Multiple Imputation Using SAS Software. **Journal of Statistical Software 45:**1-25, 2011

39. Zhang G, Young BB, Ezura Y, Favata M, Soslowsky LJ, Chakravarti S, et al: Development of tendon structure and function: regulation of collagen fibrillogenesis. **J Musculoskelet Neuronal Interact 5:**5-21, 2005

Chapter 7. Conclusions and Future Directions

A. Overall Conclusions

This chapter will summarize findings from each of the previous chapters and discuss future directions for this research. The overall aim of this dissertation was to evaluate collagen fiber re-alignment and the uncrimping of fibers in response to mechanical load and to determine if structural changes are dependent on the age of the tendon (maturity of the collagen fibril network) or tendon location. Elucidating tendon structure-function relationships is an important step towards understanding the mechanical etiology of tendon injury as well as how tendon transfers load from muscle to bone. In this dissertation, local tendon structural response to load was first characterized in a mature mouse model of the supraspinatus tendon (SST) (Chapters 3 and 4). A developmental model was then utilized to determine if the ability of tendons to respond to load through collagen fiber re-alignment and the uncrimping of fibers was dependent on the age of the tendon or collagen fibril matrix maturity (Chapters 5 and 6). In this study, we identified that collagen fiber re-alignment may depend on the age, or more likely the maturity of the collagen network. Tendon locations demonstrated different collagen fiber re-alignment and crimp behavior and were suggested to have different preferred mechanisms in response to tensile mechanical load. Further, a new, quantitative method for analyzing collagen fiber crimp at specific points in the mechanical test was established and validated using a previously established semi-quantitative method. Surprisingly, we also

identified increases in crimp frequency during preconditioning and decreases in crimp frequency with increasing number of preconditioning cycles at 28 and 90 days old.

A1. The Effect of Preconditioning and Stress Relaxation on Local Collagen Fiber Re-Alignment: Inhomogeneous Properties of the Rat Supraspinatus Tendon

Chapter 2 examined the effect of preconditioning and stress relaxation on local collagen fiber re-alignment in a rat supraspinatus tendon model and characterized local collagen fiber distributions and mechanical properties. Cyclic preconditioning is a commonly accepted initial component of most tendon mechanical testing protocols. Preconditioning provides tendons with a consistent "history" and stress-strain results become repeatable, allowing for rigorous evaluation and comparison. While it is widely accepted that preconditioning is important, the mechanisms of preconditioning are not well understood. Micro-structural alterations, such as the re-arrangement of collagen fibers, is one proposed mechanism of preconditioning[47,61,65] and recently a strong correlation between changes in collagen fiber alignment and mechanical response during preconditioning has been reported.[47] However, the dependence of collagen fiber re-alignment during preconditioning on location had not yet been examined. Additionally, the re-arrangement of collagen fibers during stress relaxation or a tensile ramp-to-failure following preconditioning had not been examined in tendon. Therefore, we sought to quantify local collagen fiber re-alignment and corresponding mechanical properties in a rat SST model throughout tensile mechanical testing to address mechanisms of preconditioning and stress relaxation.

Interestingly, while a correlation was identified between cyclic preconditioning

and the early re-alignment of collagen fibers regardless of location, no significant changes in fiber re-alignment were found during stress relaxation. The large shift in collagen fiber re-alignment during preconditioning suggests that the re-alignment of collagen fibers may be an underlying mechanism of preconditioning as well as a potential explanation for the increase in tendon strength seen after preconditioning in highly aligned tendons.[54,65] This study also found that collagen fiber re-alignment became significantly more disorganized following a return to zero displacement following the stress relaxation test; however, no changes in alignment were identified during any of the holds at a constant load rate throughout the test. These findings, in combination with the lack of collagen fiber re-alignment identified during stress relaxation, suggest that a shift in the structural organization of collagen fibers may not be responsible for stress relaxation.[14,71] Additionally, this work supports previous work in a tissue-equivalent structure demonstrating a recovery of fiber alignment during a stress-free return to zero-displacement, but not during a return to zero-force, suggesting that fiber alignment away from the direction of loading occurred only after a return to an unstretched length during unloading.[72]

Also in this chapter, the inhomogeneous, nonlinear mechanical properties and collagen fiber alignment of the rat SST were reported. While similar patterns of collagen fiber alignment were found between the midsubstance and insertion site locations at all mechanical testing points, the insertion site location was found to be more disorganized than the midsubstance at all points throughout the mechanical test. Additionally, a lower linear modulus was found at the insertion site compared to at the midsubstance location.

The local differences found in cross-sectional area, linear modulus, transition strain and collagen fiber alignment at all regions of the mechanical loading profile demonstrate that the rat SST is inhomogeneous.

Further, the lower linear modulus and more disorganized collagen fiber distribution found at the insertion site compared to the midsubstance location support the idea that the insertion site experiences multi-axial loads, which may affect both the structure and mechanics of the tissue.[30,31,67] The potential correlation identified between collagen fiber alignment and preconditioning in this chapter supports previous studies[47] and provides information on the local re-alignment of collagen fibers in tendon throughout a mechanical testing protocols. Preloads and the specific preconditioning protocols used are not consistently reported in literature and the information presented in this chapter suggests that the mechanical testing protocol itself may have implications on the consistency and repeatability of the mechanical properties measured. Further, this chapter provides valuable data regarding the specific mechanical and organizational properties of the rat SST. Finally, this study reports information on how the collagen fiber distribution changes in response to various loading conditions. Collagen fiber distribution in relation to tendon macroscopic deformation is an important constituent of structurally based continuum models and it is important to be able to predict mechanical behavior during initial loading as well as unloading and reloading.[8,29]

A2. Collagen Fiber Re-Alignment, Mechanics and Correlations in a Mature Mouse Supraspinatus Tendon Model

Chapter 3 identified structure-function relationships in a mature mouse SST model. Collagen fiber re-alignment is one postulated mechanism of tendon structural

response to mechanical load. In Chapter 2, a large shift in collagen fiber orientation was found during preconditioning in a rat SST model. While preconditioning is commonly accepted to be an important part of mechanical testing protocols, the mechanisms of preconditioning are not well understood. Further, the effect of the number of cycles of preconditioning on collagen fiber re-alignment and mechanical properties had not been examined. Additionally, while the rat model is a well-established model for examining clinical problems in the shoulder, the mouse model provides additional opportunities to further examine structure-function relationships in tendon including an established developmental model and a wide range of genetically modified animals. However, local collagen fiber alignment and mechanical properties had not been characterized in the mouse SST. Therefore, we sought to locally measure collagen fiber re-alignment during 3 preconditioning protocols (5, 10, and 20 cycles) as well as throughout tensile mechanical testing and to compare local differences in collagen fiber distribution and corresponding mechanical properties in a mature mouse SST. Additionally, we examined correlations between structure and mechanical properties.

Mature mouse SSTs demonstrated a more disorganized collagen fiber distribution and a lower linear modulus at the insertion site compared to the midsubstance location. This result supported previous findings from Chapter 2 in the rat SST as well as previous work in the human SST.[30,31] Additionally, a low but significant correlation was identified between collagen fiber alignment before preconditioning and linear modulus supporting work in the human SST.[30] Further, the insertion site of the mature mouse SST re-aligned throughout the entire mechanical testing protocol supporting the results found in Chapter

2 in the rat SST. However, interestingly, the midsubstance location only re-aligned during preconditioning and in the linear-region of the stress-strain curve. This suggests that the more disorganized insertion site may require additional collagen fiber re-alignment compared to the midsubstance location. It is possible that the midsubstance location "pauses" recruiting fibers in the toe-region to allow the insertion site ample time to recruit additional fibers before transitioning to the linear-region. Further, other structural components of collagen, including collagen fiber crimp or cross-links, may affect collagen fiber re-alignment and may be distributed inhomogeneously throughout the tendon. An increase in collagen fiber crimp or cross-links at the midsubstance location compared to the insertion site may explain the lack of fiber re-alignment during the toe-region. Further, fibers initially recruited at the midsubstance location during preconditioning may be beginning to fail in the toe-region.

Surprisingly, no differences in collagen fiber re-alignment or mechanical properties were identified with increasing number of preconditioning cycles. This study found that mature mouse tendons respond via the re-alignment of collagen fibers to the small loads seen during preconditioning, regardless of the number of loading cycles or tendon location. This suggests that the mature collagen fiber network can communicate quickly and efficiently across the entire tendon length in the presence of small external loads.

A3. Collagen Fiber Crimp Behavior in a Mature Mouse Model

Chapter 4 presented a new, quantitative method for analyzing collagen fiber crimp. While collagen fiber crimp has been previously studied at slack or nondescript loading

conditions,[10-13] few studies have examined crimp at specific, quantifiable loads. Therefore a method to quantitatively evaluate crimp frequency at specific, quantifiable loads would provide additional information on tendon structural response to load in addition to identifying how crimp behavior may relate to tendon mechanical properties. Further, it has been speculated that collagen fiber crimp frequency may vary by location.[60] In Chapter 3, we determined that the insertion site of the mature mouse SST demonstrates a more disorganized collagen fiber distribution, a lower modulus and different collagen fiber re-alignment behavior than the midsubstance location. Therefore, the objective of this chapter was to validate a new, quantitative method of analyzing crimp frequency and to locally measure crimp frequency throughout a mechanical testing protocol in a mature mouse SST.

First, the quantitative method was presented and validated with a previously established semi-quantitative method.[71] The quantitative method demonstrated good inter- and intra-user reliability and a Bland-Altman analysis identified a normal distribution of error between the quantitative and previously established semi-quantitative methods. The quantitative method was then utilized to examine local changes in collagen fiber crimp behavior in a mature model SST model. Collagen fiber crimp frequency was quantified at the insertion site and midsubstance locations at 6 points in the mechanical testing protocol. An additional shoulder from each litter was also analyzed at an "in situ" reference configuration for comparative analysis. A decrease in collagen fiber crimp frequency was identified during the toe-region at both locations, supporting the idea that collagen fiber crimp frequency contributes to tendon nonlinear behavior.[19,25,75] While no

significant changes in crimp frequency were identified between the insertion site and midsubstance locations of the SST, results indicate that the magnitude of the crimp response to load is greater at the midsubstance location compared to the insertion site. Further, we identified a possible pattern of decreasing crimp frequency with increasing number of preconditioning cycles at the midsubstance location.

A4. Collagen Fiber Re-Alignment, Mechanics and Correlations in a Postnatal Developmental Mouse Supraspinatus Tendon Model

Chapter 5 builds from the work reported in Chapter 3 examining local collagen fiber re-alignment, mechanical properties and correlations in a mouse supraspinatus tendon model. In Chapter 3, we established that the mouse SST demonstrates different mechanical properties, collagen fiber distributions as well as collagen fiber re-alignment behavior at the insertion site and midsubstance locations. However, these properties had not yet been examined throughout postnatal development and it was not known if the changing structure and composition noted throughout postnatal development[3,5,6] affected the tendon's ability to respond to mechanical load. Therefore, the objective of this chapter was to examine local collagen fiber re-alignment and corresponding mechanical properties throughout postnatal development in a mouse SST model. Additionally, this chapter identified correlations between collagen fiber alignment and mechanical properties throughout postnatal development.

As expected, mechanical properties increased throughout development. Additionally, a decrease in transition strain and an increase in collagen fiber alignment was identified with increasing developmental age. Interestingly, this study found that significant collagen fiber re-alignment occurred at different points throughout the

mechanical loading protocol at each age group, indicating that the tendon's ability to structurally respond to load is dependent on developmental age and more importantly, on level of tissue organization or maturity. Overall, collagen fiber re-alignment was delayed at early development, suggesting that immature networks of collagen fibrils required a longer exposure to load to re-align and then transition into the linear-region.[5,6] Interestingly, different collagen fiber alignment behavior was noted at 4 days old between the midsubstance and insertion site locations, suggesting that the locations develop differently and at different rates.

Further, this study identified a low but significant negative correlation between collagen fiber alignment before preconditioning and linear modulus for the 4, 10 and 28 day time points. This finding provides additional support for the correlation identified in Chapter 3 as well as in work in the human SST.[30] Additionally, a positive and significant correlation was established between collagen fiber alignment and transition strain at early development. The correlation between collagen fiber alignment and transition strain at 4 days old further supports the theory that the insertion site and tendon midsubstance develop separately and at separate rates, as the more highly aligned midsubstance responded to load in a quicker manner and time scale than the less developed insertion site. This study demonstrated that the maturity of the collagen fiber network may influence the tendon's ability to respond to mechanical load and identified additional structure-function relationships throughout development.

A5. Examining Differences in Local Collagen Fiber Crimp Frequency Throughout Mechanical Testing in a Developmental Mouse Supraspinatus Tendon Model

Chapter 6 builds from the work presented in Chapter 4 examining how local collagen fiber crimp frequency changes throughout a tensile mechanical test. This chapter utilizes the software presented in Chapter 4 to quantify local changes in crimp frequency throughout postnatal development. In Chapter 4, the mature mouse SST model demonstrated significant changes in crimp frequency during the toe-region of the mechanical test at both locations. Additionally, a pattern of decreasing crimp frequency with increasing number of preconditioning cycles was noted. However, the dependence of collagen fiber crimp behavior on developmental age and in response to increasing number of cycles during preconditioning had not yet been examined throughout postnatal development. Therefore, the objective of this study was to quantify local collagen fiber crimp frequency throughout a mechanical testing protocol in a developmental mouse SST model.

Results from this study confirmed that the uncrimping of collagen fibers occurs primarily in the toe-region of the mechanical test and may contribute to tendon nonlinear behavior.[19,25,56,75] Additionally, results identified changes in collagen fiber crimp frequency with increasing number of preconditioning cycles at 28 days, supporting our hypothesis in Chapter 4. Changes in crimp frequency with increasing number of preconditioning cycles may have implications on the measurement of mechanical properties, in addition to identifying a proper reference configuration for strain analysis. Further, while no differences in local collagen fiber crimp behavior were identified, local differences in crimp behavior were found at 28 days between the insertion site and the

midsubstance location supporting observations in Chapter 4 in the mature tendon. In both 28 and 90 day SSTs, the midsubstance location demonstrated larger changes in crimp frequency with increasing number of preconditioning cycles compared to the insertion site location. This suggests that the more highly aligned collagen fiber distribution at the midsubstance location may increase sensitivity to the number of preconditioning cycles and the ability of tendon to respond quickly to mechanical load by the uncrimping of collagen fibers.

B. Future Directions

This dissertation expanded the current knowledge of tendon structure-function relationships, in particular it investigated how tendon structurally responds to load through collagen fiber re-alignment and the uncrimping of collagen fibers. Additionally, this study characterized mechanical properties, collagen fiber re-alignment and crimp frequency in the mouse SST throughout postnatal development. This work characterizes the normal structural response to load throughout postnatal development, which can be compared to future studies utilizing the mouse SST model in genetically modified or injury models to further elucidate structure-function relationships. Further, this study identified correlations between mechanical and structural properties throughout postnatal development. However, this study also identified several areas that merit further exploration. The following section describes several potential future research directions developed from the results and methodologies presented in this dissertation.

B1. Investigation of structure-function relationships in uninjured tendon

The previous chapters of this dissertation quantified structural changes in response

to mechanical load and identified correlations between structure and mechanical properties throughout postnatal development. However, collagen fiber re-alignment and crimp behavior do not fully explain tendon mechanical behavior and as a result, additional factors that may affect tendon mechanical properties and structural response to load which should be investigated. Therefore, further studies are necessary to identify, quantify and characterize the behavior of additional constituents and potential structural mechanisms that may affect tendon structural response to mechanical load. Ideally, these studies need to be performed in the mouse SST, as tendons located in different parts of the body have different functions and structural properties.

a. Tendon structural response to mechanical load across multiple hierarchical scales

Collagen is a versatile structural molecule and fundamental component of various types of tissues. Hierarchical structure, from molecular to tissue level, allows collagen to fulfill a variety of mechanical functions. Collagen orientation plays a fundamental role in establishing tissue mechanical properties.[35] Tendon is hierarchical, highly organized and composed primarily of type I collagen. Initially, immature type I collagen molecules assemble to form fibrils. Throughout development, fibrils associate laterally to create a wide range of fibril diameter sizes.[5,6,78] Fibrils are organized into collagen fibers, which form fascicles, which in turn coalesce to form tendon. In order to understand the process of tendon injury, we must first understand how native tendon responds to and transfers mechanical load across each hierarchical scale.

Recently, a molecular-based model of collagen fibril mechanics has been developed.[16,64] This model coupled molecular structure and biochemical information

with experimental mechanical results from collagen fibrils.[64] The results from these studies provide foundational information on structural changes at the collagen molecule level in addition to describing how molecular structural changes translate to collagen fibril dynamics. Collagen fibrils initially deform by the straightening of twisted triple-helical collagen molecules at small strains, then stretch axially, followed by molecular uncoiling.[64] Additionally, tropocollagen molecule deformation is influenced by fibril length, width and cross-linking density.[16,64] Recently, a technique was developed to examine strains within individual collagen fibrils within an Achilles tendon.[52] Following a prescribed mechanical loading protocol, fibrils were fixed in glutaraldeyde solution and atomic force microscopy was used to examine fibril mechanical properties.[52] Strain measured in collagen fibrils was at least 5% behind the applied macroscopic strain in the intact tendon. This indicates that collagen fibrils are not strained in the toe-region of the mechanical test. In addition, the collagen fibril network stretched uniformly both locally and across various anatomic tendon subregions.[52] Experiments in the excised rat tail tendon fascicle identified that collagen fibers also experience smaller strains than the strain applied to excised fascicle.[55] Additionally, it was suggested that strain no longer increases at the fiber level after the fibers have re-aligned in the direction of loading within the excised fascicle.[56] This dissertation examined structural response to load at the tendon level scale, examining local multi-fascicle or fascicle level structural changes. Further, the changes identified at the macroscopic level were speculated to be influenced by fibril level structure.

While tendon macroscopic mechanical properties are well established, there is a lack

of understanding of how microstructural elements respond to load and contribute to macroscopic mechanical behavior. Additionally, while collagen fibers are thought to be the primary load bearing structures in tendon that drive macroscopic mechanical behavior, the mechanisms by which collagen responds to and transfers load across multiple hierarchical scales is not well understood. While recent technological advances have provided opportunities to examine tendon mechanics and structural behavior during loading at smaller scales,[52,56] a consistent body of interpretable literature does not currently exist. It is vital to examine mechanical properties and structural changes in the same tendon with the same boundary conditions (intact tendon versus excised fascicles) to further support the suggested mechanisms in response to load and to understand how load is transferred across hierarchical scales. Further, structural changes and mechanical properties may be dependent on mature tendon composition and structure (e.g., crosslink density, presence of PGs or minor collagens, length of collagen fibrils, fiber crimp frequency, etc.). A developmental model, with changes in structure and composition,[3,5,6,36,78] would provide an appropriate system where the dependence of structural changes across hierarchy levels on tendon structure and composition could be examined. It is important to determine if structural changes at the fibril level can affect macroscopic mechanical properties or vice versa.

Therefore, the objective of this study would be to characterize inhomogeneity of local mechanical and structural properties, as well as structural changes in response to load, at multiple hierarchical scales in a postnatal developmental mouse SST model. This study would identify potential mechanisms of tendon load transfer between hierarchical levels

and further elucidate mechanisms of tendon structural response to load at each hierarchical level. In particular, the properties of the collagen fascicles in relation to fibril level structural changes must be quantified in an intact tendon, in addition to examining strain at the fibril and molecular scale, throughout postnatal development in the mouse SST. Finally, this study would locally characterize the content of proteoglycans, minor collagens, crosslink density, fibril diameters and lengths for the developing mouse SST.

For the proposed study, we hypothesize that the predominant mechanisms of structural response to load will vary by hierarchical level. In this dissertation, collagen fiber re-alignment and uncrimping were identified as potential mechanisms at the multi-fascicle level. However, previous work has suggested that collagen fiber sliding may be the dominant mechanism at the fiber level scale.[56] Therefore, we expect each hierarchical level to have a "preferred" mechanism to handle mechanical load and that these mechanisms may be dependent on the type of load or strain experienced by each hierarchical level.

Additionally, we hypothesize that structural changes will begin at the tendon level, then transfer down the hierarchical scale to the fascicle level, fiber level and fibril level followed by the collagen molecule itself. This hypothesis is supported by recent work in the Achilles tendon which identified a 5% lag in strain measured at the fibril level compared to the applied macroscopic strain.[52] The collagen fibrils may not bear load until fascicle and fiber levels have re-organized their structure in response to load. For example, collagen fibrils may not be tensioned until collagen fiber crimp has been

extinguished at the fiber level and all fibers are aligned in the direction of loading. Further supporting this hypothesis, microscopic collagen fiber crimp has been identified after the disappearance of crimp on the macroscopic level.[10]

We hypothesize that throughout development, local structural changes will be inhomogeneous at multiple hierarchical levels. Previous work in the Achilles tendon identified that collagen fibril strain was relatively homogeneous throughout the tendon.[52] However, the SST insertion site demonstrates a more disorganized collagen fiber distribution, lower mechanical properties and different collagen fiber behavior compared to the midsubstance location.[30,36,37] Additionally, previous studies have speculated that the insertion site experiences larger strains compared to the midsubstance location.[60] A homogeneous strain distribution at the fibril scale could potentially be explained by an inhomogeneous distribution of structural changes at higher hierarchical scales. In addition, fibril bundles at the insertion site may respond to load differently than bundles at the midsubstance location, accounting for the local differences in mechanical properties noted previously.[30,31,36,37]

Finally, we hypothesize that structural changes will be dependent on local composition and structure. Previous studies have identified a negative correlation between collagen fiber alignment and mechanical properties.[30,31,36] Additionally, in this dissertation it was suggested that collagen fiber re-alignment and uncrimping may be dependent on collagen fibril crosslinking or matrix maturity.

This study would utilize experiments as well as structural and mathematical models to understand load transfer between hierarchical levels. The objectives of this proposed

study could be completed by quantifying local structural changes and mechanical properties at smaller hierarchical levels (fascicle, fibril and molecular levels) as well as performing the necessary biochemical and structural analysis described for the SST. In order to quantify local structural changes and mechanical properties across multiple hierarchical scales, recent experimental techniques must be combined.[16,25,36,52,55,56] Further, the techniques described in this dissertation must be integrated with a confocal microscope to simultaneously take images at the multi-fascicle and fiber level scales.[36,55,56]

After successfully completing these experiments, the experimental results could be used to derive and validate an expansion of the previously established molecular-based model of collagen tissues.[16] The expansion of this model could be used to further elucidate structure-function relationships across multiple hierarchical scales, providing insight into the specific mechanisms of tendon structural response to load at each hierarchical scale as well as the mechanisms of load transfer between hierarchical scales. The information obtained in these experiments would improve our understanding of how tendons transfer load, both across hierarchical scales as well as from muscle to bone, thus enhancing ability to design tendon equivalent tissue engineered structures, modify clinical treatments and to further elucidate potential mechanisms of tendon injury with mechanical etiology.

b. Effect of matrix interconnectivity on mechanical properties and tendon structural response to load

This dissertation identified that where collagen fiber re-alignment occurs throughout a tensile mechanical test may depend on the tendon's age or maturity of the collagen

matrix. In Chapter 5, at early development, tendons demonstrated delayed collagen fiber re-alignment in response to load compared to tendons at 28 and 90 days old. The change in re-alignment behavior identified throughout postnatal development may be explained by the formation of additional connections between collagen fibers and the extracellular matrix as the tendon matures.[36] Additional fiber-fiber and fiber-matrix connections may increase the rate and efficiency that loads can be transferred across the tendon. Recent work in developing embryonic tendon demonstrated that inhibiting collagen crosslink formation resulted in a decrease in modulus.[34] This suggests that developmental tendon mechanical properties may be dependent on crosslink formation. Further, studies in tissue-engineered structures have shown that high densities of fiber interconnections were associated with higher strain energies and mechanical anisotropies.[2] The insertion site and midsubstance locations of the SST may demonstrate different quantities of collagen crosslinks and connections with surrounding fibers, which may explain the differences in mechanics and structure identified between locations throughout this dissertation.

However, the presence of collagen fibril crosslinks and fiber connections such as proteoglycans, FACITs or minor collagens have not yet been quantified in the SST or throughout postnatal development. Additionally, the number of connections each collagen fibril maintains with the surrounding matrix has not yet been examined in tendon or throughout postnatal development. Further, correlations between the presence of collagen crosslinks and connections with the surrounding matrix on tendon structural response to load or mechanical properties throughout development have not been examined.

Therefore, the objective of this study would be to: 1) Quantify local collagen fibril crosslinks and fiber-fiber interactions throughout development; and to 2) Identify correlations between the presence of collagen crosslinks and tendon structural response to load or mechanical properties throughout development. For the proposed study, we hypothesize that local collagen fiber crosslink density will increase throughout development at both locations and that collagen matrix connectivity will increase throughout development. Supporting this hypothesis, tendons increase in strength throughout development.[3,36] Further, a delayed structural response to mechanical load has been identified at early development, which may be explained by a low number of connections and crosslinks between fibers preventing effective load transmission.[36] Additionally, we hypothesize that a correlation will exist between collagen connectivity and mechanical properties. In this dissertation we identified a negative correlation between collagen fiber alignment and mechanics. A more highly connected collagen fiber network may result in a stronger, more unified tendon response.[34] Finally, we hypothesize that incorporating experimental information on fiber-fiber connections will improve the ability of mathematical models to predict mechanical data. Experimentally obtained information on the local microstructural network could be used to refine the parameters for fiber-fiber and fiber-matrix interactions currently incorporated into tendon constitutive models, thus improving their predictive capability.[18,29]

If successful, the proposed study would enhance our current understanding of structure-function relationships in tendon. Further, it will provide additional information on the mechanical and structural differences between the insertion site and midsubstance

locations. Clinically, tears begin and propagate at the SST insertion site. A better understanding of the insertion site microstructure is necessary to improve tendon repairs, injury diagnosis and the design of clinical treatments. Finally, a better understanding of the dependence of tendon mechanical properties on microstructure will help to further elucidate tendon injury with mechanical etiology in addition to providing necessary structural information for improving designs of tissue engineered replacements for injured tendons.

The proposed study could be achieved by utilizing a recently developed automated software system, which characterizes the tissue fiber network topology from scanning electronic microscope images.[2,7] The automated software detects and quantifies fiber orientation, connectivity, intersection spatial density and diameter.[7] In addition, previously established methods to analyze covalent crosslinking will be used.[1,74] Using the model system from this dissertation, insertion site and midsubstance samples from tendons throughout postnatal development would be characterized.

c. Conditions for re-alignment and fiber crimp behavior to return to initial configurations

In this dissertation, we characterized the response of collagen fibers to the presence of mechanical load. In Chapter 2, large changes in collagen fiber re-alignment towards the direction of load were identified during preconditioning in the rat SST. In Chapters 3 and 5, similar results were found during late development and maturity in the mouse SST model. The changes in collagen fiber re-alignment were identified despite the small loads and small number of cycles used in the preconditioning protocols. These results suggest that mature collagen fibers can respond quickly to the presence of mechanical

load through fiber re-alignment. Additionally, in Chapter 6, we identified an increase in collagen fiber crimp frequency compared to the preload with 5 and 10 cycles of preconditioning. However, while this dissertation identified changes in collagen fiber crimp frequency and fiber re-alignment in response to load, it is currently not known if these changes are permanent or if the tendon can "recover" or return to its initial configuration in the presence of certain conditions.

In Chapter 2, changes in collagen fiber re-alignment away from the direction of load, representing an increase in disorganization, were identified following a return to zero displacement after the stress relaxation (SR) test was applied.[37] However, changes in collagen fiber alignment were not identified following a 300 second hold after preconditioning or during a 600 second SR test. Recall in Chapter 1, previous work examining collagen fiber crimp behavior in ligament found no changes during SR tests.[71] However, changes in crimp frequency were identified during creep tests,[71] supporting previous results suggesting that creep and SR are governed by different mechanisms.[71,76,77] Further, tendon's ability to "recover" from loading regimes and stress relaxation are also thought to be separate phenomenon governed by different mechanisms.[8] The specific mechanisms of recovery are currently unknown. Additionally, it is unknown if the ability of tendon to return to its initial structural configuration is dependent on the loading conditions experienced, such as: loads reached during preconditioning, number of repeated cycles, loads reached during the mechanical testing protocol, strain levels reached, etc. The effect of increased hold times on collagen fiber re-alignment and crimp behavior following a return to zero displacement throughout

each mechanical testing component has not yet been examined.

Therefore, the objectives of this proposed study would be to: 1) To characterize additional mechanical loading protocols and determine which parameters result in permanent changes in tendon structure; and 2) To investigate potential mechanisms of tendon recovery. For the proposed study, we hypothesize that extended rest periods of 600 seconds or greater following preconditioning will result in a significant re-alignment of collagen fibers away from the direction of load. Following preconditioning, the tendons are returned to the initial length following the application of the preload. While no changes in collagen fiber distribution were found after a 300 second hold following preconditioning in the rat SST, an extended period of time may give the tendon time to re-orient fibers away from the direction of loading.[37] Secondly, we hypothesize that after reaching loads in the toe-region a) returning to zero displacement will result in a significant re-alignment of fibers away from the direction of loading, and b) following extended rest periods of 900 seconds or greater after the toe-region (following a return to zero displacement) will return with 5% of the original collagen fiber distribution after preload. In the rat SST, a significant re-alignment of fibers away from the direction of loading was identified following a return to zero displacement after a SR test; therefore, we expect a similar response following strains in the toe-region in the mouse SST.[37] Further, we expect the extended rest period following the return to zero displacement to allow fibers to continue to re-align away from loading towards their initial reference configuration. Next, we hypothesize that collagen fiber alignment will not return to its initial distribution after reaching loads in the linear-region (following a return to zero

displacement). In Chapters 4 and 6, several fibers were catastrophically damaged in the linear-region based on histologic identification. Therefore, we hypothesize that some fiber populations will begin to fail late in the toe-region and early in the linear-region of the mechanical test, preventing the tendon from returning to its initial configuration. Finally, we hypothesize that age, maximum load reached and rest period duration will significantly contribute to the ability of collagen fibers to return to their initial distribution following a return to zero displacement.

If successful, the proposed study will identify the parameters necessary for tendon to return to its initial structural configuration. Understanding how tendon responds to and subsequently recovers from mechanical load is necessary to identify parameters that may result in tendon injury with mechanical etiology. Further, this study will help identify what strains result in long-term or permanent structural changes, which may be indications of permanent fiber damage. Overall, this study will improve our understanding of how tendon structure corresponds to mechanical function and further our understanding of tendon physiology during load transfer.

To accomplish the proposed objectives, the methods utilized in this dissertation to quantify collagen fiber re-alignment and uncrimping will be applied to an expanded mechanical testing protocol to examine structural changes in response to: 1) extended periods of rest following preconditioning; 2) the effect of returning to zero displacement after reaching a point the toe-region; 3) the effect of adding holds following the return to zero displacement; 4) the effect of returning to zero displacement after reaching a point the linear-region; 5) the effect of adding a hold following the return to zero displacement.

The proposed study will utilize a multiple regression model to determine the contribution of each loading parameter (strain rate, hold time, etc.) to identify conditions that are necessary for tendons to return to their initial configuration. Additionally, studies are needed to further elucidate the role of collagen fiber re-alignment and crimp behavior during SR, in addition to the effect of increased strains and different hold times, as well as to examine the effect of fatigue loading followed by rest periods.

d. Detecting fiber damage and identifying load levels that result in damage

This dissertation identified significant changes in collagen fiber re-alignment throughout a mechanical testing protocol and identified correlations between mechanical properties and collagen fiber re-alignment behavior before and after preconditioning. However, recent work in ligament has utilized a vector correlation technique to associate abnormal changes in collagen fiber re-alignment behavior with the onset of local collagen fiber damage and a subsequent decrease in local mechanical properties.[45,46,48] In addition, software has recently been developed to identify regions of collagen fiber damage marked by an increase in crimp behavior utilizing second-harmonic generation (SHG) images.[58] The current software presented in Chapter 4 could be refined utilizing the standards previously established for SHG images[58] to identify areas of fiber rupture. Additionally, criteria must be established to augment the software to identify the return of fibers to their initial configuration. These techniques would be instrumental in identifying an appropriate strain cutoff for repeated mechanical tests. Frequently, experimental protocols necessitate re-testing samples to either run multiple assays or measure mechanical properties at different strain rates or loading conditions. However, it

is important to ensure that the samples are not being damaged during the loading protocols and thus affecting the subsequent tests. Utilizing the proposed techniques in combination with our current mechanical testing set-up would provide valuable information on the appropriate load levels to repeatedly test samples. Additionally, these techniques would aid efforts to further elucidate the specific structural response at each loading level and component of the mechanical testing protocol. Therefore, the objective of this proposed study would be to: 1) utilize vector correlation software to identify abnormal collagen fiber re-alignment behavior; 2) to identify the onset of local collagen fiber damage throughout tensile mechanical testing through abnormal collagen fiber re-alignment and crimp behavior; 3) correlate the onset of local collagen fiber damage with local decreases in mechanical properties. For the proposed study, we would hypothesize that 1) abnormal collagen fiber re-alignment would correlate with areas with decreased linear moduli; and that 2) abnormal or an increase collagen fiber crimp frequency following the transition strain would correlate with decreased mechanical properties.

e. Tendon remodeling in response to mechanical load

The work in this dissertation provides a foundational understanding of how tendon's structurally respond to mechanical testing in the ex vivo testing condition. While the ex vivo condition provides important and more easily interpretable information on how tendon responds to load, it is vital to obtain an understanding of the effect of cells and the subsequent mechanobiological response to mechanical load. However, in order to examine the effect of cells on tendon structural response to mechanical load, an ex vivo tendon culture model must be developed. Further, mathematical models are an important

tool for investigating and interpreting complex relationships between structure and mechanical function and there is an increasing need for integrative multi-scale models that can capture both cellular and molecular mechanisms and their associated responses at the tissue level.[20,70] Previous studies have shown that coupling a discrete, stochastic agent-based model (ABMs) of cell-level processes with continuum-based constrained mixture models (CMMs) of tissue-level phenomena demonstrated potential to increase our understanding of how biology and physiology contribute to disease processes.[20,70] Agent-based models simulate interactions of autonomous agents (individual cells) with each other and with their environment based on a literature-derived rule set.[69,70] Continuum-based models employ phenomenological constitutive relations and are an important tool toward understanding the relationship between tendon structure and corresponding mechanical properties.[20,29]

However, currently neither a constitutive growth and remodeling model nor an ABM model exist for tendon. Therefore, the overall aim of the proposed study would be to establish a growth and remodeling model for tendon that can be adapted to be applied to development, injury and changing loading conditions. The specific objectives associated with this aim are: 1) To develop an ex vivo tendon culture mechanical testing system that can be incorporated with the current techniques measuring structural changes; 2) To develop a constitutive mixture model of growth and remodeling for tendon; 3)To develop an agent-based model of tenocytes in response to mechanical load based on previously published literature; and 4) To refine the parameters of both model systems by establishing congruency between the model systems. For the proposed study, we

hypothesize that 1) tendons will demonstrate a more robust structural response to load in the presence of live cells; and 2) the multi-scale model will provide a closer in vivo prediction of mechanical properties compared to the ABM or CMM alone.

B2. Investigation of structure-function relationships in models with altered loading conditions

a. Collagen fiber crimp frequency and collagen fiber re-alignment in an injury model

The mechanical properties of healing tendons have been shown to be effected by the amount of activity allowed during the healing process,[17,44,53,68] which has motivated additional work examining the affect of periods of immobilization or altered loading conditions following rotator cuff injury and repair.[40-44] Ideally, immobilizing the shoulder post-rotator cuff repair would allow the complex tendon-to-bone insertion site time to heal and lay down a more organized collagen fiber matrix in the absence of multi-axial loads. In Chapters 3 and 5, we demonstrated that a more organized collagen fiber alignment may result in a tendon with higher tensile mechanical properties, which may prevent the tendon from re-tearing in response to early loading before the tendon-to-bone insertion site is re-developed.

Additionally, collagen fiber crimp frequency is thought to influence tendon mechanical properties.[26] While Chapters 4 and 6 of this dissertation examined collagen fiber crimp frequency and behavior throughout a tensile mechanical testing protocol, the affect of an injury on crimp behavior has not been examined in tendon. In previous studies, healing ligament examined within scanning electron microscopy was found to have dramatically different collagen fiber crimp patterns in the scar region compared to

controls.[26] Tendon may have a similar response to injury and an alteration in crimp behavior may affect the ability of tendons to structurally respond to load. Further, alterations in crimp behavior following injury may contribute to the high re-tear rate seen clinically with, for example, supraspinatus tendon repairs. A better understanding of healing tendon's response to load will aid in the appropriate clinical treatment of tendon injuries.

Further, in Chapters 3 and 5 significant correlations were identified between collagen fiber alignment and mechanical properties. Collagen fiber organization may be an appropriate measure of the progress of tendon healing post-injury. Recent developments in imaging technology have demonstrated the ability to noninvasively measure collagen fiber alignment and collagen fiber crimp properties and may be applicable to clinical problems.[27,38,49-51] However, imaging measures of collagen fiber properties have not yet been compared to the ex vivo experimental measures. Linking experimental ex vivo measures with clinically available in vivo measures would enhance our understanding of how the information obtained ex vivo applies to clinical problems. Additionally, it will provide more information on tendon structure-function relationships, which will help to elucidate mechanisms and markers of tendon healing.

Therefore, the objectives of this study would be to: 1) Determine how injury affects tendon structure and structural response to load and 2) corresponding mechanical properties; and 3) To correlate imaging measurements of collagen structure and organization obtained from in vivo and ex vivo measurements throughout the injury time course. In this proposed study, we would hypothesize that following injury, newly

formed collagen will demonstrate a higher frequency of collagen fiber crimp. As seen in Chapter 6, crimp in early stages of postnatal development demonstrated a higher frequency than crimp at maturity. Therefore, we expect newly assembled collagen fibrils and fibers to display a higher frequency of collagen fiber crimp compared to the surrounding matrix, which may affect local mechanical properties. Additionally, we hypothesize that as the tendon heals, collagen fiber crimp frequency will decrease with time. As the tendon heals, the newly formed collagen fibers will mature and adapt in response to the surrounding matrix environment supporting observations made in healing ligament.[26] Next, we hypothesize that a correlation will be present between collagen fiber crimp data from MRI and experimental frequency measurements and that a correlation will be present between collagen fiber organization measures obtained from imaging techniques and linear modulus.

Overall, if successful, the proposed study will provide significant insight into the consequences of injury on tendon structure, as well as the subsequent effect on tendon mechanical function. Further, correlations between ex vivo and noninvasive imaging measures of collagen fiber characteristics will provide new avenues for tracking the progress of healing tendons as well as initial injury diagnosis.

In this proposed study, the methods described in this dissertation could be used in an established tendon injury model to examine the local effects of injury and subsequent remodeling on tendon collagen structural behavior. Additionally, fluorescent markers could be used to denote newly formed collagen in response to injury.[28] This would provide the opportunity to distinguish between the structural properties and response of

newly formed collagen versus remodeled collagen in the presence of an injury. In addition, magnetic resonance imaging (MRI) and ultrasound (US) can be used to track collagen fiber structural characteristics in vivo and for comparison with ex vivo measures. Finally, this study will attempt to identify linear correlations between collagen fiber alignment from injured and healing tendons. To identify correlations between in vivo imaging and ex vivo measures of collagen structure, the following comparisons could be attempted between: 1) Crimp frequency obtained with MRI[38] and the experimentally derived measure (Methods from Chapters 4 and 6); 2) Collagen fiber alignment obtained with double-quantum filtered MRI (DQF) imaging[27] with cross polarizer measurements; 3) Measurements of anisotropy from diffusion tensor imaging (DTI)[21,49-51] and experimental measures; and 4) US measure collagen fiber distribution and alignment from experimental measures.[15,22-24] Further, the information obtained from the experimental and imaging studies could be utilized couple constitutive mixed model (CMM)-agent-based model (ABM) model[20,70] to predict mechanical behavior as described in section B1.5 utilizing developmental injury data from previous studies.[3,4]

b. Collagen fiber crimp frequency and collagen fiber re-alignment in an overuse model

This dissertation quantified collagen fiber crimp frequency and fiber re-alignment behavior throughout postnatal development. In Chapters 3 and 5, we found that the insertion site demonstrated a more disorganized collagen fiber distribution and lower modulus compared to the midsubstance location.[36] Additionally, the insertion site and midsubstance locations showed different collagen fiber re-alignment and crimp responses throughout postnatal development. The differences observed in tendon structure and

ex vivo structural response to load may occur in response to multi-axial loads experienced at the supraspinatus tendon insertion site in vivo.[36,37] An established overuse model has demonstrated that collagen fiber distributions become more disorganized, cross-sectional area increases and modulus decreases in response to downhill treadmill running.[59] However, collagen fiber re-alignment behavior and crimp behavior have not been examined in an overuse model. Therefore, the objectives of the proposed study would be: 1) To determine if overuse results in a) changes in collagen fiber crimp frequency, b) the ability of the tendon to structurally respond to load, or c) exacerbates the differences between the midsubstance and insertion site locations; and 2) To identify correlations with a) structural properties and mechanical properties and b) structural properties and functional measures. For the proposed study, we hypothesize that overuse activity will result in a decrease in crimp frequency. Previous studies in the horse identified a decrease in crimp frequency with exercise in the central third of the superficial digital flexor tendon;[39] therefore, we expect the insertion site of the SST to demonstrate a decrease in crimp frequency with overuse activity over time. Second, we hypothesize that the tendon will exhibit smaller changes in crimp frequency throughout the mechanical test. In this dissertation, we identified that the insertion site demonstrated more modest changes in collagen fiber crimp behavior compared to the more highly aligned midsubstance location. Overuse activity has been shown to decrease collagen fiber organization; therefore we expect overuse tendons to require additional collagen fiber re-alignment and demonstrate a decreased crimp response.[57]

c. Identifying necessary constituents for proper tendon growth and development

After establishing a growth and remodeling model for tendon as described in Section B1.5, the model could be adapted to stimulate tendon development.[62,63,73] In order to properly design tissue engineered structures and therapeutic intervention for tendon injuries, it is necessary to further elucidate the process of normal tendon development and the contribution of each individual constituent to tendon mechanical behavior. Therefore, the objective of the proposed study is to adapt an ABM-CMM model to examine alterations to the normal process of tendon development,[20,62,63,70,73] to further our knowledge of tendon mechanobiology and to elucidate the individual role of each constituent in the process of tendon structural development. For the proposed study, we hypothesize that, after 10 days postnatal, the collagen fiber distribution of tendon is dependent on mechanical load. This hypothesis is supported by previous work using a botox model to investigate changes throughout development in a mouse SST.[66] Additionally, we hypothesize that cross-link formation will be positively correlated to mechanical properties in early development. This hypothesis is supported by preliminary work in embryonic tendon.[34] In addition to utilizing botox injections[66] to alter the loading environment throughout development, genetically modified mice could be used to determine the potential role and compensatory mechanisms of individual components of tendon throughout development.

d. Identifying changes in structural response and mechanical properties with alterations in Type III collagen

Type III collagen is a fibrillar forming collagen and is colocalized with type I collagen in several tissues.[32] Studies have demonstrated the coexistence of type I and

type III collagens within individual fibrils and have suggested that these interactions may regulate fibril formation and growth.[9] An increase in type III collagen has been associated with healing or ruptured tendons and is thought to be an abnormal healing response resulting in scar tissue with inferior mechanical properties. In particular, areas of tendons associated with stress or potential microtrauma are thought to produce an increased amount of type III collagen which may predispose them to rupture.[33] Tissues with increased amount of type III collagen demonstrate decreased resistance to tensile forces and rupture more frequently.[33] Additionally, studies in animal deficient in type III collagen demonstrated severe cardiac defects and are subject to rupture of blood vessels or intestines as well as aortic aneurysms.[32] Further the distribution of collagen fibril diameters were highly variable in type III collagen deficient mice and type I collagen fibrils in the adventitia of the aorta were disorganized compared to wild type controls.[32] However, the effect of type III collagen on tendon structural response and local mechanical properties is currently unknown. Therefore, the objective of this study would be to examine local collagen fiber re-alignment behavior as well as the transition point in collagen type III deficient mice. We hypothesize that tendons deficient in type III collagen would demonstrate an altered structural response to load and transition region. This hypothesis is supported by previous work identifying a more disorganized collagen fibril population in type III deficient animals which may result in a delayed structural response and longer transition region.[32] However, given that type III collagen deficient animals are prone to aneurysms and spontaneous blood vessel and intestinal ruptures, it is also possible that the tendons would demonstrate an accelerated structural response and

very short toe-region with tendons reaching very high stresses with minimal amounts of strain. Regardless, literature strongly indicates that samples deficient in type III collagen would demonstrate an altered structural response to mechanical load and toe-region properties compared to control animals which merits further study. The information obtained from these studies could improve our understanding of the role of type III collagen in regulating collagen fibrillogenesis, the properties of healing tendon, in addition to providing insights into the pathology of diseases such as Ehlers-Danlos syndrome.

C. Final Conclusions

The studies conducted in this dissertation demonstrated that the ability of collagen fibers to structurally respond to mechanical load through fiber re-alignment or uncrimping depends on the age of the tendon and maturity of the collagen fiber matrix. Additionally, studies examining collagen fiber crimp showed that the number of preconditioning cycles and mechanical testing protocol affects crimp frequencies, which may affect experimentally measured mechanical properties. Finally, at all time points, the insertion site demonstrated a more disorganized collagen fiber distribution and lower linear modulus compared to the midsubstance location.

D. References

1. Aldous IG, Veres SP, Jahangir A, Lee JM: Differences in collagen cross-linking between the four valves of the bovine heart: a possible role in adaptation to mechanical fatigue. **Am J Physiol Heart Circ Physiol 296:**H1898-1906, 2009
2. Amoroso NJ, D'Amore A, Hong Y, Wagner WR, Sacks MS: Elastomeric electrospun polyurethane scaffolds: the interrelationship between fabrication conditions, fiber topology, and mechanical properties. **Adv Mater 23:**106-111
3. Ansorge HL, Adams S, Birk DE, Soslowsky LJ: Mechanical, compositional, and structural properties of the post-natal mouse Achilles tendon. **Ann Biomed Eng 39:**1904-1913
4. Ansorge HL, Hsu JE, Edelstein L, Adams S, Birk DE, Soslowsky LJ: Recapitulation of the Achilles tendon mechanical properties during neonatal development: a study of differential healing during two stages of development in a mouse model. **J Orthop Res 30:**448-456
5. Birk DE, Nurminskaya MV, Zycband EI: Collagen fibrillogenesis in situ: fibril segments undergo post-depositional modifications resulting in linear and lateral growth during matrix development. **Dev Dyn 202:**229-243, 1995
6. Birk DE, Zycband EI, Woodruff S, Winkelmann DA, Trelstad RL: Collagen fibrillogenesis in situ: fibril segments become long fibrils as the developing tendon matures. **Dev Dyn 208:**291-298, 1997
7. D'Amore A, Stella JA, Wagner WR, Sacks MS: Characterization of the complete fiber network topology of planar fibrous tissues and scaffolds. **Biomaterials**

31:5345-5354

8. Duenwald SE, Vanderby R, Jr., Lakes RS: Stress relaxation and recovery in tendon and ligament: experiment and modeling. **Biorheology 47:**1-14

9. Fleischmajer R, Perlish JS, Burgeson RE, Shaikh-Bahai F, Timpl R: Type I and type III collagen interactions during fibrillogenesis. **Ann N Y Acad Sci 580:**161-175, 1990

10. Franchi M, Fini M, Quaranta M, De Pasquale V, Raspanti M, Giavaresi G, et al: Crimp morphology in relaxed and stretched rat Achilles tendon. **J Anat 210:**1-7, 2007

11. Franchi M, Ottani V, Stagni R, Ruggeri A: Tendon and ligament fibrillar crimps give rise to left-handed helices of collagen fibrils in both planar and helical crimps. **J Anat 216:**301-309

12. Franchi M, Quaranta M, Macciocca M, Leonardi L, Ottani V, Bianchini P, et al: Collagen fibre arrangement and functional crimping pattern of the medial collateral ligament in the rat knee. **Knee Surg Sports Traumatol Arthrosc 18:**1671-1678

13. Franchi M, Raspanti M, Dell'Orbo C, Quaranta M, De Pasquale V, Ottani V, et al: Different crimp patterns in collagen fibrils relate to the subfibrillar arrangement. **Connect Tissue Res 49:**85-91, 2008

14. Fung YC: **Biomechanics : mechanical properties of living tissues, ed 2nd.** New York: Springer-Verlag, 1993

15. Garcia T, Hornof WJ, Insana MF: On the ultrasonic properties of tendon.

Ultrasound Med Biol 29:1787-1797, 2003

16. Gautieri A, Vesentini S, Redaelli A, Buehler MJ: Hierarchical structure and nanomechanics of collagen microfibrils from the atomistic scale up. **Nano Lett 11:**757-766

17. Gimbel JA, Van Kleunen JP, Williams GR, Thomopoulos S, Soslowsky LJ: Long durations of immobilization in the rat result in enhanced mechanical properties of the healing supraspinatus tendon insertion site. **J Biomech Eng 129:**400-404, 2007

18. Guerin HA, Elliott DM: The role of fiber-matrix interactions in a nonlinear fiber-reinforced strain energy model of tendon. **J Biomech Eng 127:**345-350, 2005

19. Hansen KA, Weiss JA, Barton JK: Recruitment of tendon crimp with applied tensile strain. **J Biomech Eng 124:**72-77, 2002

20. Hayenga HN, Thorne BC, Peirce SM, Humphrey JD: Ensuring congruency in multiscale modeling: towards linking agent based and continuum biomechanical models of arterial adaptation. **Ann Biomed Eng 39:**2669-2682

21. Helm P, Beg MF, Miller MI, Winslow RL: Measuring and mapping cardiac fiber and laminar architecture using diffusion tensor MR imaging. **Ann N Y Acad Sci 1047:**296-307, 2005

22. Hoffmeister BK, Gehr SE, Miller JG: Anisotropy of the transverse mode ultrasonic properties of fixed tendon and fixed myocardium. **J Acoust Soc Am 99:**3826-3836, 1996

23. Hoffmeister BK, Handley SM, Wickline SA, Miller JG: Ultrasonic determination

of the anisotropy of Young's modulus of fixed tendon and fixed myocardium. **J Acoust Soc Am 100:**3933-3940, 1996

24. Hoffmeister BK, Verdonk ED, Wickline SA, Miller JG: Effect of collagen on the anisotropy of quasi-longitudinal mode ultrasonic velocity in fibrous soft tissues: a comparison of fixed tendon and fixed myocardium. **J Acoust Soc Am 96:**1957-1964, 1994

25. Houssen YG, Gusachenko I, Schanne-Klein MC, Allain JM: Monitoring micrometer-scale collagen organization in rat-tail tendon upon mechanical strain using second harmonic microscopy. **J Biomech 44:**2047-2052

26. Hurschler C, Provenzano PP, Vanderby R, Jr.: Scanning electron microscopic characterization of healing and normal rat ligament microstructure under slack and loaded conditions. **Connect Tissue Res 44:**59-68, 2003

27. Ikoma K, Kusaka Y, Takamiya H, Eliav U, Navon G, Seo Y: Evaluation of collagen fiber maturation and ordering in regenerating tendons employing H-1 double quantum filtered NMR spectroscopy. **J Orthop Res 21:**149-156, 2003

28. Krahn KN, Bouten CV, van Tuijl S, van Zandvoort MA, Merkx M: Fluorescently labeled collagen binding proteins allow specific visualization of collagen in tissues and live cell culture. **Anal Biochem 350:**177-185, 2006

29. Lake SP, Cortes DH, Kadlowec JA, Soslowsky LJ, Elliott DM: Evaluation of affine fiber kinematics in human supraspinatus tendon using quantitative projection plot analysis. **Biomech Model Mechanobiol 11:**197-205

30. Lake SP, Miller KS, Elliott DM, Soslowsky LJ: Effect of fiber distribution and

realignment on the nonlinear and inhomogeneous mechanical properties of human supraspinatus tendon under longitudinal tensile loading. **J Orthop Res 27:**1596-1602, 2009

31. Lake SP, Miller KS, Elliott DM, Soslowsky LJ: Tensile properties and fiber alignment of human supraspinatus tendon in the transverse direction demonstrate inhomogeneity, nonlinearity, and regional isotropy. **J Biomech 43:**727-732

32. Liu X, Wu H, Byrne M, Krane S, Jaenisch R: Type III collagen is crucial for collagen I fibrillogenesis and for normal cardiovascular development. **Proc Natl Acad Sci U S A 94:**1852-1856, 1997

33. Maffulli N, Ewen SW, Waterston SW, Reaper J, Barrass V: Tenocytes from ruptured and tendinopathic achilles tendons produce greater quantities of type III collagen than tenocytes from normal achilles tendons. An in vitro model of human tendon healing. **Am J Sports Med 28:**499-505, 2000

34. Marturano JE KC: Mechanical and biochemical effects of inhibiting collagen crosslinking in developing embryonic tendon. **Trans Orthop Res Soc 37:**2302, 2012

35. Masic A, Bertinetti L, Schuetz R, Galvis L, Timofeeva N, Dunlop JW, et al: Observations of multiscale, stress-induced changes of collagen orientation in tendon by polarized Raman spectroscopy. **Biomacromolecules 12:**3989-3996

36. Miller KS, Connizzo BK, Soslowsky LJ: Collagen Fiber Re-Alignment in a Neonatal Developmental Mouse Supraspinatus Tendon Model. **Ann Biomed Eng**, 2012

37. Miller KS, Edelstein, L., Connizzo, B. K., and Soslowsky, L. J... Effect of Preconditioning and Stress Relaxation on Local Collagen Fiber Re-Alignment: Inhomogeneous Properties of Rat Supraspinatus Tendon. **Journal of Biomechanical Engineering In press**, 2012

38. Mountain KM, Bjarnason TA, Dunn JF, Matyas JR: The functional microstructure of tendon collagen revealed by high-field MRI. **Magn Reson Med 66:**520-527

39. Patterson-Kane JC, Wilson AM, Firth EC, Parry DA, Goodship AE: Exercise-related alterations in crimp morphology in the central regions of superficial digital flexor tendons from young thoroughbreds: a controlled study. **Equine Vet J 30:**61-64, 1998

40. Peltz CD, Hsu JE, Zgonis MH, Trasolini NA, Glaser DL, Soslowsky LJ: Biceps tendon properties worsen initially but improve over time following rotator cuff tears in a rat model. **J Orthop Res 29:**874-879

41. Peltz CD, Hsu JE, Zgonis MH, Trasolini NA, Glaser DL, Soslowsky LJ: Decreased loading after rotator cuff tears leads to improved biceps tendon properties in a rat model. **J Shoulder Elbow Surg 20:**698-707

42. Peltz CD, Hsu JE, Zgonis MH, Trasolini NA, Glaser DL, Soslowsky LJ: The effect of altered loading following rotator cuff tears in a rat model on the regional mechanical properties of the long head of the biceps tendon. **J Biomech 43:**2904-2907

43. Peltz CD, Hsu JE, Zgonis MH, Trasolini NA, Glaser DL, Soslowsky LJ: Intra-

articular changes precede extra-articular changes in the biceps tendon after rotator cuff tears in a rat model. **J Shoulder Elbow Surg**

44. Peltz CD, Sarver JJ, Dourte LM, Wurgler-Hauri CC, Williams GR, Soslowsky LJ: Exercise following a short immobilization period is detrimental to tendon properties and joint mechanics in a rat rotator cuff injury model. **J Orthop Res 28:**841-845

45. Quinn KP, Bauman JA, Crosby ND, Winkelstein BA: Anomalous fiber realignment during tensile loading of the rat facet capsular ligament identifies mechanically induced damage and physiological dysfunction. **J Biomech 43:**1870-1875

46. Quinn KP, Winkelstein BA: Altered collagen fiber kinematics define the onset of localized ligament damage during loading. **J Appl Physiol 105:**1881-1888, 2008

47. Quinn KP, Winkelstein BA: Preconditioning is correlated with altered collagen fiber alignment in ligament. **J Biomech Eng 133:**064506

48. Quinn KP, Winkelstein BA: Vector correlation technique for pixel-wise detection of collagen fiber realignment during injurious tensile loading. **J Biomed Opt 14:**054010, 2009

49. Raya JG, Arnoldi AP, Weber DL, Filidoro L, Dietrich O, Adam-Neumair S, et al: Ultra-high field diffusion tensor imaging of articular cartilage correlated with histology and scanning electron microscopy. **MAGMA 24:**247-258

50. Raya JG, Horng A, Dietrich O, Krasnokutsky S, Beltran LS, Storey P, et al: Articular cartilage: in vivo diffusion-tensor imaging. **Radiology 262:**550-559

51. Raya JG, Melkus G, Adam-Neumair S, Dietrich O, Mutzel E, Kahr B, et al: Change of diffusion tensor imaging parameters in articular cartilage with progressive proteoglycan extraction. **Invest Radiol 46:**401-409

52. Rigozzi S, Stemmer A, Muller R, Snedeker JG: Mechanical response of individual collagen fibrils in loaded tendon as measured by atomic force microscopy. **J Struct Biol 176:**9-15

53. Sarver JJ, Peltz CD, Dourte L, Reddy S, Williams GR, Soslowsky LJ: After rotator cuff repair, stiffness--but not the loss in range of motion--increased transiently for immobilized shoulders in a rat model. **J Shoulder Elbow Surg 17:**108S-113S, 2008

54. Schatzmann L, Brunner P, Staubli HU: Effect of cyclic preconditioning on the tensile properties of human quadriceps tendons and patellar ligaments. **Knee Surg Sports Traumatol Arthrosc 6 Suppl 1:**S56-61, 1998

55. Screen HR, Lee DA, Bader DL, Shelton JC: Development of a technique to determine strains in tendons using the cell nuclei. **Biorheology 40:**361-368, 2003

56. Screen HR, Lee DA, Bader DL, Shelton JC: An investigation into the effects of the hierarchical structure of tendon fascicles on micromechanical properties. **Proc Inst Mech Eng H 218:**109-119, 2004

57. Sellaro TL, Hildebrand D, Lu Q, Vyavahare N, Scott M, Sacks MS: Effects of collagen fiber orientation on the response of biologically derived soft tissue biomaterials to cyclic loading. **J Biomed Mater Res A 80:**194-205, 2007

58. Sereysky JB, Andarawis-Puri N, Jepsen KJ, Flatow EL: Structural and

mechanical effects of in vivo fatigue damage induction on murine tendon. **J Orthop Res**

59. Soslowsky LJ, Thomopoulos S, Tun S, Flanagan CL, Keefer CC, Mastaw J, et al: Neer Award 1999. Overuse activity injures the supraspinatus tendon in an animal model: a histologic and biomechanical study. **J Shoulder Elbow Surg 9:**79-84, 2000

60. Stouffer DC, Butler DL, Hosny D: The relationship between crimp pattern and mechanical response of human patellar tendon-bone units. **J Biomech Eng 107:**158-165, 1985

61. Sverdlik A, Lanir Y: Time-dependent mechanical behavior of sheep digital tendons, including the effects of preconditioning. **J Biomech Eng 124:**78-84, 2002

62. Taber LA: Biomechanics of cardiovascular development. **Annu Rev Biomed Eng 3:**1-25, 2001

63. Taber LA: Mechanical aspects of cardiac development. **Prog Biophys Mol Biol 69:**237-255, 1998

64. Tang Y, Ballarini R, Buehler MJ, Eppell SJ: Deformation micromechanisms of collagen fibrils under uniaxial tension. **J R Soc Interface 7:**839-850

65. Teramoto A, Luo ZP: Temporary tendon strengthening by preconditioning. **Clin Biomech (Bristol, Avon) 23:**619-622, 2008

66. Thomopoulos S, Kim HM, Rothermich SY, Biederstadt C, Das R, Galatz LM: Decreased muscle loading delays maturation of the tendon enthesis during

postnatal development. **J Orthop Res 25:**1154-1163, 2007

67. Thomopoulos S, Williams GR, Gimbel JA, Favata M, Soslowsky LJ: Variation of biomechanical, structural, and compositional properties along the tendon to bone insertion site. **J Orthop Res 21:**413-419, 2003

68. Thomopoulos S, Williams GR, Soslowsky LJ: Tendon to bone healing: differences in biomechanical, structural, and compositional properties due to a range of activity levels. **J Biomech Eng 125:**106-113, 2003

69. Thorne BC, Bailey AM, DeSimone DW, Peirce SM: Agent-based modeling of multicell morphogenic processes during development. **Birth Defects Res C Embryo Today 81:**344-353, 2007

70. Thorne BC, Hayenga HN, Humphrey JD, Peirce SM: Toward a multi-scale computational model of arterial adaptation in hypertension: verification of a multi-cell agent based model. **Front Physiol 2:**20

71. Thornton GM, Shrive NG, Frank CB: Ligament creep recruits fibres at low stresses and can lead to modulus-reducing fibre damage at higher creep stresses: a study in rabbit medial collateral ligament model. **J Orthop Res 20:**967-974, 2002

72. Tower TT, Neidert MR, Tranquillo RT: Fiber alignment imaging during mechanical testing of soft tissues. **Ann Biomed Eng 30:**1221-1233, 2002

73. Varner VD, Voronov DA, Taber LA: Mechanics of head fold formation: investigating tissue-level forces during early development. **Development 137:**3801-3811

74. Willett TL, Labow RS, Aldous IG, Avery NC, Lee JM: Changes in collagen with

aging maintain molecular stability after overload: evidence from an in vitro tendon model. **J Biomech Eng 132:**031002

75. Woo SL: Mechanical properties of tendons and ligaments. I. Quasi-static and nonlinear viscoelastic properties. **Biorheology 19:**385-396, 1982

76. Woo SL, Debski RE, Zeminski J, Abramowitch SD, Saw SS, Fenwick JA: Injury and repair of ligaments and tendons. **Annu Rev Biomed Eng 2:**83-118, 2000

77. Woo SL, Johnson GA, Smith BA: Mathematical modeling of ligaments and tendons. **J Biomech Eng 115:**468-473, 1993

78. Zhang G, Young BB, Ezura Y, Favata M, Soslowsky LJ, Chakravarti S, et al: Development of tendon structure and function: regulation of collagen fibrillogenesis. **J Musculoskelet Neuronal Interact 5:**5-21, 2005

Appendix: Experimental and Analysis Protocols

A. Postnatal Mouse Dissection and Preparation for Mechanical Testing Protocol

Thaw out mouse at room temperature, Note: Work through this protocol one mouse at a time so that the tendons are exposed for as small a time as possible.

Equipment:

Small development grips, grip holder, Allen key, dovetails and corresponding pieces

2 Jeweler's forceps

Microscissors

Large microscissors (for 24+ day dissections)

Scalpel Holder

#11 Blades

Black mat

Super glue

Small pieces of sandpaper (0.5mm-1mm squares depending on age)

Weigh boat with Verhoeff stain

A1. Dissection

a. BLUNT DISSECTION

1. Tape the mouse down on the black mat, fixing it behind the shoulder as well as above the neck
2. Make incision in the skin
3. Rotate and visualize shoulder, tape down in ~30° external rotation

4. Locate and break the acromioclavicular (AC) joint with jeweler's forceps

5. Follow spine of scapula with the forceps to gently free the supraspinatus tendon-muscle unit from the scapula

6. 'Flip' supraspinatus tendon and muscle to rest on humeral shaft.

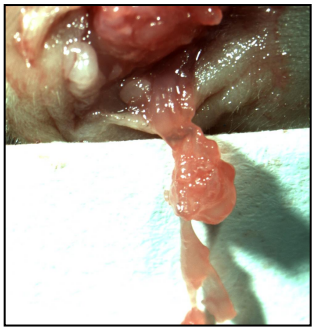

Figure A.0.1 Tendon-Muscle-Humerus Complex

7. Cut (Large microscissors for 24+ days old, microscissors for younger ages) the humeral head at the tendon-to-bone insertion site to release a bone chip-tendon-muscle unit. Clear any remaining fascia away before cutting to ensure that you can visualize the insertion site. Cut the smallest bone chip as possible without damaging the insertion site.

**Note: It is easiest to cut the bone chip with as much tissue still naturally attached to anchor the humerus and scapula

8. Remove the tendon-muscle-bone chip complex from the shoulder

b. FINE DISSECTION

1. Place jewelers over the Supraspinatus tendon and move proximally to gently detach the muscle.

2. Use microscissors to trim any additional pieces of the humeral head that would impede visualizing the insertion site

3. Use microscissors to shape the bone chip so you can easily fit it between pieces of sandpaper. We want to try and have as flat of a bone chip as possible.

4. Under dissecting scope carefully remove excess muscle and fascia from tendon using the jeweler's forceps

5. Carefully clean up capsule or additional fascia near the tendon insertion site

Make sure to keep the tendon hydrated with a SMALL amount of PBS at all times. A large amount of PBS will cause the tendon to delaminate. It is best to keep using small drops of PBS and reabsorbing with a Kimwipe if necessary

Figure A.0.2 Supraspinatus tendon and bone chip

A2. Cross-sectional Area

1. Allow GisMO at least 20 minutes to warm up
2. Place laser 5cm from ceramic plate to minimize spot diameter (0.045mm)
3. Launch Mogware
4. Place the tendon on top of a flat dissection ruler. Align the insertion site of the tendon with a millimeter marker
5. Move entire ruler and tendon to the GISMO stage; make sure that the ruler is lying flat on the stage. If necessary, weights to hold the ruler flat are located in the GisMO drawer.

a. Lightly dab excess PBS off with Kimwipe. Make sure time tendon is without PBS is

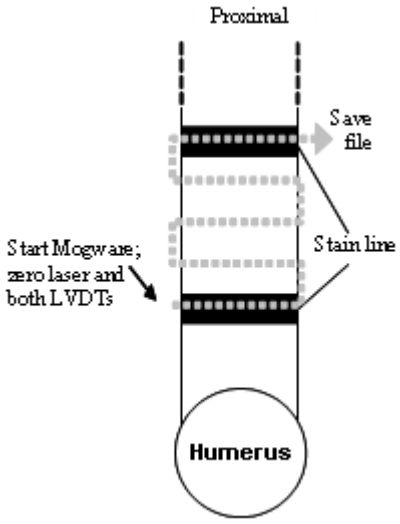

Figure A.0.3 GisMO Test Sequence

minimized (less than 60 seconds)

b. Lay tendon and ruler flat on the ceramic within the LVDT measuring range (4 blue dots) – helps to lightly drag along ceramic [The insertion site should be your left]

c. The laser should be just to the right of the insertion site and on the opposite side from where you are (see Figure A.3)

6. Press the Run (➔) button in Mogware and ensure that the oval Capture button beneath the Start button is activated (lit) so that your data will be captured. Press the Start button to begin recording data.

a. Zero both LVDTs and laser **Make sure you zero on the ruler and stay on the ruler at all times during the measurement.

7. Measure the appropriate area of the tendon depending on age by following the key above in Figure 3 (½ turn in y direction = 0.25mm):

a. 4–10 day – 1.5 mm

b. 28-90 day – 2.5 mm

8. Press Stop button and save file in the appropriate folder

A3. Stain Lines

1. Place the tendon on top of a flat dissection ruler. Align the insertion site of the tendon with a millimeter marker

2. Prepare the Verhoeff's stain (see "recipe" below)

a. Stain works best if 'suture' is soaked in it at least 15 minutes prior to use

b. Need to use extremely fine thread or hair for the stainlines

Verhoeff's Stain Recipe

Ingredients:

A) 5% hematoxylin solution 0.4 g Hematoxylin + 20 ml 95% EtOH

B) 10% aqueous ferric Chloride 2 g Ferric chloride + 20 ml dH_2O

C) Wiegert's iodine solution 2 g Potassium iodide + 1 g Iodine + 100 ml dH_2O

Dissolve all solids and add **in order –** B to A, then C to A

A = 4 mL

B = 2 mL

C = 2 mL

Solutions A, B and C can be made up ahead of time and stored separately. Store C in a dark bottle. The shelf life of each solution is as follows: A – 100 years, B – 1 day to a week, C – up to 3 months. After mixing, stain may be stored at room temperature (1 week max). However, it is better to make up fresh stain for the testing day.

3. Dip suture into stain and apply appropriate stain lines

a. Ensure there are no stain droplets on the suture before application on tendon as these will sped across the tissue

4. First stain line will be place on the insertion of the humerus and the rest the appropriate distance away as follows for each age:

a. 4 days old – stainlines every 0.5mm. gage length ~1.5 mm. Insertion site

denoted as first 0.5 mm, midsubstance from 0.5 to 1mm. Gripped at 1.5 mm.

b. 10 days old – stainlines every 0.5 mm, gage length ~2mm. Insertion site denoted as first 0.5 mm, midsubstance from 0.5 to 1mm. Gripped at 2 mm.

c. 28 days old - stainlines every 0.5 mm, gage length ~2.5mm. Insertion site denoted at 0-1mm, midsubstance denoted as 1-2mm, Gripped at 2.5 mm

d. 90 days old – stainlines every 0.5 mm, gage length ~2.5mm. Insertion site denoted at 0-1mm, midsubstance denoted as 1-2mm, Gripped at 2.5 mm

5. Make stain lines as clear as possible – keep stain "fresh" and apply to a relatively "dry" tendon (dab on kimwipe first, work fast). The clearer the stain lines are, the easier optikos will be.

A4. Sample Prep

1. Sand paper both the insertion site and the tendon

a. Place a small layer of glue along the sandpaper before placing the bone chip

b. Place insertion site sand paper as close to the insertion stain line as possible without covering it

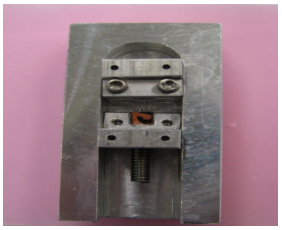

Figure A.0.4 Grip-Boat with grips

c. Crush the bone chip into the glue using either the blade handle of the scalpel or the opposite end of the forceps (This step is only necessary if you cannot appropriately trim the bone chip during fine dissection

d. Place an additional small amount of glue on top of the bone chip

e. Sandpaper the top of the bone chip

f. For the myotendinous junction side of the tendon, place the tendon on top of the sandpaper and align it with the appropriate gauge length insertion site.

g. Add a small amount of glue on top of the tendon

h. Place additional piece of sandpaper on top.

i. Make sure the tendon is hydrated and not glued to the mat before removing

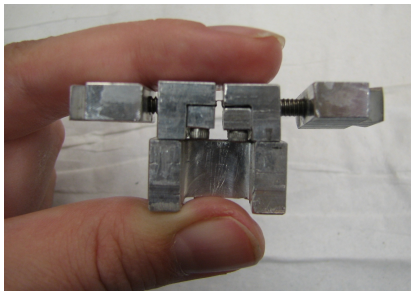

Figure A.0.5 Grips with grip holder and dovetails attached.

2. Place grips into grip-boat (Figure A.4)

a. Designed to eliminate grip movement while tightening grips

3. Place each sandpaper end on one grip and secure the tendons in the grips

a. The insertion site should be placed in the bottom grip and the muscle origin in the top grip. The top grip has a notch milled out if image calibrations are needed (not pictured).

b. Figure 2 shows top grip secure, bottom grip open

4. Secure the grip holder on both the top and bottom grips

5. Remove grip+grip holder complex (Figure A.5) and attach the top stem that connects to the cross bar on the instron. Then attach the bottom plate which gets secured to the floor of the tank.

6. Carefully move the whole complex into the instron and attach it to the crosshead. Lower the crosshead down until it is just touching the tank. Secure the bottom to the tank and remove the grip holder.

7. Visualize the tendon and make sure it is straight, both front/back and left/right. Make careful, careful adjustments if necessary. Once satisfied tighten bottom plate to tank.

A5. Instron and software preparation

1. Attach 10N load cell to Instron.
2. Turn on Instron and start Bluehill
3. Calibrate load cell
4. Load either "MouseSupra_earlydev" or "MouseSupra_latedev" in Bluehill (Early for 4, 10 days; Late for 28, 90 days)
    a. Check to make sure appropriate parameters are set in the Bluehill protocol (Need to change distances and speeds based on grip to grip gauge length)
5. Start *Digi-vlepo* for Crimp Images and *Redonkulous* for Cross Polarizer Tests
    a. Set up camera – Basler Scout-1600fm with Nikon 200mm Micro lens
    b. Place fixture stem in cross head and lower to approximate testing location
    c. Visualize fixture in LABview and optimize image
        i. If camera settings need to be changed, LABview must be closed and MAX opened -- MAX and LABview cannot operate together
        ii. Change camera settings in MAX, SAVE and close

**For CP testing, make sure that the shutter is not above 2000 as the camera cannot operate at the necessary frame rate.

Set sample name and image capture folder

B. Tensile Testing Profile for Postnatal Mouse Supraspinatus Tendons

Preload	Block # 1	Tensile Extension
		Absolute Ramp
		Delta 0.005 N (or 0.02)
		Rate 0.0025 mm/s or 0.0015 mm/s (0.1%/s)
Precycling	Block # 2	Tensile Extension
		Triangle
		Maximum 0.008 N (or 0.04)
		Minimum 0.005 N (or 0.02)
		Rate 0.0025 mm/s or 0.0015 mm/s (0.1%/s)
		Number of cycles 10
Hold	Block # 3	Tensile Extension
		Hold
		Delta 60 s
Test to failure	Block # 4	Tensile Extension
		Relative Ramp
		Delta 1200 s
		Ramp 0.0025 mm/s or 0.0015 mm/s (0.1%/s)

(**Based on 2.5mm (28, 90 days) or 1.5mm (4, 10 days) grip to grip gauge length**)

C. Cross Polarizer Testing Protocol

Equipment:

2 NEMA stepper motors

Cross polarizer base plate

Frank the tank

4 metal cylinders

4 long screws

2 wooden blocks

Light box – old slide containers and wooden blocks to reach correct height

DC power supply – alligator clips to connect to box

Brian box

Cords to attach motors to box

Cords to convert motor attachments to USB ports

Protocol for Cross Polarizer:

1. Open up the *Redonkulous* software in LABview.
2. Change the directory and file name.
    a. For example file name might be 200L_afterpre, marked as sample number, shoulder of mouse_type of test
3. Make sure all of the equipment is properly set up, i.e. camera plugged in, DC power supply turned on, motors connected properly.
    a. Motor address needs to match the correct COM port tagged in LABview

4. Make sure the camera settings are appropriate for cross polarizer testing, if camera settings need to be adjusted you must CLOSE LABview and then open up MAX. (MAX and LABview cannot be open at the same time.)

a. Make sure the shutter setting is not above ~2500 or the camera cannot operate at its natural 14.14 fps

b. SAVE the settings after adjusting them and record in the lab notebook

c. Close MAX and re-open *Redonkulous* when you are done

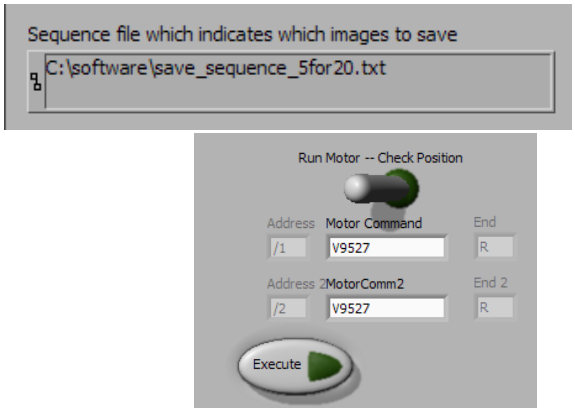

Figure A.0.6 Above, Input for *.txt file (step 6). Below, Command Line for motors in Redonkulus

5. Make sure the tendon is oriented properly, i.e. straight and in the plane of the camera.

6. Make sure you input the correct *.txt file for your tissue. This file determines which images the computer will save. For example, the file in Figure A.7 will save an alignment map every 20 seconds.

7. Start the motors using the following commands

a. **V9527** to set the velocity – this velocity has been determined in order to take a 14 image alignment map every 5 seconds starting at angle zero

b. **z0** to zero the encoder at the start point, this should be done with the tabs aligned on the wooden blocks. One tab should have a small mark on it. Make sure after zeroing the encoder that the discs did not shift and offset from each other.

c. **P0** will cause the discs to move continuously forward until commanded otherwise

d. **T** will stop the discs from moving, always try and stop the discs close to their initial start point.

e. If you ever need to move the discs to align them with the zero start position you can move them slowly by entering a number of steps after a P or A, for example P1000 will move the discs forward a 1000 steps on the encoder, A1000 will move then backwards a 1000 steps

8. Once the tendon is slightly slack, zero the load.

9. Manually load the tendon to the appropriate preload:

a. *4-10 days* – 0.005N

b. *28-90 days* – 0.02N

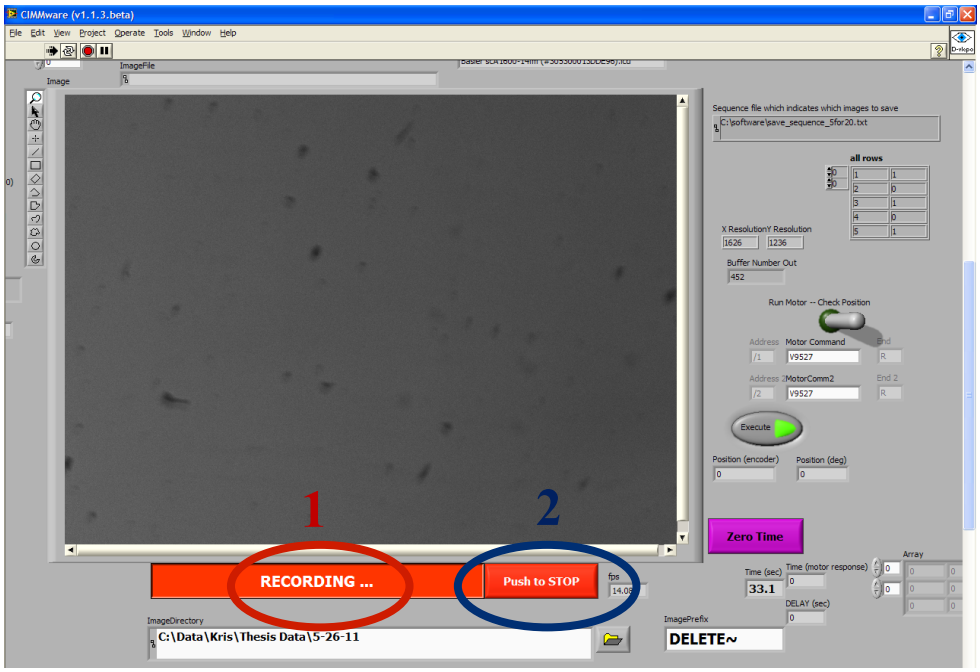

Figure A.0.7 Screenshot of Redonkulus Program, highlighting the PUSH to RECORD button (step 17, red) and the Push to STOP button (step 20, blue).

Zero the displacement on the Instron

10. Take a set of Cross Polarizer images starting at zero degrees before beginning test (_slack/before)

a. Make sure to unclick to STOP taking images and STOP the program in order to save the output file.

b. Always immediately change the file name to avoid saving over one

11. Change the file name to '_after'.

12. Start test by zeroing the time on *Redonkulous* and pressing start on the Instron at the same time

13. **Take a set of Cross Polarizer images starting at zero degrees** after the tendon has finished precycling, record the time at the end of preconditioning.

14. **Change the file name to '_ramp'.**

15. **After restarting the program, record the offset between the Instron and image capture program**

16. **Take Cross Polarizer images (starting at zero degrees) for the entire ramp**

17. After tendon fails, stop image capture by un-clicking the "capture images button" on the left and save Bluehill file by pressing "Finish". Make sure that you have stopped capturing images on *Redonkulous* by pressing the capture images button on the left.

18. Stop the motors using the command "T" on the *Redonkulous* software.

19. Manually increase displacement to observe failure. Record failure location.

20. Stop the *Redonkulous* program to save the output file by pressing the red stop button on the right.

21. Change the file name on the program for your next test.

22. See below for testing protocol figure and blocks

Always check gage lengths of tendons and make sure you are using the appropriate

protocol and strain rates

For precycling:

4-10 days – early development protocol, precycling occurs at 0.005 - 0.008N

28-90 days – late development protocol, precycling occurs at 0.02 – 0.04N

D. Crimp Testing Protocol

Equipment:

Open tank

Razor blade

Plastic backing

Plastic specimen holders

Colored OCT

2 jeweler's forceps

#11 blade

Freeze spray

Liquid nitrogen

Large Hemostat

Liquid nitrogen Dewar flask

Protocol for Crimp:

1. Open up the *Digivlepo_Baslerscout* software in LABview.
2. Change the directory and file name.
    a. For example, file name might be 200L_afterpre, marked as sample number, shoulder of mouse_type of test
3. Make sure all of the equipment is properly set up, Dewar flask full of liquid nitrogen, freeze spray full, etc.
4. Make sure the camera settings are appropriate for crimp testing, if camera settings

need to be adjusted you must CLOSE LABview and then open up MAX. (MAX and LABview cannot be open at the same time.)

b. SAVE the settings after adjusting them and record in the lab notebook

c. Close MAX and re-open *Digivlepo_Baslerscout* when you are done

5. Make sure the tendon is oriented properly, i.e. straight and in the plane of the camera.
6. Once the tendon is slightly slack, zero the load
7. Manually load the tendon to the appropriate preload:

d. *4-10 days* – 0.005N

e. *28-90 days* – 0.02N

8. Zero displacement

9. Start test by zeroing the time on *Digivlepo_Baslerscout* and pressing start on the Instron at the same time.
10. Start taking images before the ramp to failure begins.
11. See below for testing protocol figure and blocks

Always check gage lengths of tendons and make sure you are using the appropriate protocol and strain rates

For precycling:

4-10 – early development protocol, precycling occurs at 0.005-0.008N

28-90 – late development protocol, precycling occurs at 0.02 – 0.04N

Protocol for Flash Freezing Specimens

1. Once the test has reached the desired point stop the test on the Instron.

2. Immediately begin freeze spraying the tendon from approximately 10 cm away (Spray until some frost appears on the tendon; the further away you are from the specimen, the longer you will have to spray)

3. Carefully place plastic backing behind the dovetails

4. Use a razor blade to sharply detach the tendon at the Insertion site

5. Freeze spray the tendon again

6. Remove the top dovetail and tendon from the Instron

7. Spray the tendon again

8. Detach the frozen tendon from the top grip using the scalpel with a #11 blade

9. Use the jeweler's forceps to orient the tendon appropriately in the plastic specimen holder as fast as possible

10. Cover the tendon in OCT (Be careful not to turn the specimen while squeezing the OCT into the dish)

11. Use large forceps to place tendon in plastic holder in the liquid nitrogen Dewar flask until completely frozen

12. Place in labeled plastic bag and store in freezer until sectioning

Notes for Sectioning on Cryostat Microtome

1. Make sure the tendon is as level as possible and in the same plane

2. Section tendon in 8μm increments

3. Try and keep the orientation of all samples the same so it is easy to identify the midsubstance and insertion site of the tendon

4. If the tendon keeps shredding, increase slice thickness to 10μm and cut the tissue very slowly. Be patient -- sometimes it just needs to be sectioning enough of the tendon to not rip it.

E. Protocol for Cryostat Microtome Sectioning of Samples

1. To begin, the cryostat microtome should be set to approximately -22 to -25 degrees Celsius, which is optimal for sectioning tendon. Also, turn on the light.
2. Next, prepare the block containing your specimen by squeezing OCT onto one of the metal chucks, which should be sitting in one of the holes of the Peltier elements.
3. Quickly place the block on top of the button and situate it so that its top is parallel to the surface of the button. Squeeze more OCT around and on top of the block to entirely embed your sample.
4. Press the 'Freeze Object' button on the microtome. Wait approximately five to ten minutes for the OCT to harden until it appears white.
5. On the disposable blade carrier, pull the clamping lever towards you to loosen the gap where you will insert a blade. Push the lever back to secure the blade.
    a. Note: Use the knife guards to cover the blades when done.
6. Grab the button and place it within the specimen clamping.
7. Twist the clamping lever to firmly hold the chuck and pull the orienting lever to situate the chuck such that its surface is parallel to the metal plate behind the clamp.
8. Turn the knob controlling thickness to 8 or 10 microns and also reset the section counter to keep track of how far you have sectioned into the block.
9. Adjust the entire position of the block with respect to the blade by using the arrow buttons to retract or pull it closer. Test the best position by removing the knife guard and turning the handwheel on the right side of the machine until you are able to section a very thin part of the block.

10. Adjust the orienting lever until sections span the entire block and the blade is slicing parallel to the button.
11. Slice away the excess OCT until you encounter your specimen. Begin taking sections and collecting them on Posi-Slides.

F. In Situ Postnatal Mouse Crimp Protocol

Thaw out mouse at room temperature, Note: Work through this protocol one mouse at a time so that the tendons are exposed for as limited time as possible.

Equipment:

2 Jeweler's forceps

Microscissors

Scalpel Holder

#11 Blades

Black mat

Liquid Nitrogen in Dewar Flask

Large Forceps/Hemostat

Freeze Spray

Tissue Freezing Medium

1. DISSECTION
    a. Tape the mouse down on the black mat, fixing it behind the shoulder as well as above the neck
    b. Make incision in the skin and peel away skin so that the shoulder is exposed. (It might be useful to do this prior to taping down the mouse for older specimens.)
    c. Rotate and visualize shoulder. Then tape the arm in ~30° external rotation.
    d. Follow the spine of the scapular lightly with the forceps in order to remove the trapezius and deltoid muscles. Once removed, cut out the fat pad just above the

humerus and the acromioclavicular (AC) joint.

e. Locate and cut the AC ligament to break the AC joint with microscissors.
f. Cut away the clavicle and then break off the acromion to expose the supraspinatus, infraspinatus, and subscapularis tendons. At this point the entire rotator cuff is exposed with no overlying tissue.
g. Using the microscissors carefully cut the infraspinatus and subscapularis tendon at their insertions. Remove these tendons and their associated muscles.
h. Continue to cut away some of the surrounding fascia but be careful not to move the scapula's position in order to maintain in situ stress on the tendon.

2. FLASH FREEZING

a. Begin freeze spraying the tendon from approximately 10 cm away (Spray until some frost appears on the tendon; the further away you are from the specimen, the longer you will have to spray) **During the remainder of the protocol, monitor the joint carefully for signs of thawing and periodically refreeze with the spray to preserve the tendon's loading environment
b. Carefully cut the bone-tendon-muscle complex out by cutting a rectangular piece out with a scalpel blade. Do this by removing the muscles of the humerus, cutting the humerus free and then removing the scapulohumeral joint.
c. Spray the tendon again if necessary to make sure the tendon piece is frozen throughout the removal process.
d. Use the jeweler's forceps to orient the tendon appropriately in the plastic

specimen holder as fast as possible. This is the most difficult part. It is important to get the tendon to lie flat against the bottom of the dish.

e. Cover the tendon in OCT (Be careful no to turn the specimen while squeezing the OCT into the dish)
f. Use large forceps/hemostat to place tendon in plastic holder in the liquid Nitrogen dewar flask until completely frozen (about 30 seconds).
g. Place in labeled plastic bag and store in freezer until sectioning

3. SECTIONING

a. Make sure the sectioning block is as level as possible as well as the bone-tendon-muscle complex is parallel to the plane of the blade
b. Section tendon in 10μm increments
c. If it is difficult to section (this will happen with older samples that have more developed bone), try a different section of the blade or wipe down the surface with cryostat oil. *ALWAYS put the blade safety on when doing this.
d. Try and keep the orientation of all samples the same so it is easy to identify the midsubstance and insertion site of the tendon
e. If the tendon keeps shredding, increase slice thickness to 12-15μm and cut the tissue very slowly. Be patient -- sometimes it just needs to be sectioning enough of the tendon to not rip it.

4. IMAGE

a. After sectioning and staining (see *Picrosirius Red and Hematoxylin Staining* protocol), image slides using the *Protocol for Polarized Light Imaging for Crimp Analysis*.

G. Picrosirius Red and Hematoxylin Staining Protocol for Crimp Analysis

Tap H_2O	1 minute
Picrosirius Red	45 minutes
Acidified H_2O	5 minutes
Hematoxylin	10-15 minutes
Tap H_2O	3 minutes
Acid EtOH	20 seconds
Tap H_2O	3 minutes
Scott's Buffer	20 seconds
Tap H_2O	3 minutes
95% EtOH	1 minute
95% EtOH	1 minute
100% EtOH	1 minute
100% EtOH	1 minute
CitroSolv	1 minute

H. Protocol for Polarized Light Imaging

1. Turn on the microscope and the camera (plus firewire cable into either input on side of camera).
2. Obtain microscope micrometer scale (1 mm with 20 subdivisions) and place on the stage so it is centered and in focus. Start with the 5X objective.
3. Under the *Measure* file menu, select *Calibration* and then *Spatial Calibration Wizard*. This will walk you through the steps in order to create reference calibrations.\
4. Read through the instructions and click "Next" on the bottom of each prompt until you come to a screen with a button "Edit/Add Objectives."
5. Create reference calibration files by clicking "Edit/Add Objectives" and adding a new file for each objective. Name them by the objective in use, i.e. "5x". Once you have made them, start with the 5X objective and click "Next."
6. The program will now prompt you to focus the micrometer scale bar in the frame and to snap a picture. It's important to use the correct binning and resolution when performing this step in order to visualize the scale bar as best as possible.
7. Once you have taken an image, click "Next."
8. The next prompt is to create a reference bar that has a known length. The default units for this section are micrometers. Draw a reference bar and input the appropriate number of micrometers for the bar. (This is done by knowing how big each tick mark is on the scale bar and drawing straight lines between ticks. Make sure you are going from the beginning of one mark to the beginning of the last one for consistency.) Repeat this step several times in order to get the most accurate measurement of

calibration. Once finished, click “Next.”

9. The program will then ask you if you want to edit more, or finish. Repeat this process until you have made a calibration for each objective.
10. Now you have made calibration references. There are two ways to use this now. You can either set a system calibration reference or you can use it to measure and create scale bars in your images. If you set both, the calibration will not be correct as it will be double calibration. Every time you want to measure in a snapped image, you need to pick the reference calibration (5X, 10X, 20X) with the calibration tool before using the measure tool.

IMAGING

1. Turn on the microscope and the camera (plug firewire cable into either input on side of camera).
2. Using the 5X objective, focus the condenser so that the edges of the hexagon are sharp. (Dial at bottom left of microscope, on the base, changes the size of the hexagon. Condenser is focused using black knobs under stage).
3. Find the region of interest (e.g., insertion site or midsubstance) and focus the specimen.
4. As you change objectives from 10X and then to 20X, ensure that the edges of the hexagon are still in focus and that the specimen is still in focus.
5. Upon reaching the desired magnification, move the condenser hexagon out of view.
6. On the computer connected to the microscope, load QCapture Pro software. Click on

the camera icon to bring up the capture menu. Click Preview to view the image.

7. Rotate the stage until the tendon is at a ~45 degree angle (bottom left to top right) and then lightly tighten the stage.
8. Set the analyzer to 180 degrees and the polarizer to 270 degrees. This position will be considered 45 degrees when saving the images.
9. Turn the light all the way up and ensure that all light is directed toward the camera.
10. **Take the noncompensated images first.** With the 20X objective in place, load the PLuncomp profile. Adjust exposure as needed. This can be done by checking that the image is not too bright (with the analyzer at 180° and the polarizer at 270°) or too dark (with the analyzer at 135° and the polarizer rotated 45° clockwise to the blue line).
11. Rotate both the analyzer and polarizer in a clockwise direction by the same increment (5 or 10°). For both noncompensated and compensated images, pictures need to be taken across a 90° range in 5 or 10° increments.
12. Press Snap and save each picture as a .tiff file. For each specimen, create a folder with the specimen number. Within this, create separate folders for compensated and noncompensated images. Save pictures using a 3 digit filename format. For example, a picture taken at 45° should be saved as 045. Repeat until a span of 90° (image named 135) has been reached.
13. **Take the compensated images.** Insert the compensator in its slot above the polarizer with the nail pointing down. The compensator must be oriented 45° counterclockwise from analyzer and polarizer (i.e., compensator nail should be pointing at 225 degrees

– the blue line – on the polarizer).

14. Load the PLcomp profile and adjust exposure as needed.
15. Repeat steps 11 and 12. *However*, this time rotate the compensator in a clockwise direction with the analyzer and polarizer (make sure that compensator is always oriented 45° from the analyzer and polarizer while you are rotating). Instead of going from light to dark (or vice-versa) as you rotate analyzer compensator and polarizer, the images should go from blue to red (or vice versa).
16. When you have finished, turn off camera by unplugging fire wire cable.
17. Put away the compensator and analyzer and turn off the microscope lamp.

I. Protocol for Analyzing Fiber Crimp Frequency Using Noncompensated Polarized Light Images

1. Open MATLAB (v7.0 or later).
2. Set a new path to \\max\krism\Software
3. In the command window, type " [dt1,dt2, magnitude, distance, amp, meanamp, MeanDistance, MeanAmplitude,RegionDistMeans, RegionAmpMeans, NUMpixs, RegionPeriod,MeanPeriod] = fft_profile_kris_allangles3reg_mag_fig2"
4. Choose the image file you want to analyze (should be a *.tif file extension). For this analysis, choose the noncompensated image taken at a 75 degrees angle (please see the "Protocol for Polarized Light Imaging" for more details).
5. First, draw a rectangle by clicking four points around a representative section of crimp for the image. Then click 'Enter.'
    a. Note: It is important to draw these lines so that opposite sides of the rectangle are parallel to each other and the fibers as possible.
    b. Note: Pressing 'Delete' will remove the previous click and allow you to choose a new corner instead.
6. Now you want to draw a line in the direction of the collagen fibers. Choose to follow a fiber that has visible differences in light intensity (crimp). Click once to start drawing a line and again to finish the line. You may edit this line until you click 'Enter.' This line should represent the fiber direction of the tissue but ideally should be oriented towards 45 degrees.
7. Next, you will be prompted to save the Excel file and the MatLab figure to your desired location.

a. For example, save the image in the !LizQual! folder as Samplename_location_slidenumber
    1. Ex. HHHippos_mid_S1

8. This program splits the rectangle into three regions and averages the intensity across many lines within that region. The user will have to pick the peaks from those average plots for each region, and for each angle. The Intensity vs. Length plot will come up for the first angle.
9. Before beginning to click, make sure the rectangles (regions) within the blue lines on the original image are appropriate for qualitative analysis and parallel to the fiber direction.
10. In the Intensity vs. Length plot, select the **peaks** of intensity in order to obtain the coordinates of crimp peaks. Hit enter after all of the peaks have been chosen. The next sub-region in the rectangle will come up. Continue to pick peaks on each region for each angle until complete (5 regions/angle, 10 angles).
    a. Only choose peaks that cross the mean intensity threshold (noted by a red dashed line at 0 degrees – This line comes from a dtrend of the data) and drop below the mean intensity by 20 pixels (noted by a green line).
    b. Note: For type III uncrimped tissue, it is important to pay attention to there being too numerous peaks that falsely represent the tissue due to artifact from flattened crimps.
11. SAVE the following data from the command prompt into an Excel file:
    a. RegionAmpMeans

b. MeanAmplitude

c. RegionPeriod

d. MeanPeriod

** Do NOT choose peaks that are not separated by a substantial dip (must cross the mean intensity threshold in red) and do not include those that do not reach the green line (20 pixels below the mean intensity) Fig A.8.

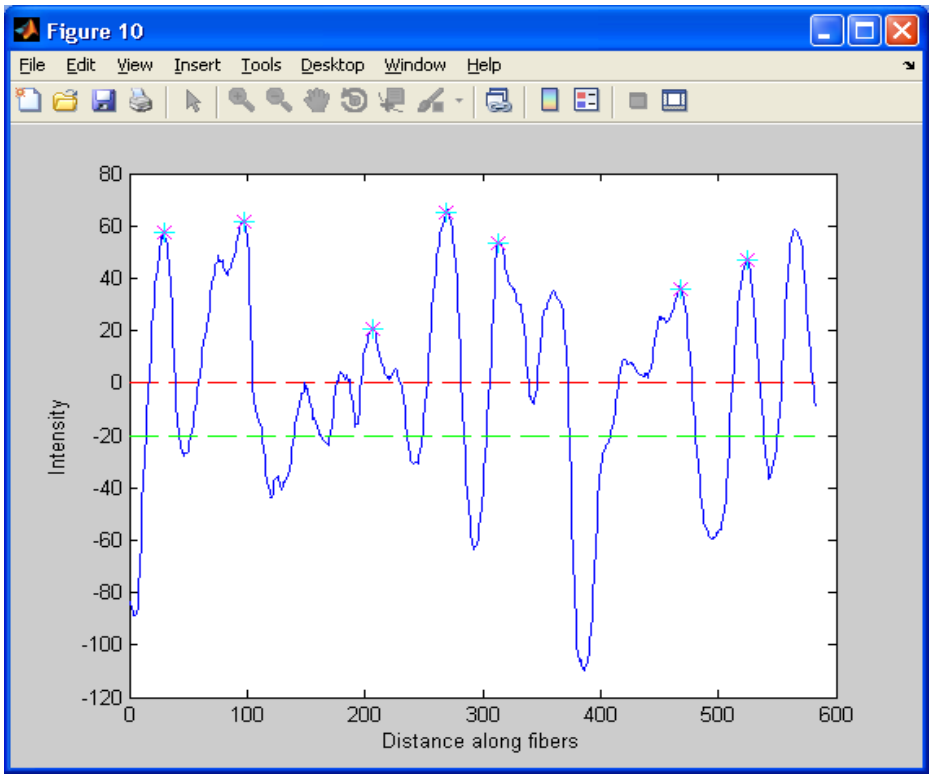

Figure A.0.8 Length vs. Intensity Plot With Peaks Highlighted. For each sub-region, the user selects peaks that cross both the red (mean pixel intensity) and green (deviation of 20 pixels from the mean intensity) lines.

12. Repeat for all specimens, for midsubstance and insertion.

OUTPUT FILES

This program outputs a combined plot of all of the transforms for each region as well as

an Excel file with the FFT data.

J. Protocol for Fiber Alignment Analysis

FILES NEEDED TO RUN ALIGNMENT MAP ANALYSIS

1. Images (preferably *.tiff files, 15 images per set)
2. CIMMware output text dile ('filename'~OUTPUT.txt) – contains the timestamp of each image, corresponding motor encoder counts and angle (degrees), and delay in image capturing.
3. Instron output file ('filename'.is_tcyclic_raw) OR output text file (as generated by "rawful.m", 'filename'.is_tcyclic_taw.tvt) – contains time, displacement and load data from Instron

RUNNING ALMAP.M

1. Open Matlab
2. Direct working directory towards folder containing images (**Analysis will run much faster if images are on local computer rather than on network drive or external hard drive)
3. Run "ALMAPv14fps_7dres.m" for 4 and 10 day specimens or "ALMAPv14fps_24dres.m" for 28 and 90 day specimens by typing the program name at the Matlab command prompt, or by opening up the m-file and clicking "F5".
4. User is asked to enter in the following:
    a. Rotation speed of polarizer (encoder counts/second): _____ (9527)
    b. Number of images per alignment map: _____ (13)
    c. Number of regions across width: _____ (5 for 4,10 days, 10 for 28,90 days)

d. Number of regions across height: _____ (10 for 4,10 days, 20 for 28,90 days)

e. Tip – total number of regions is width multiplied by height, so default is 450 regions across the surface of the sample.

5. User is then asked to select folder containing images. This is done by finding desired folder and double clicking on any image (with appropriate filename extension) in that folder.
6. User is then asked if they would like to determine the failure cutoff level. This refers to finding the stress/strain point of failure in the mechanical test such that alignment analysis is only done up until the point of failure. The options are:

   f. "Yes – pick cutoff now"

   g. If user selects this option, they are then prompted to find the *.raw file.

   h. After selecting the *.raw file, the user is prompted to save the output text file. Use the default name for saving the text file.

7. The user is then asked to select the *.txt file. Double-click on the name of the file that was saved in the previous step.
8. User is then asked for the time offset (Instron-images) in seconds. This command is used if there is a delay in timing between the Instron timestamps and the CIMMware timestamps. If there is a delay, enter the amount of time delay here. Otherwise, leave the default value of 0.
9. The user is then asked to draw a rectangle around the failure region. Click and hold to start drawing a rectangle, then release when appropriate shape is dawn around the

approximate area of failure.

10. A zoomed in plot of the selected data is now shown. Click once at a point as close as possible to the failure point.
11. The full load-time curve is then displayed, with the chosen cutoff time shown. This cutoff should inform the user of the pre-failure time range, which can be used when selecting which image sets to analyze (see next step). Click OK.
    a. "Yes – select exisiting *cutoff.fig file"
        i. Locate the *cutoff.fig file for this sample (that may have been created during strain analysis or a prior alignment map analysis) and double click on it. The load-time curve for the sample isdisplayed, with the chosen cutoff time shown. This cutoff should inform the user of the pre-failure time range, which can be used when selecting which image sets to analyze (see next step). Click OK.
    b. No
        i. No failure point is selected and the analysis carried on without it
12. Next question is "How would you like to select images for analysis?" After selecting one of the options below, the title of the image selection window (that appears upon selection of one of these options) indicates the time representing the cutoff in order for the user to know what the pre-failure time ranges are. This value may be used to inform the user on which image sets to select for analysis. The options for this question are:
    a. All ALMAPs for sample

i. If this option is selected, the user is asked to identify the first and last image of the sample (or in other words, the first and last iamge that span the range of images you want analyzed). Click on the first one, then hold CTRL and click on the last iamge. Click OK.

b. Manually

i. If this option is selected, the user needs to select the first image from each alignment map image set that is desired for the analysis. Click on the first image of the first desired set, and then hold CTRL to click on subsequent images. Click OK

c. Every X seconds

i. If this option is selected, the user is asked to identify the first and last image of the sample (or in other words, the first and last image that span the range of the images you want analyzed). Click on the first one, then hold CTRL and click on the last image. Click OK.

ii. A second box will pop up and ask "Analyze an image every ____ seconds (multiple of 10)." Input an appropriate spacing value depending on the time range of image sets to be analyzed, and on the number of alignment maps you would like to span that range. For example, if you are analyzing image sets from 120 seconds to 420 seconds, and you want 10 image sets to span that range, take 300 seconds and divide by 10 and input 30 as the answer to this question. **The increment for this question must be a factor of 10 due to the

timing of image acquisition.

13. Next question is “What is the testing orientation of the sample?” This will center the output angle values around 90° (longitudinal) or 0° (transverse). Select one of:
    a. Longitudinal
    b. Transverse
    c. Cancel
14. The user is then asked “Would you like to save the files (cropped images, histogram & contour)?” Options are:
    a. Yes -- User is asked to select folder to where the files should be saved
    b. No
    c. Cancel
15. The first image of the first image set will then appear. At the top center will be a set of numbers indicating which image set (and hence alignment map) the current image represents, and also the total number of image sets/alignment maps to be analyzed. For example, 1 of 10 refers to the first image set of 10 total. Using the cursor, draw a rectangle around the desired area of interest for the alignment analysis. This is likely to be the center region of the sample, or the area contained within the strain beads. Try to place the borders of the rectangle using recognizable landmarks of the sample in order to be able to repeatedly select this area on subsequent images. After drawing a rectangle for the first sample, the user will then draw rectangles on the remaining images until rectangles have been placed on all alignment maps in the analysis. Starting at the 2nd image set, a second window will appear which shows the previous

rectangle's position in order to assist the user in placing a rectangle on the current image. **Note – the previously drawn rectangle may appear slightly smaller or cropped than what was drawn. This is because the total pixel numbers are cropped in order to result in similar sized areas across the sample surface for alignment analysis.

OUTPUT FILES FROM ALMAP.M

contour_(filename-timestamp).fig

a. shows a 2D contour plot of fiber alignment values – NOTE: 90° range only (45-135° for longitudinal, 0-90° for transverse)
b. stored userdata = number of thrown out angle values

histo_data_(filename-timestamp).xls

c. single column of all angle values for this alignment map values – NOTE: 90° range only (45-135° for longitudinal, 0-90° for transverse)

histogram_(filename-timestamp).fig

d. histogram of all angle values for that particular timestamp values – NOTE: 90° range only (45-135° for longitudinal, 0-90° for transverse)
e. stored userdata = matrix containing all angle values from histogram

meanangle_(filename).fig

f. plot showing the mean and median angle values for each alignment map analyzed for that sample
g. stored userdata = matrix containing timestamp, median and mean angle values

meanangle_(filename).xls

h. matrix containing timestamp, median and mean angle values for each alignment map/histogram analyzed

quiver(v2)_(filename-timestamp).fig

i. alignment map (quiver plot) of all angle values for that particular timestamp – NOTE: 90° range only (45-135° for longitudinal, 0-90° for transverse)

j. stored userdata = number of thrown out angle values

S90_(filename-timestamp).fig

k. histogram *centered about 90°* of all angle values for that particular timestamp – NOTE: 90° range only (45-135° for longitudinal, 0-90° for transverse)

l. stored userdata = mean, median and mode of incrementally-shifted histograms until it was centered about 90°. "Shift" value indicates how many degrees the histogram was shifted at the end

S90_(filename-timestamp).fig.xls

m. single column of all angle values for histogram *centered about 90°* – NOTE: 90° range only (45-135° for longitudinal, 0-90° for transverse)

(filename)-ORIANA.xls

n. contains timestamp and VAR values for each alignment map analyzed

K. Protocol for the Structural Fit Model Program for Fiber Recruitment

RUNNING THE PROGRAM

1. Open MATLAB (v7.0 or later).
2. Set a new path to Y:\Software\TendonMechanics\cooker.
3. In the command prompt, type "r2f_structfit;"
4. Choose the file you want to analyze (should be a *raw.txt file extension).
5. The program will then prompt you to choose a failure/yield strain. Normally we would choose this at the peak of the load-displacement curve, but this program will work better if you choose a point that is still in the linear region. For example, Figure A.9.

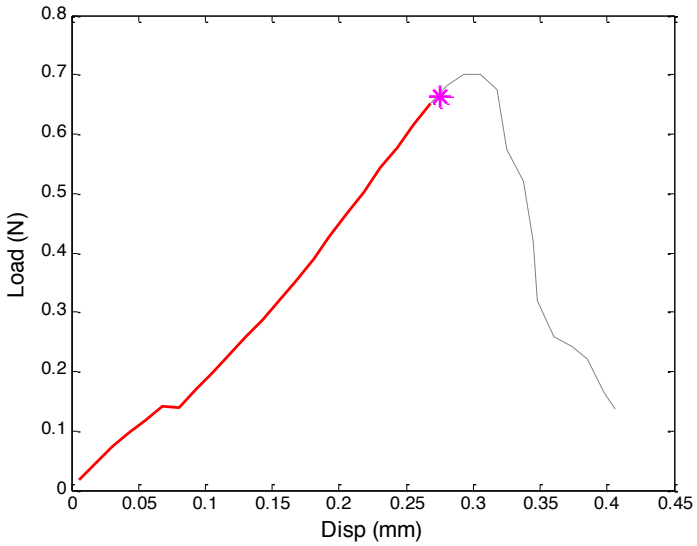

Figure A.0.9 Load-Displacement curve that has the yield/failure strain marked with a magenta star. Note that this is still in the linear region.

6. Let the program run and it will fit a structural fiber recruitment model to the data.
7. The program will prompt you to save a *_sfit.txt file. This will contain the fit parameters for the whole model. Choose to save by clicking "save" or cancel.
8. Repeat for all samples.

1. A plot of the data and the structural fit is outputted. You can use this figure to determine whether the model has fit the data well or not. See A.10 – On the left is a bad fit since there is a discontinuity in the plot and on the right is a very good fit. These plots also write the L0m, L0s, Kel and err of the fit. These parameters are also given in the MATLAB output.
2. In addition to the plots, the program will output a *_sfit.txt file that contains the fit parameters for the entire data set.

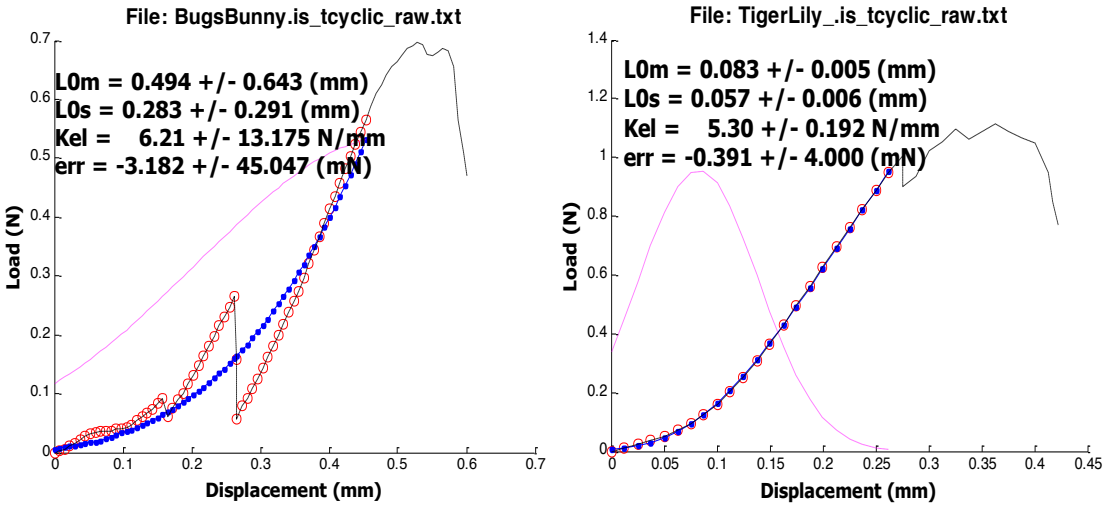

Figure A.0.10 Two examples of a structural fit model output. Bugs Bunny is a bad fit, but TigerLily is a good fit.

3. Finally, text is outputted into MATLAB that is required for analysis.
   a. Copy and paste the output in the MATLAB command window into an Excel file. The file should have the following headings:
      i. %File, dFmax(mm), Fmax(N), sL-mn(mm), sL-sd(mm), Kel(N/mm), CI sLmn(%), CI sLsd(%), CI Kel(%), err-mn(mN), err-sd(mN), rmse(mN)

b. If the confidence interval (CI) of any of the three parameters is greater than 50, than that parameter is considered a bad point. These points are up to the discretion of the user as to whether they should be discarded or not. If all three CIs are greater than 50, that point should be discarded.

c. Next you must calculate the displacement at each percentage of fiber recruitment.

i. To do this, create a matrix in MATLAB by typing "dt1 = []".

ii. Then go into the command workspace and copy and paste the columns "sL-mn(mm)" and "sL-sd(mm)" into the variable matrix. See Figure A.11.

iii. In the command prompt, type "dP = icdf('normal'**,.50***ones(length(dt1),1), dt1(:,1), dt1(:,2))." The "0.50" is the percentage of fiber recruitment so for each percentage, you will change this number. Typically, 50% is for the transition strain and 75% is in the linear region.

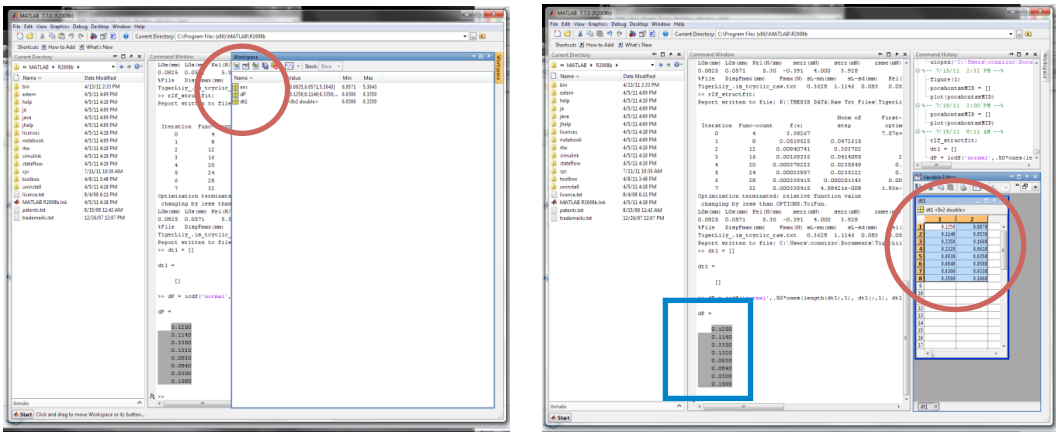

Figure A.0.11 Screenshots showing (left) where to find the variables in the workspace (Double-click on the variable to open it), and (right) how to input the data columns into the variable matrix. Both shots also showing the output of the command used in item iii for 50% fiber recruitment (blue rectangle).

iv. This prompt will output one column of data; this is the displacement for the 50% fiber recruitment mark. In order to get the strain, simply divide by the gauge length.

**Note: A template for this analysis exists in Y:\Software\TendonMechanics.